

Ministry of Higher Education and Scientific Research
Hassiba Benbouali University of Chlef
Faculty of Exact Sciences and computer science
Department of Chemistry



THESIS

Submitted in fulfillment of the requirements for the degree of doctorat

Field : Chemistry

Specialty: Security, Reliability and Enhancement of Gas Pipelines

By

SOUDANI MOHAMED

Title:

CORROSION AND SCALE GREEN INHIBITORS ON CORROSION EFFECTS ON THE FRACTURE MECHANICS PROPERTIES OF GAS PIPELINES

Defended on 12/02 /2019, before the examining committee composed of:

Abdallah Labbaci	Professor	UHB-Chlef	Chair
Željko Božić	Professor	University of Zagreb	External examiner
Chahinez Fares	MCA	UHB-Chlef	Internal examiner
Abdelkader Khadraoui	MCA	UDB - Khemis Meliana	External examiner
Mohammed Benarous	Professor	UHB-Chlef	Invited
Khaled El-Miloudi	MCA	UHB-Chlef	Supervisor
Mohammed Hadj Meliani	Professor	UHB-Chlef	Co-supervisor

Scholar Year 2018-2019

This work is dedicated to my parents SOUDANI Mbeirick & EBIDE Beiba, and my wife KHADIJA Alouch for their incessant support.

This is dedicated to three influential persons in my life:

My mom and dad for their love, prayers and encouragement;

My brothers and my sisters and my family;

My Best friends B,Omar, Hocine Boukortt, B.G.N.Muthanna.

Thank you all

SOUDANI MOHAMED

Aknowledgement

I would like to express my sincere gratitude to my supervisor, Dr. Khaled EL-MILOUDI for his constant guidance, encouragement and support throughout my graduate studies program, and invaluable comments throughout the PhD period and preparation of this thesis.

I would like to use this opportunity to express my sincere thanks and appreciation to my co-supervisor Dr. Mohammed HADJ MELIANI. I am eternally grateful for everything you've taught me.

I would also like to extend my sincere appreciation to the Chair person Pr. Labbaci Abdallah and the members of examining committee Pr Željko Božić, Dr.: Chahinez Fares, Dr. Khadraoui Abdelkader, for giving me the honor and to agree to review this work and evaluate the contents of this doctoral thesis.

I also wish to thank Pr. Mohammed BENAROUS for accepting the invitation to be member of my jury examining committee.

I would like to thank all my teachers and colleagues from the Laboratory of Theoretical Physics and Materials Physics.

I would like to express my gratitude to Pr. Zitouni Azari, Dr. Djamel Meziani from the Laboratory of Biomechanics, Polymer and Structures Mechanics Metz-France for their vital hands-on experience and for facilitating the testing requirements.

I wish to acknowledge a scholarship, granted by the faculty of exact sciences and computer science which enabled me to do the work without financial burden.

I am grateful to my friends and colleagues at the University of Hassiba Benbouali of Chlef and The last, but certainly not the least, I wish to express my special thanks to my mum, who has constantly supported me unconditionally with her understanding, patience, encouragement and unwavering love. She maintained the belief that initiating and completing a PhD was my natural path to travel.

Research objectives

Research objectives

One of the important thoughts came to mind after experience in running projects of asset assessment, failure analysis case studies and materials research activities, is the proposal on creating a scientific network studying the significance of sour environment on gas Industry with and without the presence of green inhibitors. This proposal is aimed to establish a data base account and information resources describing the situation of the existing components as well as knowing their performance in environment contains H_2S , HCl , and H_2SO_4 above the designed with the inhibitors environment.

The overall objective of this research was site from the following topics.

- ✓ Process the protective thin film with inhibitor effect or by combination between inhibitor ions and metallic surface ;
- ✓ Process the degradation of the properties mechanical steel API 5L X52 in acid media;
- ✓ Process the efficiency the green inhibitors corrosion on the degradation of the Properties mechanical steel API 5L X52 and X65 in acid media;

Abstract

The degradation of metal structures in pipelines can caused accidents. Some studies and research, indicate in the field oil and gas industry, that the effects of acidic chemical cleaning solution to an important role in the process of internal corrosion. In this context we performed an inspection of a corroded gas pipe by metallographic analyzes. Then we studied the mechanical behavior of the pipe in the presence and absence of green corrosion inhibitors (Ruta Chalepensis " FIDJILE ") and synthetic. Two pipe grades were studies API X52 and API X65 mechanical tests were performed by Charpy test, Drop weight test, three point bending test and tensile test.

Keywords: *corrosion, green inhibitors, failure, fracture mechanics, pipelines.*

Résumé:

La dégradation des structures métalliques des pipelines, peut causer des accidents graves. Certaines études et recherches, indiquent dans le domaine industrie pétrolière et gazière, que les effets de la solution acides de nettoyage chimique à un important rôle dans le processus de la corrosion interne. Dans ce contexte nous avons effectué une inspection d'une pipe de gaz corrodé par des analyses métallographiques. Puis nous avons étudié le comportement mécanique du pipe en présence et en absence d'inhibiteurs de corrosion vert (Ruta Chalepensis " FIDJILE") et synthétique. Deux nuances de pipe ont été études API X52 et API X 65 des essais mécaniques ont été réalisé par des tests essais de Charpy, essais de Drop weight, essais de flexion à trois points et traction.

Mots-clés: *corrosion, inhibiteurs verts, rupture, mécanique de la rupture, pipelines.*

الملخص:

يمكن أن يؤدي تدهور الهياكل المعدنية في خطوط الأنابيب إلى وقوع حوادث خطيرة. بعض الدراسات والبحوث، تشير في مجال صناعة النفط والغاز، أن آثار محلول التنظيف الكيميائي الحمضي له دور مهم في عملية التآكل الداخلي. في هذا السياق، أجرينا فحصاً لأنبوب غاز متآكل من خلال تحاليل فحص المعادن. ثم قمنا بدراسة الخواص الميكانيكية للأنبوب في وجود وغياب مثبطات التآكل الخضراء (Ruta Chalepensis " FIDJILE ") والتركيبية. يتم تقييم الخواص الميكانيكية بواسطة اختبار Charpy و اختبار Tensil test. اختبار Three point و اختبار Drop weight

الكلمات المفتاحية: التآكل، مثبطات خضراء، الفشل، ميكانيكا الكسر، خطوط الأنابيب.

Table of Contents

I.1.GENERAL INTRODUCTION.....	1
Chapter . I	
I.1. INTRODUCTION	4
I.2.ALGERIA OIL AND GAS RESERVES.....	6
I.3. NATURAL GAS IN ALGERIA.....	8
I.4. STATISTICAL ANALYSIS OF PAST PIPELINES ACCIDENTS IN ALGERIA.....	9
I.5 LEAKS OR EMISSIONS OF GAS FROM PIPELINES	11
I.6.EXPERTISE OF PIPE LINE	12
I.6.1. INSPECTION INTERVENTION 2004:	12
I.6.2. INSPECTION INTERVENTION 2009:	13
I.7. FAILURE OF PIPELINES	14
I.7.1. INTERNAL SERVICE PRESSURE	15
I.7.2. MECHANICAL DAMAGE OF PIPELINES.....	15
I.7.3..EXTERNAL CORROSION.....	16
I.7.4..INTERNAL CORROSION.....	16
I.7.4.1. INTERNAL CORROSION BY CARBON DIOXIDE (CO ₂)	17
I.7.4.2. INTERNAL CORROSION BY HYDROCHLORIC ACID (HCl)	17
I.7.4.3. INTERNAL CORROSION BY SULFURIC ACID (H ₂ SO ₄)	17
I.7.4.4 INTERNAL CORROSION BY HYDROGEN SULFIDE (H ₂ S)	18
I.7.4.5. INTERNAL CORROSION REACTIONS	18
I.8. PREVENTION AND PROTECTION OF PIPELINES FROM CORROSION.....	18
I.8.1 FROM EXTERNAL CORROSION:.....	18
I.8.1.1.CATHODIC AND ANODIC PROTECTION.....	18
I.81.2. COATING PROTECTION.....	19
I.8.2. FROM INTERNAL CORROSION	20
I.8.2.1. CLEANING PIGS PROCESS	20
I.8.2.2. CORROSION INHIBITORS	21
I.9. CONCLUSION.....	23
REFERENCES CH.I.....	24
Chapter . II	
II.1 INTRODUCTION	26
II.2. CORROSION INHIBITORS	26
II.3. ACTION MECHANISM OF CORROSION INHIBITORS.....	26

Table of Contents

II.4. ELECTRODE REACTIONS OF CORROSION INHIBITORS.....	27
II.4. 1 ANODIC OR CATHODIC PROCESS OF INHIBITORS	27
II.4.2. ADSORPTION INHIBITORS	28
II.4.2.1. PHYSICAL ADSORPTION.....	29
II.4.2.2. CHEMICAL ADSORPTION	29
II.5. ORGANIC INHIBITORS	29
II.6. STEEL SURFACE ADSORPTION	31
II.7. ROLE OF GREEN CORROSION INHIBITORS.....	32
II.7.1 EFFECT OF CORROSION INHIBITORS	32
II.7.2.EFFECT OF CORROSION INHIBITORS ON MECHANICAL PROPERTIES ..	33
II.8. CONCLUSION	33
REFERENCES CH.II. ..	34

Chapter. III

III.1. INTRODUCTION.....	38
III.2. PRESENTATION OF API 5L X52 AND X65 STEEL GRADES.....	38
III.2.1. API 5L X52 STEEL GRADE	38
III.2.2. CHEMICAL COMPOSITION OF X52.....	39
III.2.3.MICROSTRUCTURE ANALYSIS OF THE API 5L X52 STEEL	39
III.2.4. API 5L X65 STEEL GRADE	41
III.3. CHARPY MECHANICAL TEST	43
III.3.1. OBJECTIVES OF THE CHARPY TEST.....	44
III.3.2. CHARPY MECHANICAL TEST MACHINE.....	44
III.3.3. PRINCIPLES OF CHARPY MECHANICAL TEST.....	45
III.3.4. CHARPY TEST SPECIMENS	46
III. 4. DROP-WEIGHT TEST.....	48
III. 4. 1. DROP-WEIGHT TEST PRINCIPLE	48
III. 4.2. DROP-WEIGHT TEST MACHINE.....	49
III. 4. 3. IMPACTORS OF DROP-WEIGHT TEST	50
III.5.THREE POINT BENDING TEST.....	51
III. 5. 1. THREE POINT TEST MACHINE.....	51
III. 5. 2. THREE POINT BENDING TEST SPECIMENS.....	52
III. 5. 3. MECHANICAL PROPERTIES MEASURED BY 3-POINT BENDING TEST	53

Table of Contents

III. 6. TENSILE TEST	54
III. 6. 1. THE TENSILE TEST MACHINE.....	54
III. 6. 2. TENSILE TESTING SPECIMENS	55
III. 6. 3. MECHANICAL PROPERTIES MEASURED BY TENSILE TEST	57
III.7.THE PREPARATION METHOD OF THE GREEN CORROSION INHIBITOR.....	58
III.7.1. PRESENTATION OF THE PLANT	58
III.7.2. EXTRACTION METHODOLOGY	58
III.7.3.THE PREPARATION OF THE TESTING MEDIA.....	59
REFERENCES CH.II.	60

Chapter. IV

IV.1. INTRODUCTION	62
IV.2. ANALYSIS OF CORROSION CAUSES	62
VI.2.1. VISUAL OBSERVATIONS	63
IV.2.2. OPTICAL MICROSCOPE EXAMINATION.....	64
IV.2.2.1. EXTERNAL SURFACE	64
IV.2.2.2. INTERNAL SURFACE	65
IV.2.3. SCANNING ELECTRON MICROSCOPY EXAMINATION.....	67
IV.2.4. CHEMICAL ANALYSIS BY XRD.....	68
IV.2.5. CORROSIVE FLUID	69
IV.2.6.METAL WALL THICKNESS REDUCTION	69
IV.2.7.FINAL RUPTURE.....	69
IV.2 .8. THE CORROSIVE EFFECT OF HCl.....	70
IV.2.9. CORROSION RATE	70
IV.2.10. RECOMMENDATIONS	71
IV.3. MECHANICAL TESTS	71
IV. 3. 1. CHARPY TEST (DYNAMIC STUDY).....	71
IV.3.2. CHARPY TEST OF API 5L X52 STEEL IN ACIDIC MEDIA	73
IV.3.3. CHARPY TEST OF API 5L X52 STEEL IN THE PRESENCE OF GREEN INHIBITOR.....	74
IV.3. 4. INFLUENCE OF GREEN INHIBITORS ON THE FRACTURE TOUGHNESS OF API 5L X52 STEEL	75

Table of Contents

IV.3.5. EFFICIENCY OF THE CONCENTRATION OF GREEN INHIBITOR ON THE X65 BY CHARPY TEST	77
IV.3. 6. THE TEMPERATURE EFFECT ON MECHANICAL PROPERTIES OF API 5L STEEL.....	79
IV.3.6.1. INFLUENCE OF IMMERSION TIME IN HCl/5 % GREEN INHIBITOR ON DYNAMIC FRACTURE TOUGHNESS OF API 5L X52 STEEL AT 80°C.....	80
IV.6.3.2. INFLUENCE OF IMMERSION TIME IN HCl/5 % GREEN INHIBITOR ON DYNAMIC FRACTURE TOUGHNESS OF API 5L X65 STEEL AT 80°C.....	82
IV.3.6.3. EVOLUTION OF THE FRACTURE TOUGHNESS J_c WITH IMMERSION TIME OF THE API 5L X65 AND X52 STEEL.....	84
IV.3.7. THE ACTION MECHANISM OF THE GREEN CORROSION INHIBITOR ..	85
IV.4. DROP WEIGHT TEST APPARATUS AND SPECIMEN GEOMETRY.....	85
IV.4.1. INFLUENCE OF GREEN INHIBITORS ON FRACTURE ENERGY OF THE X52 AND X65 STEEL BY THE DROP WEIGHT TEST	86
IV.4.2. IMMERSION TIME EFFECT OF THE GREEN INHIBITORS ON FRACTURE ENERGY OF THE X52 AND X65 STEEL BY THE DROP WEIGHT TEST ...	88
IV.5. THREE-POINT BENDING TEST	90
IV.5.1. SPECIMENS OF STATIC THREE POINT BENDING TEST	90
IV.5.2. INFLUENCE OF GREEN INHIBITORS ON MECHANICAL PROPERTIES OF API 5L X52 STEEL BY THREE-POINT BENDING TEST.	90
IV.6. INFLUENCE OF SYNTETIC AND GREEN INHIBITORS ON API 5L X52 BY TENSILE TESTS IN HCl ACID SOLUTIONS	92
IV.7. CONCLUSION.....	96
REFERENCES CH.IV.	97
GENERAL CONCLUSION	100
ANNEXE.....	101

List of figures

Chapter .I

Figure. I.1: Photography of pipeline.....	4
Figure. I.2. Algeria Oil /Gas network and the point's source of Oil and Gas in Algeria.....	5
Figure .I.3. Oil production in Algeria from 1998 to 2017 (in 1,000 barrels per day).....	6
Figure. I.4. Natural gas production in Algeria from 1998 to 2017.....	8
Figure.I.5 Natural gas pipeline explosion in Mohammadia-Algeria.....	9
Figure .I.6. (a) Oil pipes explosion from Hassi-Messaoud, (b) LPG pipeline was exposed to transport liquefied petroleum gas from HASSI R'mel to Arzew	10
Figure .I.7. Condensate Leak on the NZ1 28, (b) Vanishing point, (c) Repair of the leak by a Clamp.....	10
Figure. I.8. Explosion pipelines in Hassi Messaoud region.....	11
Figure. I.9. Oil pipeline leakage damage.....	12
Figure.I.10. Corrosion in Oil and Gas industry.	14
Figure.I.11. Ductile rupture of a pipe of average diameter under the effect of internal Pressure.....	15
Figure.I.12.Crack in pipelines.	15
Figure.I.13. External corrosion in pipes.....	16
Figure.I.14.Internal corrosion of pipelines.....	17
FigureI.15. Anodic / cathodic protection of pipeline.....	19
FigureI.16. Coating of outside surface of pipeline with coal tar + epoxy.....	19
Figure. I.17. Internal cleaning of pipelines and extracted dirt after cleaning process.....	20
Figure.I.18. Corroded pipe before and after the cleaning process.....	21
Figure.I.19.Injection point of the corrosion inhibitor.....	22

Chapter .II

Figure.II.1: Schematic corrosion inhibitors of the anodic reactions.....	27
Figure.II.2: Schematic corrosion inhibitors of the cathodic reactions.....	27
Figure.II.3. Schematic corrosion inhibitors of the mixed inhibitors reactions.....	28
Figure.II.4. Schematic of the adsorption modes of inhibitor molecules on a metal surface.....	28
Figure.II.5. Organic inhibitors molecule.....	30
Figure.II.6. Molecular structure of some organic inhibitors.....	31

List of figures

Chapter .III

Figure. III. 1. API 5L X52 steel pipe scheme.....	38
Figure. III.2: Microstructure of samples of X52 steel in the longitudinal direction.....	40
Figure. III. 3: Microstructure of samples of X52 steel. (left) the surface in the circumferential direction (right) the surface in the thickness direction.....	40
Figure. III. 4: X52 steel inclusions: globular oxides (left) and manganese sulfide (right) visible on the polished surface.	41
Figure III.5. Microstructure of the pipe section of API 5L X65 steel.....	42
Figure. III.6. An example of instrumented Charpy test in ductile-to-brittle transition regime..	43
Figure. III.7. Instrumented Charpy testing machine RKP 450.....	45
Figure. III.8 Description of the Charpy mechanical test.....	46
Figure. III.9 Scheme of Charpy impact test specimen.....	47
Figure. III.10 Charpy test specimen preparation.....	47
Figure. III.11. Simple illustration of the drop-weight test machine.....	48
Figure. III.12. Drop weight test machine.....	49
Figure. III.13. Schematic of the drop weight test.....	50
Figure. III. 14. Three-point bending machine, PW 310 universal machine.....	52
Figure. III.15. Scheme of the three point test specimens.....	53
Figure. III.16. Load-displacement plot from a bending test of a specimen of API 5L X52 steel.....	54
Figure III.17. Electric Static Traction Machine Zwick/Roell Z250.....	55
Figure.III.18. The specimen Geometry For Tensile Testing.....	56
Figure III.19. The rectangular sample (left) and the tensile specimens (right)	56
Figure III.20: Stress-strain curve of a high strength steel.....	57
Figure. II.21. Green and dried plant leaves process.....	58
Figure. III 22. Acid grade 37% HC, Heating operation of the dried aloe plant leaves.....	59

Chapter .IV

Figure IV.1. Schematic view of process diagram and the rupture location at the third stage...63	63
Figure IV. 2. General view of the failed gas pipe; (a) External surface and (b) internal surfaces.....	63
FigureIV. 3. Macroscopic observation on the external pipe surface (50X magnification).....	64

List of figures

Figure IV.4. Macroscopic observation on the internal pipe surface showing pitting corrosion (50X a magnification).....	65
Figure IV. 5. General view of the crack on the internal surface of the pipe (100X magnification)	65
Figure IV. 6. Close view at the internal surface of the pipe shows the crack tip and the preferable path for the crack growth (150X magnification)	66
Figure IV. 7. Thickness difference between slightly corroded and ruptured area (150X magnification)	66
Figure IV.8. SEM image on the fracture surface.....	67
Figure IV. 9. XRD analysis of corrosion product.....	68
Figure IV.10. Typical load-displacement curve and the determination of the energy absorbed by the specimen	72
Figure IV. 11. Fractured V-notched Charpy test specimen.....	73
Figure. IV. 12. Variation of the fracture work U_C vs. HCl acid concentration.....	74
Figure. IV.13. Fracture Energy as a function of immersion time for different concentrations of the corrosion inhibitor.....	75
Figure IV. 14. Load vs. displacement obtained by instrumented Charpy impact test after immersion in hydrochloric acid solution with and without green inhibitor.....	76
Figure. IV.15 Influence of green inhibitor concentration on dynamic fracture toughness of API 5L X52 steel after immersion in hydrochloric acid solution.....	77
Figure IV.16.Effect of inhibitor concentration on load-displacement curves of API 5L X65 steel.	78
Figure. IV.17 Influence of green inhibitor concentration on dynamic fracture toughness of API 5L X65 steel after immersion in hydrochloric acid solution.....	79
Figure.IV.18 Charpy V energy curve as a function of temperature for API 5L X65 steel.....	80
Figure IV. 19 Charpy impact test load-displacement curves after immersion in 1M HCl acid and 5% green inhibitor concentration at 80°C.....	81
Figure IV.20: Fracture toughness vs. immersion time in 1M HCl with 5% (v/v) green inhibitor at 80°C of API 5L X52 steel.....	82
Figure IV.21: Load-displacement curves corresponding to the different immersion solutions and immersion times of API 5L X65 steel.....	83
Figure IV.22: Fracture toughness vs. immersion time in 1M HCl with 5% (v/v) green inhibitor at 80°C of API 5L X65 steel.....	84
Figure IV. 23. Specimen of X52 and X65 steel during drop weight test.....	86
Figure. IV.24. Specimens after the drop weight test.....	86
Figure. IV.25. Absorbed energy as function of the concentration of green inhibitor in 1 M HCl API 5L X52 steel with different immersion time.....	87
Figure. IV.26. Absorbed energy as function of the concentration of green inhibitor in 1 M HCl API 5L X65 steel with different immersion time.....	87
Figure. IV.27. Absorbed energy by X52 steel as function of immersion time in 1 M HCl with different green inhibitor concentration.....	89
Figure. IV.28. Absorbed energy by X65 steel as function of immersion time in 1 M HCl with different green inhibitor concentration.....	89

List of figures

Figure IV. 29. Three point bending test, specimen under test (left), specimen after break (right).	90
Figure IV. 30. Three point bending test load- displacement curves of the specimens immersed in as indicated solutions.....	91
Figure IV. 31. The tensile specimens (a), before and (b), after tensile tests.....	92
Figure IV. 32. Stress-strain curves of API 5L X52 steel after immersion in different solutions, 1.2 M/HCl, 1.2 M HCl+ 30% Green and 1.2M HCl+ 30% synthetic inhibitors.....	93

List of tables

Chapter .I

Table I.1. Natural gas compositions from Hassi R'mel and Skikda-Algeria region.....	8
---	---

Chapter .III

Table III.1 Chemical composition of API 5L X52 steel.	39
Table III.2. Mechanical properties of API5L X52 steel.....	39
Table III.3. Summary of grain sizes in different orientations.	41
Table III.4. Chemical composition of API5L X65 steel.....	42
Table III.5. Mechanical properties of API5L X65 steel.....	42
Table III-6: The Specimen Dimensions.	56

Chapter IV

Table. IV.1. Impact testing Results.....	77
Table IV.2. Mechanical properties of the API X65 immersed on the HCl compared to the different concentration (Bb is taken as 80mm ²).....	78
Table. IV. 3 Mechanical Properties calculated for API 5L X52 steel immersed in acidic media and in the presence of 5% v/v green inhibitor (Bb is taken as 80mm ²).....	81
Table. IV. 4 Mechanical Properties calculated for API 5L X65 steel immersed in acidic media and in the presence of 5% v/v green inhibitor (Bb is taken as 80mm ²).....	83
Table. IV. 5. Evolution of the maximum load and the displacement as a function the green inhibitor concentration.....	91
Table IV.6. Tensile properties of steel API 5L X52 after immersion in different solutions from 7 days.....	93
Table IV.7. Cumulated results of the experimental test.....	94

Nomenclature

LNG	Line natural gas
LPG	Liquefied petroleum gas
GZ1 40	Hassi R'mel to Arzew
SEM	Scanning electron microscope
J_I	Fracture toughness
P_c	Critical load
U_c	Fracture energy
XRD	X-ray diffraction
API 5L	American petroleum institute specification
X52	Minimum yield stress of 52000 psi (pound force per square inch)
X65	Minimum yield stress of 65000 psi (pound force per square inch)
X70	Minimum yield stress of 70000 psi (pound force per square inch)

General Introduction

General Introduction

It is well known that, oil and gas sector is the backbone of Algeria economy accounting for up to 85 per cent of total exports. According to the 2018 annual statistical bulletin of OPEC, the country's proven reserves are about 12,200 million barrels for crude oil and 4,500 billion cubic meters for natural gas. The crude oil production reached 1,039 million barrels/day and the marketed production of natural gas reached 94,778 billion cubic meters.

The liquids and gaseous hydrocarbons transport network consists of a set of pipelines, pumping stations, compressor stations, storage yards, transporting effluents from production fields, a storage center or dispatching, to the industrial centers of processing and liquefaction, export and supply of the national market. For that, the pipeline network is a vital link in the hydrocarbons chain. It ensures the transportation, for the benefit of the users, of all hydrocarbon production from upstream to downstream. It also feeds the domestic market, LNG and LPG separation complexes and crude oil and Condensate refineries. The gas surplus is intended for export via GEM, GPDF and MEDGAZ and the surplus in crude oil and Condensate is intended for export via the ports of Arzew, Bethioua, Béjaïa and Skikda.

In 2018, more than 20,927 km length pipelines traverse Algeria. It consists mainly of 21 oil pipelines with a length of 9,946 km and 18 gas pipelines with a length of 10,981 km. They connect 83 pumping and compression stations, 127 crude oil and condensate storage tanks, 02 dispatching centers, 12 crude oil and condensate loading stations and 05 crude oil offshore loading stations. In order to fulfill this mission, the pipeline network design meets economic optimization criteria for operation at lower cost. However, the safety of people and goods and the respect of environment are of great concern. According to the 2018 annual pipeline safety report of the American Petroleum Institute (API), the USA operators have invested financial resources to ensure the reliability of the network, including spending over \$2.2 billion in 2014 to evaluate, inspect and maintain pipelines moving towards the goal of zero incidents.

According to the same report, equipment failure is the most frequent cause of liquids pipeline incidents. Over the 2013-2017 period, equipment failure represented 45% of incidents, corrosion failure 19% and incorrect operation 15% of incidents. Material pipe/weld failures include cracking, a primary source of large volume releases, but represented only 7% of incidents over the last 5 years.

At the first time, a study was carried out to investigate the probable cause or events that might have led to the failure of natural gas pipes, API 5L X52 carbon steel. The investigation was performed by visual inspection of failed pipes, and by the metallurgical analysis of the

General Introduction

corroded surface of the pipe. Investigation from the relevant pipes data suggests that the corrosion failure was the first to fail, and that is kind of failure cause serious losses in the pipe thickness. The corroded surfaces analysis showed the presence of different corrosion product and supports that the internal localized corrosion is influenced by carbon dioxide CO₂ and hydrogen sulfide H₂S content.

The use of synthetic inhibitors promotes the pipeline protection from the internal corrosion during gas transport or pipe cleaning hydrochloric acid (HCl), and sulfuric acid (H₂SO₄). These inhibitors are chemical compounds used to minimize the effect of corrosion by diminishing the rate of the chemical reactions involved. However, the environmental toxicity of synthetic corrosion inhibitors has prompted the use of ecofriendly corrosion inhibitors as they are biodegradable, non toxic and do not contain heavy metals.

In the previous investigation on the Ruta Chalepensis plant extract (known as “FIDJEL”) performed by our laboratory (LPTPM), has showed good corrosion inhibitor efficiency (about 84%) in the hydrochloric acid solutions commonly used in cleaning operations.

In this study, we focused our investigation on the mechanical properties of the API X52 and API X62, exposed to hydrochloric acid solution with the presence of Ruta Chalepensis plant extract as green inhibitor and the synthetic inhibitor. The mechanical properties are evaluated by Charpy test, drop weight test, three point bending test and tensile test.

The manuscript is divided into four chapters. The first one is an introduction on Algeria oil and gas production and reserves, the transport network, catastrophic incidents of pipeline failures and their probable causes, prevention and protection of steel pipelines methodology.

Chapter two deals with fundamentals of corrosion inhibitors: classification, mechanism of action, adsorption mechanism and the effect of green inhibitors on corrosion.

Chapter three presents the materials and methods used in this study. Chemical and physical characterization of API 5L X52 and X65 grade steels are given. Mechanical tests are described particularly Charpy test, drop weight test, three point bending test and tensile test. The preparation of the testing media is described as well as the preparation of Ruta Chalepensis plant extract, hydrochloric acid solution and their mixtures.

General Introduction

Results and discussion section is presented in Chapter four. The mechanical properties of the reference steel, the steel subjected to hydrochloric acid solution and the steel subjected to hydrochloric acid in the presence of the green corrosion inhibitor are compared and discussed.

Chapter I
Pipeline Gas/Oil
Transportation

I.1. INTRODUCTION

Pipelines play an extremely important role in the world as a means of transporting oil and gas from fields and through all stages of processing, over long distances from their sources to ultimate consumers [1]. The general public is not aware of the number of pipelines that are continually in service as a primary means of transportation of oil and gas through land, sea, and rivers to reserves or treatment station. Figure .I.1 shows a photography of a steel pipelines.



Fig. I.1: Photography of pipeline [2]

Algeria, is the largest In terms of area in Africa, is one of the biggest producers of hydrocarbons with Libya and Nigeria. Its entire economy was built around such resources, and its exports are mainly oil and natural gas. In the period of 1960s and 1970s the major capital investments is in these industries, it quickly grew into a major supplier of these energy products to Europe and other markets, including the United States.[3]

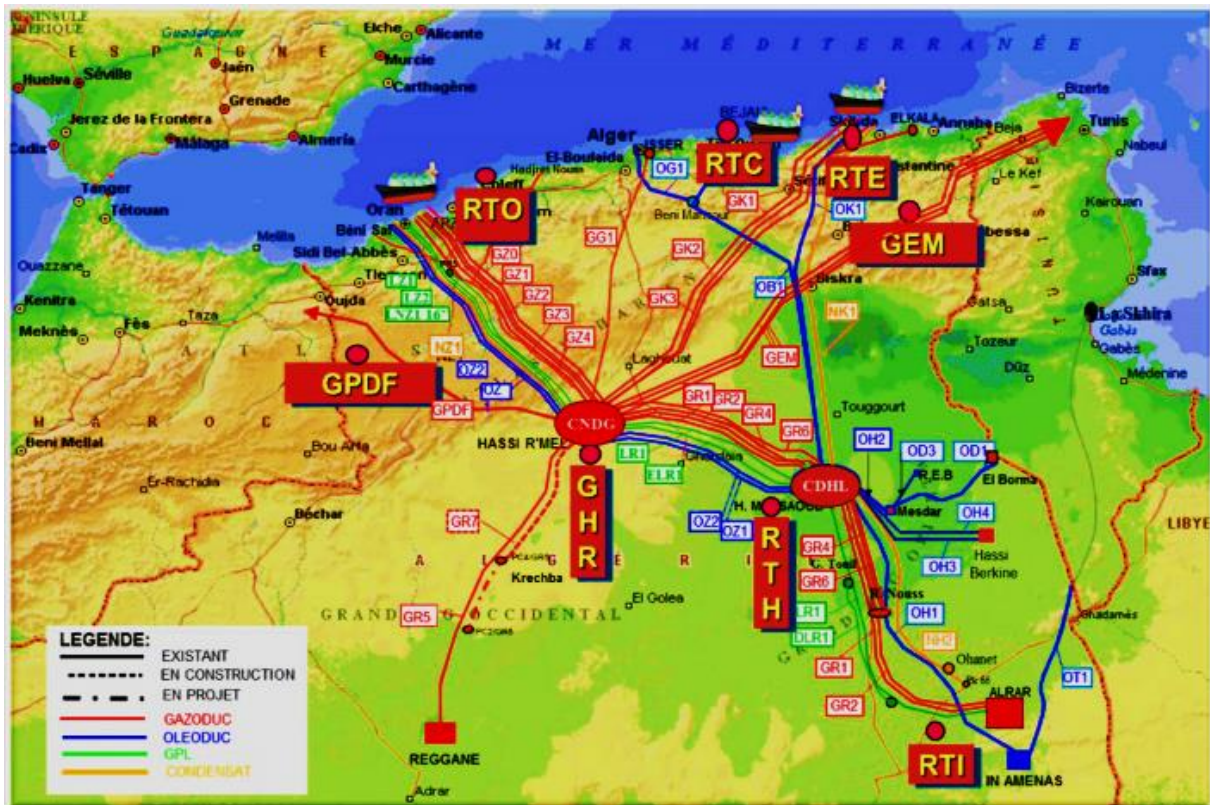


Figure. I.2. Algeria Oil /Gas network and the point's source of Oil and Gas in Algeria [4].

In Algeria today, the length of the pipeline network is estimated around the **20927 km**, based on the data from SONATRACH June 2018.

The distribution of the network in Algeria as noted below.

- ✓ 21 Oil pipelines with a length of 9946 km, with a Transport Capacity of 247,553 million tons / year, [4].
- ✓ 18 Gas pipelines with a total length of, 10,981 km, with a Transport Capacity of 195,121 Billion Sm³ / year, [4].
- ✓ 83 Pumping and compression stations, [4].
- ✓ 127 Crude oil and condensate storage bins, [4].
- ✓ 02 Liquid and Gas Dispatch Centers, [4].
- ✓ 12 Crude oil Shipping stations and Condensate dockside stations and 05 crude oil loading stations on the high seas (02 in Arzew, 02 in Skikda and 01 in Bejaia) of SPM type (Single Point Mooring), located at the terminals sailors in the various ports (Arzew, Bethioua, Bejaia and Skikda)[4].

I.2.ALGERIA OIL AND GAS RESERVES

Algeria has a large natural gas industry as a major producer in the world. Hassi R'Mel was discovered in 1956 and entered into production in 1961, supplying gas mainly to LNG export facilities and also to domestic users. In 1976, the massive field was estimated to contain 2,000 bcm of gas reserves, over half of Algeria's known total reserves at the 1978. Sonatrach already had future commitments for gas deliveries of rising to over 70 bcm per year by the mid-1980s. After that, the aggressive of the exports was increased to over 100 bcm per year through the end of the (2001). [3] Algeria's crude oil production was reported at 1039.000 Barrel/Day th in Jun 2018. This records an increase from the previous number of 1035.000 Barrel/Day [5]. Figure.I.3. shows the static of oil production from Jul 2017 to Jun 2018 in Algeria.

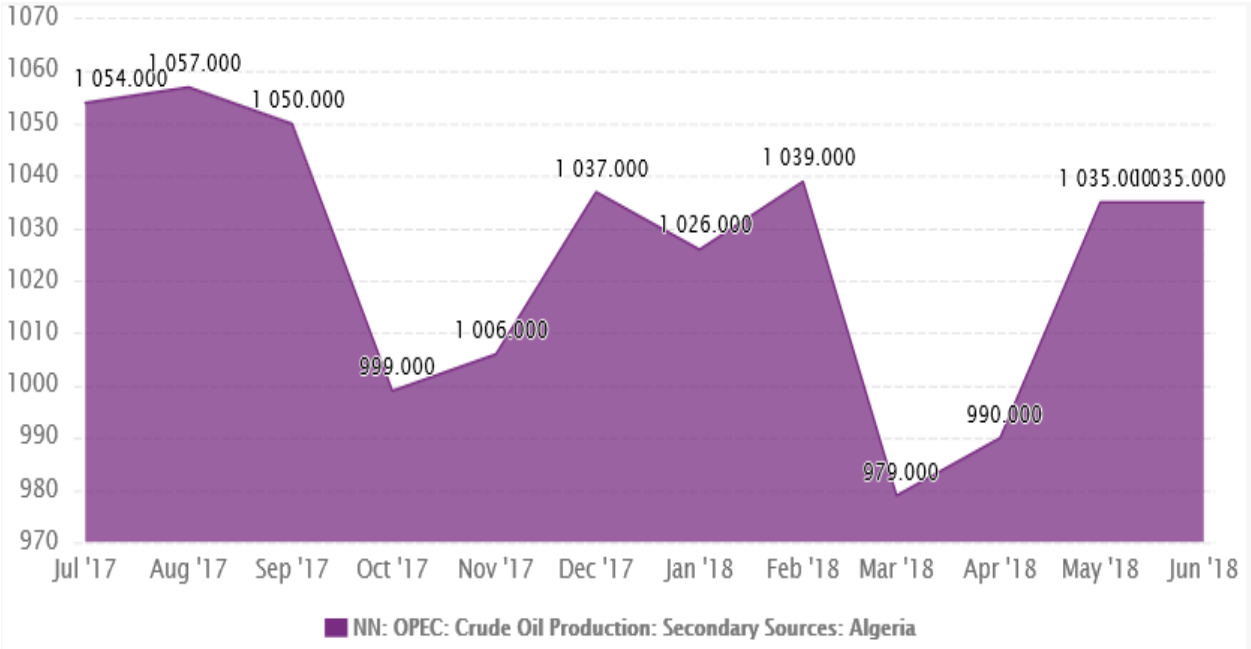


Figure .I.3. Oil production in Algeria from Jul 2017 to Jun 2018 [5]

In 2011, Algeria's estimated crude oil exports were 750,000 barrels per day (Bbl/d). The largest portion of which—around 40%—went to North America, mainly the United States. [3]. The Organization for Economic Cooperation and Development (OECD) countries import around 30% of Algeria's oil exports. [6]. Most of Algeria's proven oil and gas reserves are located in the eastern part of the Sahara. Around 67% of reserves are in the provinces of Oued Mya and Hassi Messaoud, with two giant fields: Hassi R'mel (gas) and Hassi Messaoud (oil); the basin

of Illizi comes in third position with 14% of the reserves, followed by the basins of Rhourde Nouss (9%), Ahnet Timimoun (4%), and Hassi Berkine (4%).[3]

The province of Hassi Messaoud-Dahar alone has 71% of Algeria's oil reserves, while the province of Oued Mya has corresponding to a mainly Mesozoic basin, contains mainly 50% of the gas reserves and only 6% of the oil reserves.

The basin of Illizi has 15% of oil and 14% of gas; the provinces of Rhourde Nouss and Berkine have 19% of gas, mostly in Rhourde Nouss, and 8% of oil. Finally, the basin of Ahnet-Timimoun is suspected of containing gas only (13%). [3] Terms of production, 75% of Algeria's hydrocarbon output comes from the fields of Hassi Messaoud and the Hassi R'Mel. Sixty-four percent of the total primary production volume is natural gas, 26% oil, 6% condensates and 4% LPG. In 2010, 72% of the output volume was produced by Sonatrach and the rest by foreign companies. [7] LNG is produced by the two old plants of Arzew and Skikda; two new ones are being built now.

The Arzew plant in the northwest of Algeria, a production capacity of around 53 Bcf/y of LNG, was the first of its kind in the world when it opened in 1964. It was closed in February 2011 after becoming too dangerous to operate. [3]. It is now being replaced by a new LNG plant with a mega-capacity of 218 Bcf/y; it is supplied by gas from the Gassi Touil fields and was open in 2013. The LNG plant and export terminal of Skikda in the northeast of Algeria, which has been operating since 1972, also encountered problems when on January 19, 2004, an accidental explosion.

In another hand figure .I.4 shows the statistic Algeria of the total natural gas production from 2006 to 2017[8]. In 2017, natural gas production in Algeria amounted to around 94.8 billion cubic meters. Since the data are derived directly from metric tons of oil equivalent using an average conversion factor, they do not necessarily equate with gas volumes expressed in specific national terms.

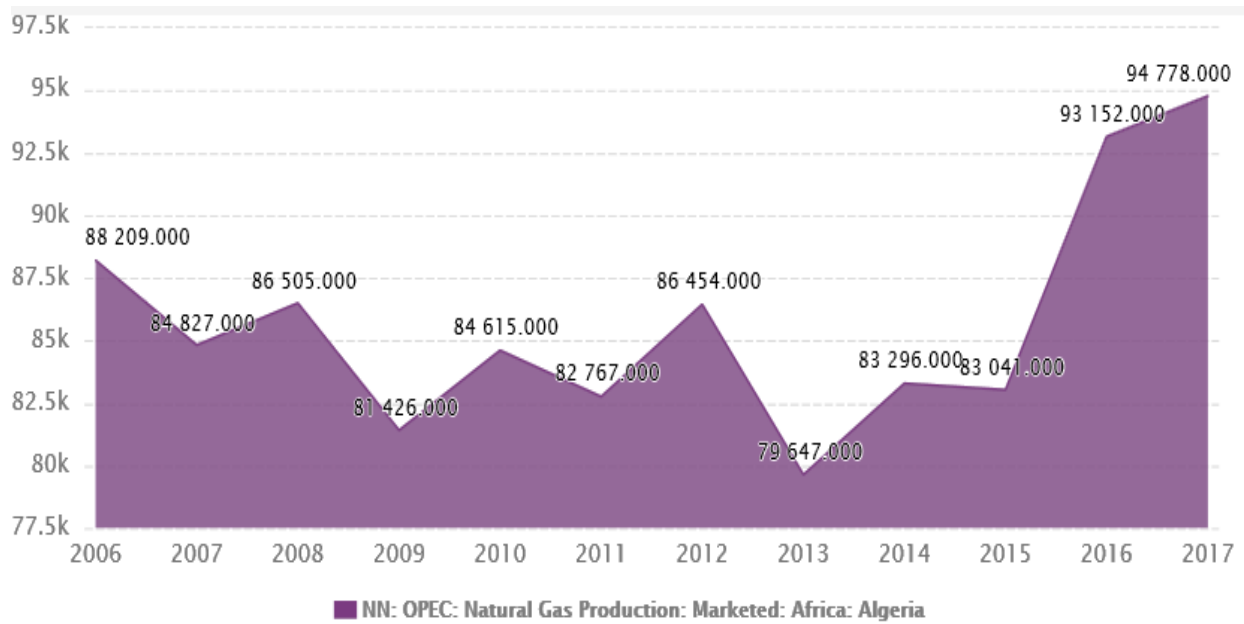


Figure. I.4. Natural gas production in Algeria from 2006 to 2017 (in billion cubic meters).[8]

I.3. NATURAL GAS IN ALGERIA

The compositions of the natural gas in Algeria contains some chemical component can play important role in the process of the internal corrosion. In the below table, we presented the chemical component from the Skikda and HassiR'mel region.

Table I.1. Natural gas compositions from HassiR'mel and Skikda-Algeria region. [9]

Chemical Composition	Skikda Algeria	HassiR'mel Algeria
Methane	82,27	83.7
Ethane	6,92	6.8
Propane	2,15	2.1
Butane	0,52	0.8
C ₅₊	0,13	0.4
Nitrogene	5,60	5.8
Hydrogen sulfide	Not available	Not available
Carbon dioxide	0,18	0.2

I.4. STATISTICAL ANALYSIS OF PAST PIPELINES ACCIDENTS IN ALGERIA

The accident temporarily reduced LNG production by more than 70%. [3]. These historical pipeline failure incidents provide valuable information about the leading causes for pipeline failures, typical failure modes, failure rate in terms of per year per unit length, consequences of failures, etc. Such information will facilitate the development of effective pipeline integrity management programs and provide baseline statistics for the quantitative risk assessment of pipelines. [3]. the risk of these accidents is associated with the presence of dangerous substances at large quantities and under such conditions that an uncontrolled accident. The consequences of these latter are at various levels and may affect not only the industrial sites, but also people, environment and economy [8]. Every year, industrial accident causes a number of deaths, injuries and property losses due to petroleum refining operations. Industrial accident has become a threat to human safety such as the accidents of Skikda refinery in January 2004 and October 2005. Another accident has been in October 19, the 2006 at 07:10 a.m. The rupture of a major underground high-pressure natural gas pipeline in Mohammadia, Algeria resulted in 78 injuries. According to local media, the fire was spread over a radius of 210m leading to air pollution because of burning of 1.3 million cubic meters of natural gas; consequently, this incident caused damages to neighboring dwellings as well as to the people who live there.



Figure.I.5 Natural gas pipeline explosion in Mohammadia-Algeria. [9].

In 2007, another accident happens in Arzew. The pipeline was buried underground carrying gas at 51 bars with a flow rate of 1450000 m³/h from Hassi R'mel to Arzew. Aerial pictures of the scene showed sheared pipe after the explosion appeared to be a trench and crater, suggesting that there was a major release of gas before the explosion occurred [9]



Figure .I.6. (a) Oil pipes explosion from Hassi-Messaoud, (b) LPG pipeline was exposed to transport liquefied petroleum gas from HASSI R'mel to Arzew[9].

Following the heavy rains on Friday 11.09.2009 at Laghouat's region, a strong current was created in Oued M'zi, where an aerial LPG pipeline was exposed to transport liquefied petroleum gas from HASSI R'mel to Arzew under pressure of 25 bars, then this pipeline has sheared at two points, which resulted on 12 September 2009 at 00:10 a.m. a strong explosion accompanied by a fire and flames up to 50 m high. Another accident because of corrosion has been appeared in Algeria on May 09, 2011, around 2:00 p.m, an oily puddle appeared near the line of the LPG pipeline in the region of El Matmar-Relizane.

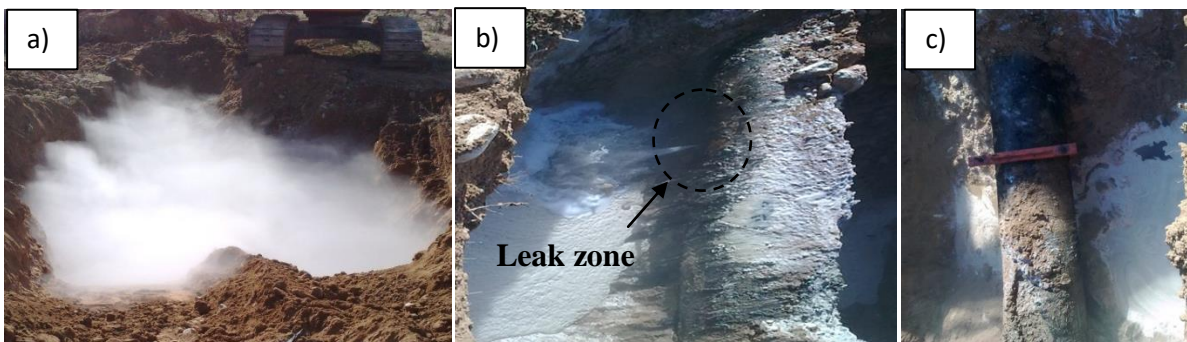


Figure .I.7. Condensate Leak on the NZ1 28, (b) Vanishing point, (c) Repair of the leak by a clamp. [9]

This pipeline was stopped at the time of incident because of a leak due to corrosion at 05:00 a.m. where the perforation has reached 0.5cm of diameter and the pressure at this point was 5 bars. Figure I.8. Shows the last accident, on Friday 11/08/2017 of oil pipeline in Hassi Messaoud region.



Figure. I.8. Explosion pipelines in Hassi Messaoud region. [9]

Besides that, Oil pollution accidents are nowadays become a common phenomenon and have caused ecological and social catastrophes. [10-11].

Petroleum refining unavoidably generates considerable volumes of oily sludge during oil production and processing activities. These, accidents statistics are important from the safety and reliability of the pipelines network. And is indicate of the impacts accidents on the success of the safety and security parameters [12].

I.5 LEAKS OR EMISSIONS OF GAS FROM PIPELINES

One another problem is noted in the line GZ1 40 "which connects Hassi R'mel to Arzew. This problem is the leaks or emissions of the gas from pipelines. Figure.I.7. Sonatrach uses a variety of methods for the detection of these leaks. One of these methods is the geothermal probes. The principle of using thermograph for the detection of leaks is as follows: gas escaping from pipe modifies thermal characteristics of the environment soil around this place when we have the leaks. In this following photo we present the leaks accident from this line "GZ1 40"



Figure. I.9 : Oil pipeline leakage damage [13]

I.6.EXPERTISE OF PIPE LINE

The detection and/or examination of pipelines is important, in order to detect the many problems that are exposed. Two inspections intervention are presented here of line connecting Hassi R'mel to Arzew the first inspection intervention in 2004 and the second was in 2009. These exhibited an advanced state of corrosion that caused an important loss of metal in different in this line. Some intervention by experts in the field of 40 inspections of the pipelines to see the state of this pipeline and take the actions required:

I.6.1. INSPECTION INTERVENTION 2004:

The report of this intervention has been drawn up defining both the state of location of the line and a plan for bringing this pipeline back into service. The defects detected were classified in three categories according to the priority

- ✓ The first priority: Some defects show important degradation of the nominal values condition of service line, in this cause it be must remove the places effected.
- ✓ The second Priority: Some defects need intervention immediate repairs.
- ✓ The third priority: Some defects need investigations.

The defects identified by the intelligent pig are as follows:

- 171306 external corrosion defects which account for 93.6% of all identified defects
- 11499 manufacturing defects of which 321 external and 11178 internal
- 111 single bumps, 15 bumps associated with the seam, 29 associated bumps loss of thickness and 4 bumps associated with both the weld, the wheel and the a loss of thickness.
- 34 metal objects.
- 1 eccentric housing tightened.

I.6.2. INSPECTION INTERVENTION 2009:

The second inspection intervention for a distance of 507 km connecting Hassi R'mel to Arzew. In this last inspection the intelligent pig was used. They can be used to the inspection of pipelines carrying gas or fluids on land or underwater and of diameter ranging from 6 to 56 inches (15 to 142 centimeters) [13].

These tools make it possible to detect the following anomalies on the pipes:

- ✓ Internal and external pitting of corrosion
- ✓ General corrosion on the pipe body
- ✓ Loss of metal near welds

These intelligent pigs are designed primarily to locate and size a metal loss greater than or equal to 10% of the thickness of the pipe.

This inspection intelligent pigs measures the thickness of the pipe wall using a technique ultrasound reflection time. Measurement using this technique is based on the interval between the reflection of the ultrasound returned by the surface of the inner wall (echo input) and that of the echo returned from the surface of the outer wall (echo of outer wall). One another technical geometric and instrumented piston leakage inspection of magnetic flux was carried out in 2009 with the aim of, [13].

- ✓ Record the restrictions and geometry faults of the pipeline and measure the dimensions
- ✓ Identify the location of pipe wall defects related to the loss of metal (internal or external corrosion, scratches, chips);
- ✓ Detect defects in circular welds;
- ✓ Detect non-welded pipe elements;

- ✓ Register building components and repair constructions of the pipe.
- ✓ Prepare the weld register for the linear part of the inspected section.

This detection process of the defect line gas connecting Hassi R'mel to Arzew was noted in three sections however, [13]

- ✚ First one section had noted 1877 defects (loss of metal) of depth up to 40.5% wt (thickness). Whose: 1540 internal and 337 external
- ✚ Sound section had noted 2686 defects (loss of metal) depth of up to 52.8% wt (thickness) between which: 1718 internal and 968 outside.
- ✚ Third section had noted 2113 defects (loss of metal) depth of up to 53.5% wt (thickness) between which 1472 Internal, and 657 external.

I.7. FAILURE OF PIPELINES

From the pipeline, the accident can be result of different metallurgical failure mechanisms including but not limited to manufacturing defects, third party damage, and corrosion. Understanding these failure mechanisms is critical to mitigating risk of future incidents and managing the future integrity of the pipeline. [13]. Out of all defects of pipeline systems the corrosion defects proportion-wise are the most significant. The general percentage distribution of all failures in the pipelines as like below noted [14].

- ✓ 34% by Mechanical fracture failure
- ✓ 15% Caused by external corrosion
- ✓ 51 % Caused by internal corrosion

Internal corrosion damage being termed as the highest cause of pipeline failures contributed 51% to overall failures. Figure. I.10 shown the static of the corrosion oil and gas industry.

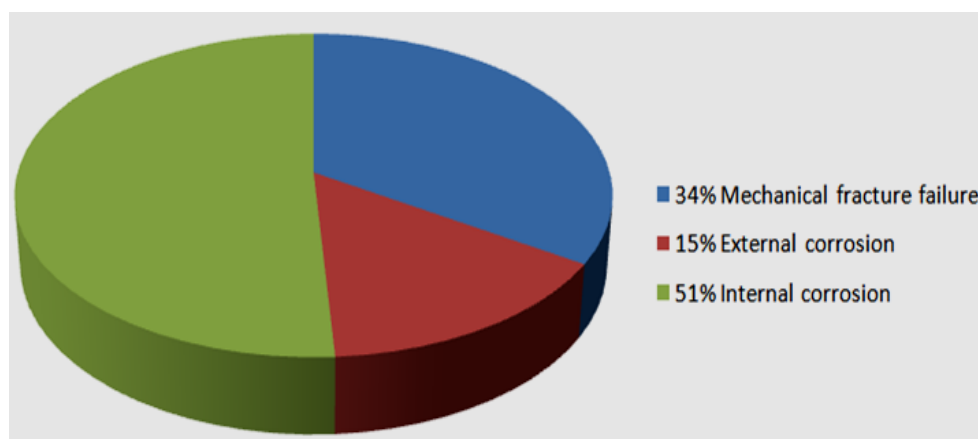


Figure.I.10. Corrosion in Oil and Gas industry.[14]

I.7.1. INTERNAL SERVICE PRESSURE

One another problem came from the internal service pressure, when the pipes can't supported the internal stress. This figure.I.11 shows that, in general, cracks propagate mainly in the longitudinal direction of the pipe, the rupture of which occurs in the same direction. Internal service pressure is usually the main cause of stress. [15]

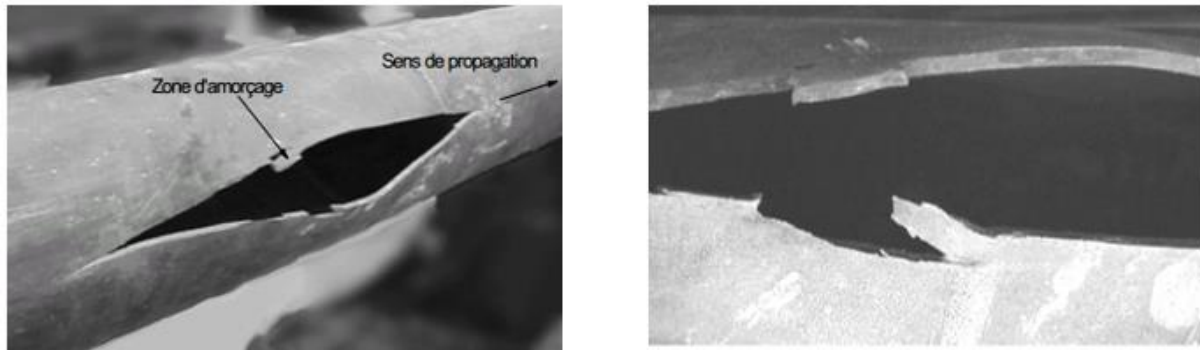


Figure.I.11. Ductile rupture of a pipe of average diameter under the effect of internal pressure. [15]

I.7.2. MECHANICAL DAMAGE OF PIPELINES

Mechanical damage of pipelines is one of some problems from pipelines. The damage came from the encroachment, which occurs when the pipe is struck by earthmoving equipment. Sometimes called a “combined defect” because it consists of both a geometry distortion and a stress-concentrator or notch. [16]. Figure .I.12. Shows the material gouge of pipe combined with crack.

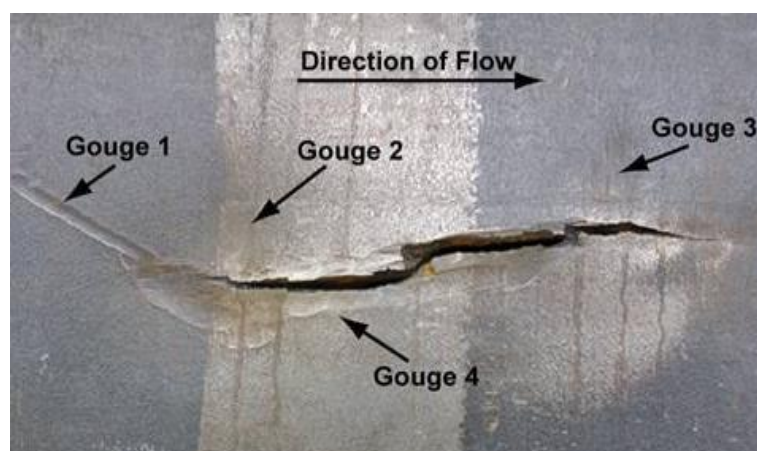


Figure.I.12.Crack in pipelines [16]

The severity of mechanical damage is rooted in the presence of micro cracks that develop at the base of the gouge during the process of dent re-rounding due to pressure (and to some extent elastic rebound). Most often the damage is seen as prominent dents on the bottom half of the pipeline, often called “plain dents”. Are defined injurious if they exceed a depth of 6% of the nominal pipe diameter.

I.7.3. EXTERNAL CORROSION

External corrosion came from the lack of coating, from this cause, it seems reasonable to assume that any buried or submerged pipeline should be identified as susceptible to external corrosion. Figure.I.13 shows the external corrosion of pipeline. However in the presence of a coating, this is an indication that the corrosion phenomenon is difficult to avoid in general.



Figure.I.13. External corrosion in pipes. [17].

I.7.4. INTERNAL CORROSION

Internal corrosion is a real problem in oil and gas industry. It is difficult to identify, especily from the pipelines to transport gas and oil in the presence of, liquids and water. From this the majority of pipelines, are a face of the internal corrosion. Figure .I.14. Shows the crack caused by internal corrosion of pipeline.



Figure.I.14.Internal corrosion of pipelines.[18]

I.7.4.1. INTERNAL CORROSION BY CARBON DIOXIDE (CO₂)

Corrosion by carbon dioxide is one of the major studied forms of internal corrosion in oil and gas industry [18]. This is generally because the crude oil and natural gas reservoir usually contains some level of carbon dioxide. Natural gas compositions from Algeria contain important value of carbon dioxide (Table. I.1). The mechanism of corrosion of carbon steel in media containing carbon dioxide is complex, inevitable in the presence of wet and in dependence of the prevailing conditions it may lead to general or local corrosion and corrosion cracking.

I.7.4.2..INTERNAL CORROSION BY HYDROCHLORIC ACID (HCl)

HCl is one of the most commonly used in petroleum industry for acid pickling and cleaning system of the internal pipe surface. Its role is to decrease the surface area of corrosion causing inactivation of the corrosion reaction part of the surface.

I.7.4.3. INTERNAL CORROSION BY SULFURIC ACID (H₂SO₄)

In some cases, the oil extraction requires the addition of chemical fluids, in the aim to facilitate the extraction process, sulfuric acid is used in this context. However many reports confirmed the sulfuric acid reacts with metal and causes internal corrosion. [19].

I.7.4.4 INTERNAL CORROSION BY HYDROGEN SULFIDE (H₂S)

Hydrogen sulfide is present in field of oil/gas, fields this gas (H₂S) combines easily with water to form a strongly corrosive acid:



Consequently, steel pipes are corroded by **H₂O** in the presence of water.

I.7.4.5. INTERNAL CORROSION REACTIONS

Corrosion is an electrochemical redox (reduction and oxidation) process, whereby localized anodic and cathodic reactions are set up on the surface of the metal. The anode of an electrolytic cell is positive whereas the cathode is negative. Therefore, the reaction at the electrodes are presented by (Equations I-3 and I-4):



I.8. PREVENTION AND PROTECTION OF PIPELINES FROM CORROSION

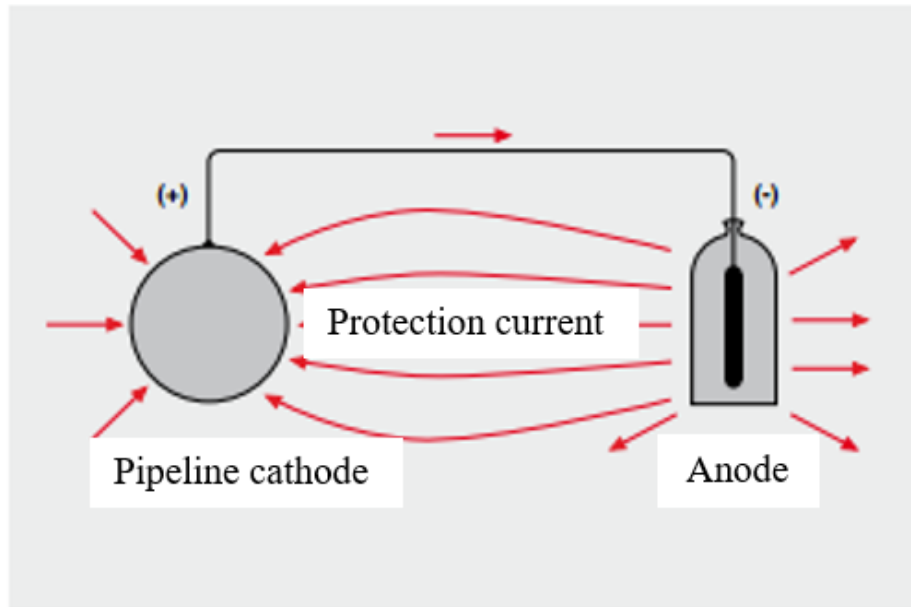
In this last part of the study we present types of the protection of pipelines from corrosion, in the below we have the major protection systems of pipelines.

I.8.1 FROM EXTERNAL CORROSION:

I.8.1.1. CATHODIC AND ANODIC PROTECTION

By using the sacrificial anode technique, the steel pipe will be protected from corrosion by another metal that will be corroded see Figure. I.15. The cathodic protection is generally credited to Sir Humphrey Davy in the 1820s. Davy found that he could preserve copper in sea water by the attachment of small quantities of iron or zinc; the copper became, as Davy put it, “cathodically protected”. Today, Davy’s procedure is still being used to minimize corrosion damage to steel vessels by installing zinc anodes on ships across the world [20]. This is achieved by applying a current to the structure to be protected (such as a pipeline) from some outside source. When enough current is applied, the whole structure will be at one potential; thus, anode

and cathode sites will not exist. Cathodic protection is commonly used on many types of structures, such as pipelines, underground storage tanks, locks, and ship hulls. Figure. I.15. below show these two types.



FigureI.15. Anodic/cathodic protection of pipeline.[21]

There are two main types of cathodic protection systems: galvanic and impressed current. [21]. Note that both types have anode (from which current flows into the electrolyte), a continuous electrolyte from the anode to the protected structure, and an external metallic connection (wire). These items are essential for all cathodic protection systems.

1.8.1.2. COATING PROTECTION

Coating is one of the corrosion protection systems for underground pipelines from external corrosion. It is a highly efficient system, provided care is taken during material selection and application of the coating. Figure.I.16. shows the external coating of pipeline.

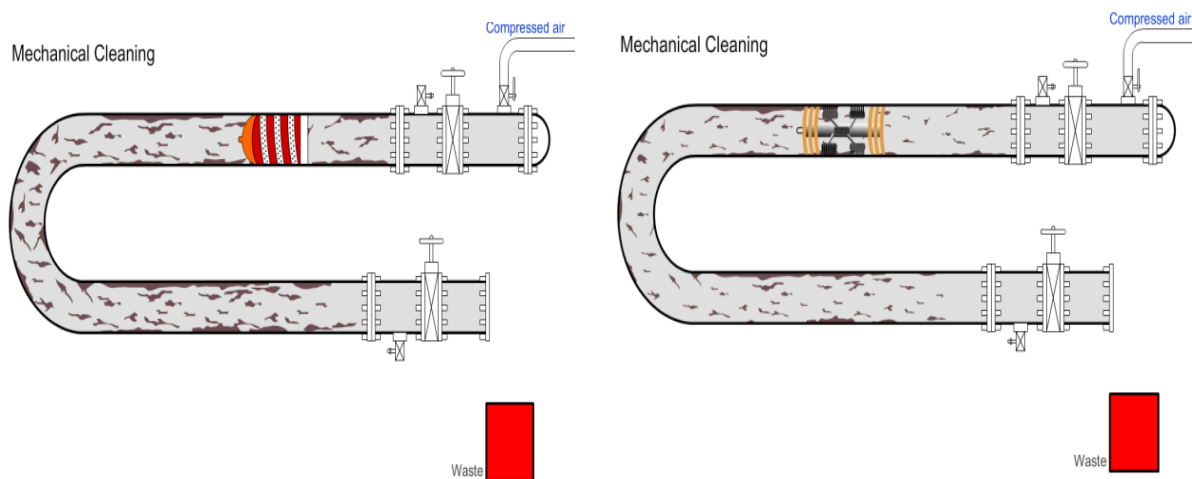


Figure I.16. Coating of outside surface of pipeline with coal tar + epoxy

I.8.2. FROM INTERNAL CORROSION:

I.8.2.1. CLEANING PIGS PROCESS

Cleaning of the internal pipeline will try to keep the integrity by means of a continuous internal protection from the aggressive environment. The aim of cleaning is designed to work on steel pipeline diameters from 4 to 36 inches, and larger diameters are possible. The protecting cleaning system using the synthetic inhibitors injection to order the facility remove the cleaning pig inside the pipeline. Figure I.17 shows the chemical and the mechanical cleaning process.



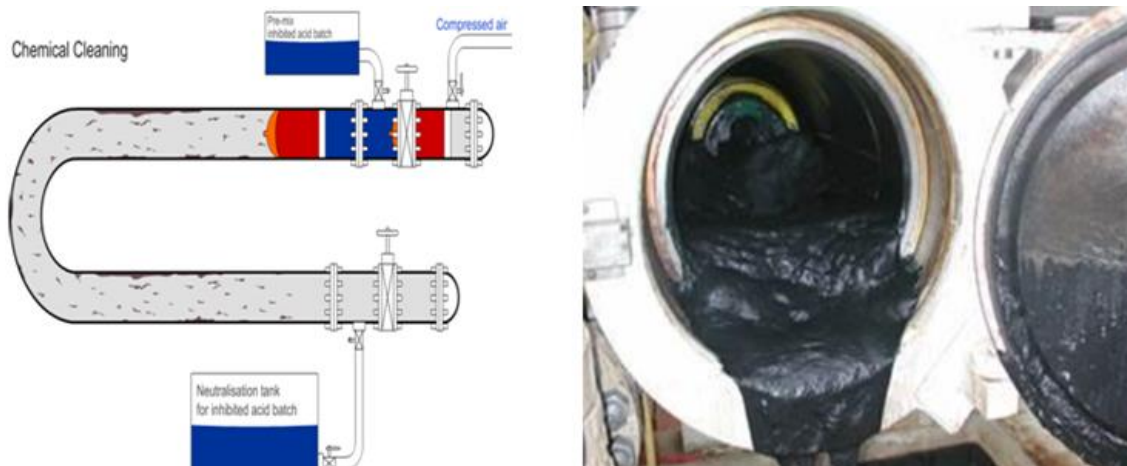


Figure. I.17. Internal cleaning of pipelines and extracted dirt after cleaning process. [22]

The beneficial effects of internal cleaning of pipelines, introduced with synthetic inhibitor, halt the damage caused by corrosion and prevent future corrosion damage. When the pipeline is in service, it is necessary to pig the line to maintain line efficiency and aid in the control of corrosion. It is necessary to remove the liquids in wet gas systems, also remove accumulated water in product pipelines, and paraffin removal and control in crude oil pipelines. When inhibitors are used in gas pipelines, the solvents in the inhibitors evaporate, create the activation of the corrosion trace on pipe walls that can be removed with cleaning pigs. It is also used in conjunction with chemical treatment of the lines to disturb the corrosion sites and remove water, microbes, and corrosion products. The following Figure. II.18. represent pipeline before and after the cleaning operation.

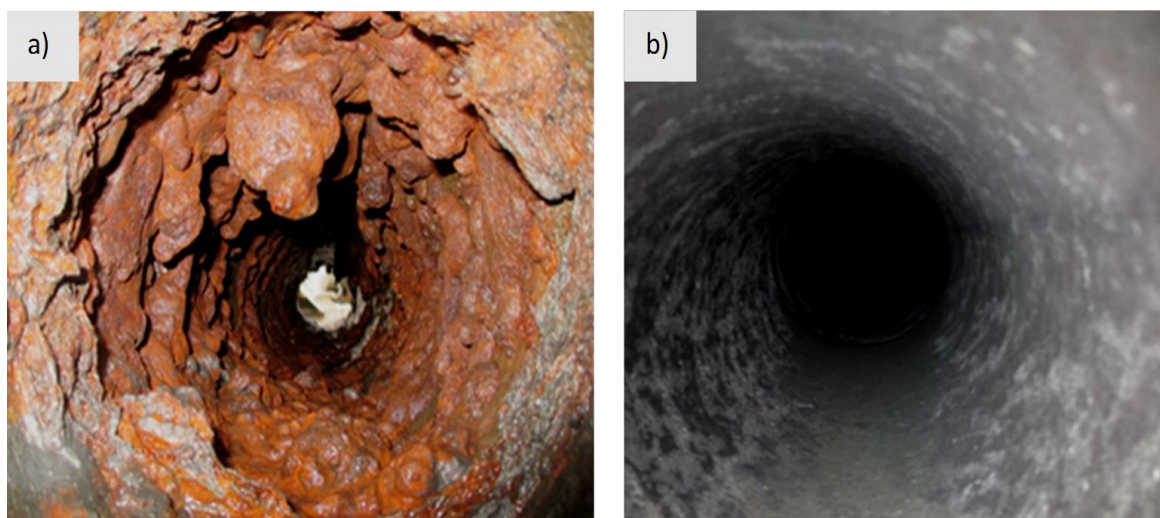


Figure.I.18. Corroded pipe before and after the cleaning process. [22]

I.8.2.2. CORROSION INHIBITORS

Corrosion inhibitors are substances that are added in small amounts to the corrosive medium to stop or slow down electrochemical corrosion reactions on a metal surface

Inhibitors can be divided into two main categories inorganic and organic.

- ✚ Inorganic inhibitors are used mainly in boilers, cooling towers, and fractionation units.
- ✚ Organic inhibitors are used mainly in oil field systems.

Figure. II.19. shows the system injection synthetic inhibitors of corrosion in Hassi R'Mel, (Algeria). When the pipeline is in service, it is necessary to cleaning the line in the aim to keep their efficacy and to control the corrosion.



Figure.I.19.Injection point of the corrosion inhibitor

The pipeline is then visually examined at predetermined inspection points for verification and total cleanliness. Generally, there are other methods for the prevention and protection of gas and oil pipelines from internal corrosion, e.g. (i) prevent or mitigate internal corrosion by dehydration,[23]; (ii) system cleaning of corroding pipe and injecting inhibitors inside pipelines, and (iii) system injection of synthetic inhibitor inside new pipelines while in service. The protective measures taken at present to combat internal corrosion are not adequate.

The methods using synthetic inhibitors are very expensive, toxic for humans and not friendly to the environment. The use of 'green' inhibitors is not a new idea. The initiative was made in some research, [24]. This work presents the new tendency is to use the 'green' inhibitor, extracted from natural plants as a solution for anti-corrosion to protect pipe steels from degradation caused by the internal corrosion in the oil transportation. The developed 'green' inhibitors are used to inhibit corrosion in steel by the natural extracts containing many families of natural organic compounds (flavonoids, alkaloids, tannins, etc.), readily available and renewable. This method is based on using an active corrosion inhibitor as a coat on the internal surface of the steel wall, such that corrosion inhibitors film will take place between the gas/oil and the internal pipeline.

I.9. CONCLUSION

The speed of demand on oil and gas, in the world is constant. This is why the energy producing companies must take attention on the transportation process and safety integrity of the pipelines, from the reserve to the station of treatment and consumers. In this chapter we presented the position of the Algeria in the world from the oil and gas reserve, and also the network pipelines installation and the estimation their length. We are presented some network accidents in Algeria and inspections from the Hassi R'mel to Arzew. We have in this chapter different failure of pipelines such as mechanical damage, internal and external corrosion. At the end we have the process of pipeline protection from corrosion by anodic and cathodic protection and also we presented the protection by synthetic and green inhibitors.

References

- [1] Hany. M. A. E, Vagif. M. A, Leylufer . I A, Teyyub. A. I, ‘‘Corrosion Protection of Steel Pipelines against CO₂ Corrosion-A Review’’, Journal of Chemistry (2012), Vol. 02, (Issue 02), pp. 52-63
- [2] Amina B, "Corrosion localisee des aciers API 5L-X52 de la ligne ASR/MP sollocite en sol Algerien", Doctoral thesis (2011) university Abou Bekr Belkaid of Tlemcen
- [3] Azzedine. L, " The changing geopolitics of natural gas: the case of Algeria", Harvard University’s Belfer Center and Rice University’s Baker Institute Center for Energy Studies (2013)
- [4] Code réseau de transport par canalisation (juin 2018). Autorité de régulation des hydrocarbures. www.arh.gov.dz. Visited on 07/12/2018.
- [5] Algeria crude oil production: OPEC: marketed production. CEIC Data (SG) Pte Ltd (data provider). www.ceicdata.com. Visited on 09/01/2019.
- [6] Mark H. H, ‘‘ Algerian Gas to Europe: The Transmed Pipeline and Early Spanish Gas Import Projects’’, Geopolitics of gas working paper series N27, Program on Energy and Sustainable Development at Stanford University and the James A. Baker III Institute for Public Policy of Rice University, 2004.
- [7] Country Analysis Brief: Algeria 2016 U.S. Energy Information Administration, www.eia.gov. Visited on .10/10/2018
- [8] Algeria natural gas production: OPEC: marketed production. CEIC Data (SG) Pte Ltd (data provider). www.ceicdata.com. Visited on 09/01/2019.
- [9] Omar B, ‘‘Harmfulness and repairing of corrosion defects in pipe mode of X70 steel’’, Doctoral thesis (2017) University of Chlef
- [10] Chettouh S, Hamzi. R, ‘‘Statistical / Dynamic approach to assess the effects of industrial Fire’’ QUALITA conference, 2015, France.
- [11] Kadri. F, Chatelet. E, ‘‘Domino Effect Analysis and Assessment of Industrial Sites Tools’’, International Journal of Computers and Distributed Systems,(2013) Vol. 2 III, pp 1-10.
- [12] Aouad. L, Abbouni B, " Petroleum-oil biodegradation by corynebacterium a quaticum and Pseudomonas aeruginosa Strains Isolated from the Industrial Rejection of the Refinery of ARZEW-Algeria", World Applied Sciences Journal, (2012), Vol 18 (8), pp 1119-1123.
- [13] AMARA Z. A , Étude du comportement des aciers API 5L X60 sollicités par contraintes mécaniques et milieu de sol Algérien Simulé, Doctoral thesis, (2014), Univeristy of Abou Bekr Belkaid – Tlemcen.

References

- [14] Khattak M.A., Zareen. N, Mukhtar. A, Kazi. S., Amena J, Zaheer A, Miraj M.J, ". Case Studies in Engineering Failure Analysis" Journal Engineering failure analyses (2016), Vol 7, pp. 1–8.
- [15] Mohammed H. M, ‘‘ Approche globale a deux parametres (K_p - T_p) Estimation des contraintes de confinements dans des structures portant des entailles’’ Doctoral thesis (2009), University of Paul Verlaine Metz
- [16] Root cause and contributory factors of gas & liquid pipeline failure, metropolitan consulting engineering & forensics, <https://sites.google.com/site/metroforensics3/root-cause-and-contributory-factors-of-gas-liquid-pipeline-failure>
- [17] Neil G., ‘‘Gas and liquid transmission pipelines’’ CC Technologies Laboratories, Inc., Dublin, Ohio.
- [18] Ilman. M.N, ‘‘Analysis of internal corrosion in subsea oil pipeline’’ Journal of Case Studies in Engineering Failure Analysis, (2014), Vol. 2, pp.1–8
- [19] Maslat S. A, ‘‘ Chloride pitting corrosion of API X80 and X100 high strength low alloy pipeline steels in bicarbonate solutions’’ (1999), King Fahd University of Petroleum and Mineral.
- [20] Amitha R. B. E, Bharathi B. J. B, Green Inhibitors for Corrosion Protection of Metals and Alloys: An Overview, journal of International Journal of Corrosion , (2011) , Vol 2012, pp 1-15
- [21] Josef, P, S. Cathodic Corrosion Protection of earthburied Pipelines, V&C Kathodischer Korrosionsschutz Ges.m.b.H www.vc-austria.com, Viseted. 14/01/2019
- [22] Mohamed. S, Mohammed H. M, El-Miloudi. K, Fares. C, Benghalia. M. A, ‘‘Corrosion effects and green scale inhibitors in the fracture mechanics properties of gas pipelines’’, Journal of Struct Integrity Life, (2017), Vol.17 (1), pp.25-31
- [23] Hachama, K., Khadraoui, A., Zouikri, M., et al. "Synthesis, characterization and study of methyl 3-(2-oxo-2H-1,4-benzoxazin-3-yl) propanoate as new corrosion inhibitor for carbon steel in 1M H₂SO₄ solution", Journal, Res Chem Interm, (2015), Vol 41(5)
- [24] Farhad A, Brian. U, James H, Paolo C, "Behaviour and design of hollow and concrete-filled spiral welded steel tube columns subjected to axial compression", Journal of Constructional Steel Research, (2017), Vol 128, pp261-288

II.1 INTRODUCTION

Algeria gas and oil transportation networks are a faces many problems. These problems can be a cause some accidents, (Chapter. I). One of them is the internal corrosion. For this case the corrosion inhibitors are used in the aim to inhibit the internal surfaces of pipeline against internal corrosion.

Generally the applications of corrosion inhibitors had been an accepted practice for their efficiency. [1-2] One of the best methods to reduce the rate of metallic corrosion is by the addition of corrosion inhibitors; even small concentrations of corrosion inhibitors can result in the decrease of the corrosion rate of the metal surface [3-7]. Corrosion inhibitors are the substances added in small amount to the corrosive medium in aim to stop the corrosion activation or slow down the electrochemical corrosion reactions on a metal surface.

II.2. CORROSION INHIBITORS

Corrosion inhibitors is one of the most practical methods for protecting metal steel in chemical industry. [8]. Sulphuric acid (H_2SO_4), and hydrochloric acid (HCl) are often used in industrial acid cleaners and pickling acids. [9] The majority of the corrosion inhibitors are organic compounds, which allow adsorption on metal surfaces [10]. Unfortunately, many common corrosion inhibitors that are still in use today are toxic to the environment and hazardous to human health [11].

II.3. ACTION MECHANISM OF CORROSION INHIBITORS

Corrosion inhibitors act by one or more of the following mechanisms.

- ✓ They form precipitates, which visibly coat and protect metal surfaces.
- ✓ They adsorb on metal surfaces to form protective films.
- ✓ They combine with corrosion product to protect metal surfaces

II.4. ELECTRODE REACTIONS OF CORROSION INHIBITORS

II.4. 1 ANODIC OR CATHODIC PROCESS OF INHIBITORS

Corrosion inhibitors protection can be classified by the reaction with metal into electrode reactions. The classification is based on anode or cathode polarizations of the reactions involved in a corrosion process [16].

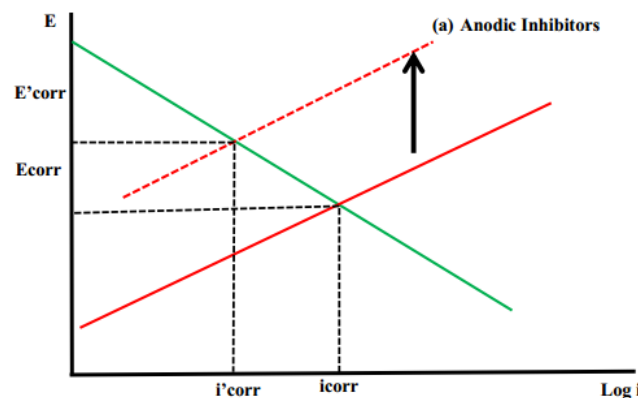


Figure.II.1: Schematic corrosion inhibitors of the anodic reactions [16]

The anodic inhibitors produce a large shift corrosion potential, E_{corr} in positive direction as shown in Fig.II.1 thereby forcing the metallic surface into the passive region with a decrease in corrosion current density, I_{corr} . However, cathodic inhibitors, the E_{corr} to a more negative value thereby increase the surface impedance and limit the migration of reducible species to the areas with corresponding decrease in I_{corr} as shown in Fig.II.2 [12-16]. Some example of anodic inhibitors are the chromates, molybdates, tungstates, [17-18], phosphate [19]. and also sodium nitrite are quite effective anodic inhibitors.

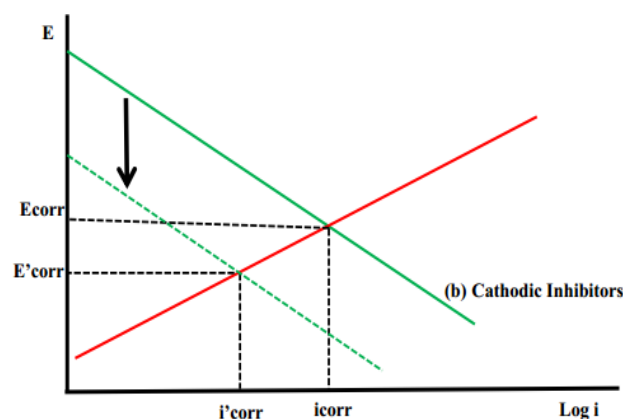


Figure.II.2: Schematic corrosion inhibitors of the cathodic reactions [16]

Figure.II.3 present another type of inhibitors as noted mixed inhibitors when there is small negative or positive change in E_{corr} with a decrease in I_{corr} . Fouda et al [16-17] also used anodic and cathodic Tafel slopes (β_a , β_c) to explain the type of inhibitor used in their work. Some examples of the inhibitors are inorganic polyphosphate (sodium polyphosphate ($\text{Na}_2\text{P}_2\text{O}_7$), Sodium tripolyphosphate ($\text{Na}_5\text{P}_3\text{O}_{10}$)). Organic compounds such as N - heterocyclic e.g. imidazole and benzimidazole. [14, 21].

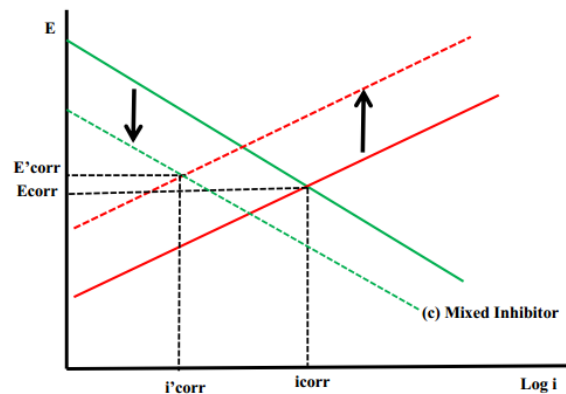


Figure.II.3. Schematic corrosion inhibitors of the mixed inhibitors reactions [16]

Benzotriazole is used widely for copper and copper alloy protection [21-23]. Quinolines and thiourea used to inhibit the dissolution of mild steel in H_2SO_4 . Amines, amides, acridines used to inhibit steel corrosion in HCl [14].

II.4.2. ADSORPTION INHIBITORS

Figure. II.4 present the adsorption modes of inhibitor molecules on a metal surface.

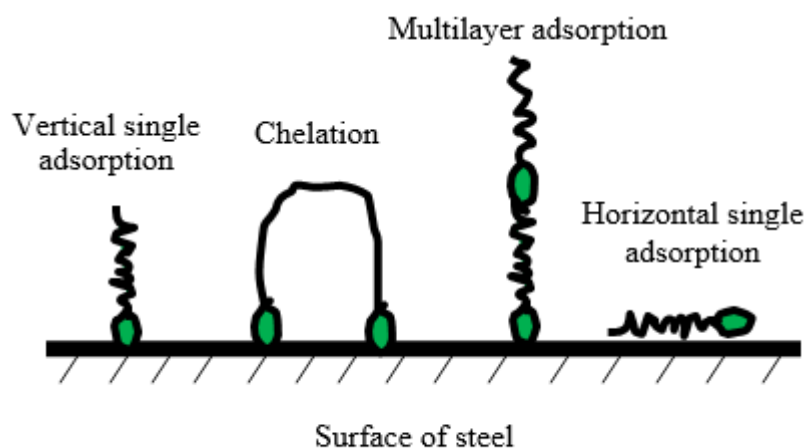


Figure.II.4. Schematic of the adsorption modes of inhibitor molecules on a metal surface.[24-25].

Two interaction types are mainly responsible for the inhibitory bond / metal surface, physisorption and chemisorption. These two types of adsorption are influenced by the nature and the charge of the metal, the chemical structure of the organic product and the type of electrolyte [24].

II.4.2.1. PHYSICAL ADSORPTION

The physical adsorption is defined from Van Der Waals by the forces or electrostatic forces existing between the ionic charge or dipoles of the inhibitory species and the surface of the metal electrically charged. The charge of the metal is defined by the position of the corrosion potential of this metal in relation to its zero charge potential (E_0) [16]. When the corrosion potential of this metal has a value less than E_0 the adsorption mechanism of the cations to be favored; on the contrary, anions are adsorbed when the corrosion potential of the metal is in the region of positive potential with respect to E_0 . In some cases, the surface charge can be modified by the adsorption of a layer of intermediate ions. [16].

II.4.2.2. CHEMICAL ADSORPTION

Chemisorption is a more common mechanism than physisorption and leads to more important efficacy of the inhibitor. It involves an electronic transfer between the orbitals of the metal and the inhibitory molecule, which leads to the formation of much more stable because they are based on higher binding energies. [16].

Generally, the transfer donor molecule / acceptor metal; there is also the transfer where the metal is the electron donor and the molecule the acceptor [16]. Chemisorption is a, irreversible and specific phenomenon for each metal. It's a fast process, depending on temperature and characterized by high activation energy.

II.5. ORGANIC INHIBITORS

Organic corrosion inhibitors are complex mixtures of different molecular compounds. Organic inhibitors affect both anodic and cathodic areas of corrosion cells. They create an organic film on the entire metal surface. Their effectiveness depends upon the following conditions:[26].

- ✓ The electrical potential of the metal
- ✓ The chemical structure of the inhibitor molecule

- ✓ The size and shape of the inhibitor molecule.

The molecule of organic inhibitor corrosion consists of a hydrocarbon chain attached to a strong polarity functional group. [26] The hydrocarbon chain of the inhibitor molecule is oil soluble. This chain provides a barrier that keeps water away from the metal surface.

Polar functional groups are based on nitrogen, sulfur, or oxygen. Petroleum industry used the organic inhibitors containing at least one nitrogen functional group. [26]. Often, these nitrogen inhibitors interact with organic acids, or they contain oxygen functional groups. The amino portion (NH_2) of the molecule is soluble in water and has a pair of unshared electrons. These electrons are available for bonding with metal surfaces. [26].

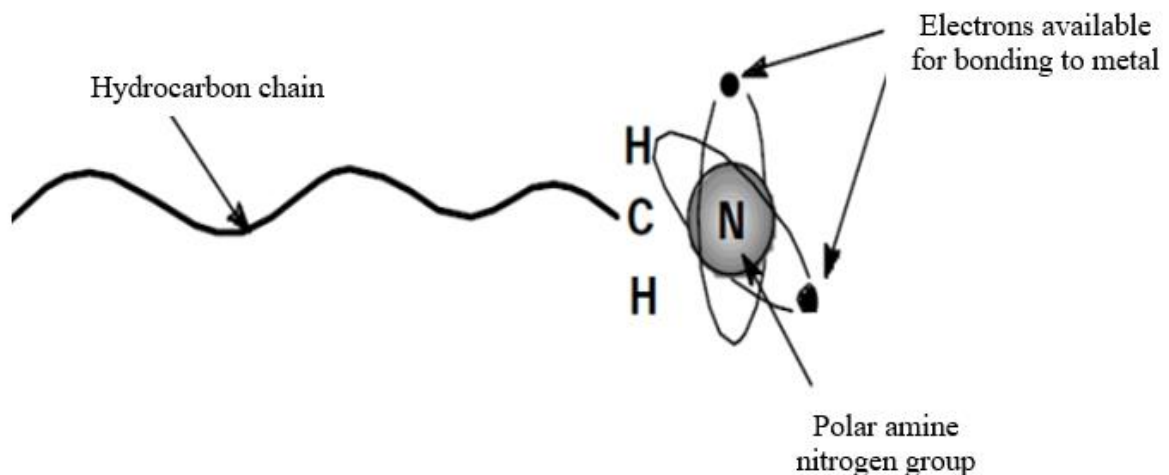


Figure.II.5. Organic inhibitors molecule. [26]

Molecules of the organic inhibitor attach to metal surfaces by both chemisorption and physisorption. Most of the metal is covered with adsorbed water molecules, when the metal is in contact with an aqueous solution. In the presence organic inhibitor in the system, the unshared electrons in the polar amine group form a chemisorption bond with the metal surface. This bond operation displaces water molecules and other corrosive agents from the metal surface. Hydrocarbon chains have important role in the inhibition process [26].

The hydrocarbon chains are soluble in oil and attract crude oil molecules in the process stream. Figure.II.6 shows the molecular structures.

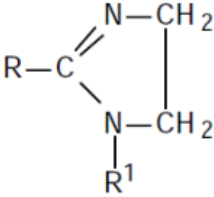
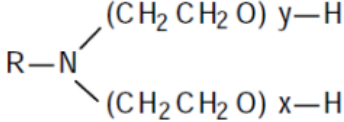
Name	Structure
Primary Amine	$R-NH_2$
Amide	$R-C(=O)NH_2$
Imidazoline	
Polyethoxylated Amines	

Figure.II.6. Molecular structure of some organic inhibitors. [26]

These are organic compounds which contain a polar group such as NH_2 (amino group), these compounds (RNH_2) adsorb on the metallic surface and isolate it from the corrosive solution (usually acids).

II.6. STEEL SURFACE ADSORPTION

The inhibitors adsorption are accepted on the surface of the steel in aim to inhibit corrosion caused by chemical reactions between the iron steel and their environment [27]. In this case, we are study the efficiency of it by experimental mechanical test of steel, such as the Charpy testing, drop weight test, three points bending test, and tensile testing [28]. We present some mechanical properties obtained from curves data and have been used in aim to determine the properties mechanical of API 5L X52 and X65 steel in HCl acid media with and without green inhibitors [29-31]. We find the adsorption efficiency is associated with increased the percent of the green corrosion inhibitors in acid media HCl [32]. Adsorption form inhibitor to the metal/solution interface, which is the driving force for the adsorption of inhibitor on steel surface [33].

General inhibitor combine with metal ions M^{+2} on surface as a result of metal oxidation or dissolution process, forming metal inhibitor complex [34]:



Depending upon the relative solubility of the resulting complex, it can further may inhibit or catalyze further metal dissolution. [35-37]. It is generally accepted that in the absence of the corrosion inhibitor, the acidic solution is in contact with the metal and porous film surface causing corrosion as a result of metal dissolution. Whereas in the presence of inhibited solution, the active or in open sites in the porous film are almost blocked by the adsorption of the inhibitor resulting a barrier or a passive layer suppressing further corrosion [37].

The prevention of corrosion reaction over the active sites of the metals surface occupied by the adsorbed corrosion inhibitor species, where corrosion reaction normally occurred on the corrosion resistance-free area. [38-39]. Adsorption mechanism is usually explained through the help of different adsorption metal inhibition by organic compounds as a result of the adsorption of (molecules and/or ions) at solid surface [33]. In the presence of inhibitor, the corrosion rate is sufficiently diminished, then the steady state adsorption. [7].

II.7. ROLE OF GREEN CORROSION INHIBITORS

II.7.1 EFFECT OF CORROSION INHIBITORS

Corrosion inhibitors are of great importance to large researchers in many industries of the field of oil and gas to protect pipelines against the corrosion of internal metal surfaces that come into contact with liquids. Aggressive acidic solutions is used in petroleum industries and applications for the aim of cleaning pipelines, rescaling, and petrochemical industry. For example, hydrochloric acid is used in the pickling processes of metals. In recent years, natural compounds such as herbal plants are employed as inhibitors in order to develop new cleaning chemicals for green environment.[40]. Several studies have been reported in the use of natural products as corrosion inhibitors in different media [40].

Today one of the good and effective methods to prevent corrosion in oil and gas industry is to use organic inhibitors [41]. These organic inhibitors are extracts from Plant, and are viewed as environmentally friendly and ecologically acceptable inhibitors.[41]. Plant products are low-cost, readily available, and renewable sources of materials. The extracts from their leaves, barks, seeds, fruits, and roots comprise of mixtures of organic compounds containing nitrogen, sulphur, and oxygen atoms. Plant extracts that contain many families of organic compounds (flavonoids, alkaloids, tannins, etc.), readily available and renewable, are shown to be effective and are presented as new " green " formulations for many metals and alloys, which can replace toxic compounds.[39-42]. The Natural inhibitors are often water soluble

and biodegradable. A great number of scientific studies have been devoted to the subject of corrosion inhibitors for mild steel in acidic media [42]. Abdelkader. K. et al has study the Mentha pulegium extract, in aim to control the corrosion steel in acid medium, they are find the highest inhibition efficiency of 84.34 % was observed with single M. pulegium extract at 33 %. [43]. And from the region of Chlef Algeria, Fares C. et al. Was studied the efficiency of green inhibitor (Ruta Chalepensis) in HCl media by (97.72%) was noticed for 30% in 1M HCl solution. [44].

II.7.2.EFFECT OF CORROSION INHIBITORS ON MECHANICAL PROPERTIES

Pipelines are used to transport oil and gas, but they face many problems. Such as fractures, stress, corrosion, fatigue, failure, and external / internal corrosion. Protecting these pipes against these problems is possible, by improving the service conditions such as diameters, pressure, surface roughness and internal service temperature. For these reasons we present the importance of this study, that is a modern idea, and modern method study the efficiency of green corrosion inhibitors to inhibit the internal corrosion of the gas and oil pipelines. Some mechanical tests of properties mechanical of steel samples grad X52 and X65 are immersed in acid solution media with different percent of these green inhibitors. In order to know the effect of these inhibitors to limit the acidity factor or to reduce the reaction rate of the acid medium with the internal surface of the gas and oil pipeline, we have obtained very good results, promising and encouraging. These results are more detailed in the last chapter of this thesis. To our knowledge, we are the first to study the effect of corrosion green inhibitors on the mechanical properties of steel pipes.

II.8. CONCLUSION

Corrosion inhibitors are one of the methods used against the corrosion problem, to protect and/or prolong the life of metallic structures. The scientific literature on corrosion inhibitors is huge, but the vast majority of it deals with fundamental studies of corrosion inhibition or industrial applications (chemical industrial, corrosion pipelines oil and gas). Protecting metals from corrosion is very important, study the different corrosion inhibitor concentrations, in order to obtain the optimal concentration of corrosion inhibitors in the aim to protect the structure of oil and gas pipelines and thereby avoid potential risks.

References

- [1] Benabdellah. M, Benkaddour. M, Hammouti. B, Bendahhou. M, Aouniti. A, " Inhibition of steel corrosion in 2 M H₃PO₄ by artemisia oil" Applied Surface Science, (2006) , Vol 252 pp 6212–6217.
- [2] Raja P.B, Sethuraman. M.G, " Atropine sulphate as corrosion inhibitor for mild steel in sulphuric acid medium" Materials Letters; (2008) Vol 62, pp 1602–1604.
- [3] Wang. L, Pu. J, Luo. H, " Corrosion inhibition of zinc in phosphoric acid solution by 2-mercaptobenzimidazole" Corrosion Science, (2003) , Vol 45 pp 677–683.
- [4] EL-Etre. A.Y., " Natural honey as corrosion inhibitor for metals And alloys I copper in neutral aqueous solution" Corrosion Science, (1998) , Vol 40, pp 1845–1850.
- [5] Radojcic. I, Berkovic. K, Kovac. S, Vorkapic. F. J, "Natural honey and black radish juice as tin corrosion inhibitors" Corrosion Science, (2008) , Vol 50, pp 1498–1504.
- [6] Ahmad. Z, "Principles of Corrosion Engineering and Corrosion Control", Elsevier, Oxford, (2006).
- [7] Philip. P. E, Schweitzer. A, "Handbook of Corrosion Engineering, McGraw-Hill", New York, 2000.
- [8] TrabANELLI. G, "Inhibitors—An Old Remedy for a New Challenge", Corrosion, (1991) Vol 47, pp 410–419.
- [9] Leelavathi. S, Rajalakshmi. R, "Dodonaea viscosa (L.) Leaves extract as acid Corrosion inhibitor for mild Steel – A Green approach", Journal of Mater. Environ. Sci, (2013) , Vol 4(5) pp 625-638.
- [10] Oguzie E. E, Enenebeaku C. K, Akalezi C. O, Okoro S. C., Ayuk A. A., Ejike E. N., "Adsorption and corrosion-inhibiting effect of Dacryodis edulis extract on low-carbon-steel corrosion in acidic media", journal of colloid Interface Sci., (2010), Vol 349, pp 283-292.
- [11] Obot I. B., Obi-Egbedi N. O., Adsorption properties and inhibition of mild steel corrosion in sulphuric acid solution by ketoconazole: Experimental and theoretical investigation, j. Corros. Sci.,(2010), Vol 52, pp 198-204.
- [12] Gil. P. M, "Exploring corrosion inhibition in Acidic and Oilfield Environments," Doctoral thesis, 2013, University of Manchester
- [13] Foss. M, Gulbrandsen. E, Sjoblom. J., "Effect of Corrosion Inhibitors and Oil on Carbon Dioxide Corrosion and Wetting of Carbon Steel with Ferrous Carbonate Deposits," CORROSION, (2009), Vol. 1, no. 65, pp. 3–14,.
- [14] Sastri. V. S, "Corrosion Inhibitors: Principles and Applications", Winston revie, series Editor, (2011).
- [15] Shreir L. L, Jarman. R. A, Burstein G. T, Corrosion control, 3rd edition, Elsevier, (1994).

References

- [16] Ajayi. F. O, ‘Mitigating corrosion risks in oil and gas equipment by electrochemical protection: top of the line corrosion’, Doctoral thesis, 2015, University of Manchester
- [17] O’Keefe JM, Geng S, Joshi S. Cerium-based conversion coatings as alternatives to hex chrome: Rare-earth compounds provide resistance against corrosion for aluminum alloys in military applications. *Met Finish* (2007); 105: 25.
- [18] Gunasekaran G, Palanisamy N, Appa Rao BV, Muralidharan VS. Synergistic inhibition in low chloride media. *Electrochim Acta* (1997) ; 42: 1427.
- [19] Blin F, Leary SG, Wilson K, Deacon GB, Junk C, Forsyth M. Corrosion mitigation of mild steel by new rare earth cinnamate compounds. *J Appl Electrochem* (2004); 34: 591.
- [20] Munn P. The testing of corrosion inhibitors for central heating systems. *Corros Sci* 1993; vol, 35(5-8).
- [21] Lorenz WJ, Mansfeld F. Determination of corrosion rates by electrochemical DC and AC methods. *Corrosion Sci* 1981; 21: 647.
- [22] Aksut AA, Lorenz WJ, Mansfield F. The determination of corrosion rates by electrochemical D.C and A.C methods — II. Systems with discontinuous steady state polarization behavior. *Corrosion Sci* (1982); 22: 611.
- [23] Fouda. A. S, Elewady. G. Y, El-Haddad. M. N, “Corrosion Inhibition of Carbon Steel in Acidic Solution Using Some Azodyes,” *Canadian Journal on Scientific and Industrial Research*, (2011), Vol. 2, no. 1, pp. 1-19,
- [24]. Asmaa M. ‘Composites à base de copolymères et de bentonite pour la rétention des polluants et pour l’inhibition de la corrosion’, Doctoral thesis 2016 University of Science and Technology of Oran Mohamed Boudiaf.
- [25] Abbasov. V.M., Hany M. Abd El-Lateef, Aliyeva. L.I, Qasimov. E.E, Ismayilov. I.T., Khalaf. M. M, ‘A study of the corrosion inhibition of mild steel C1018 in CO₂-saturated brine using some novel surfactants based on corn oil’. *Egyptian Journal of Petroleum* (2013), Vol. 22, pp. 451–470
- [26] Corrosion control, [https://www.kau.edu.sa/Files/0060757/Subjects/ %20ChE%20311.pdf](https://www.kau.edu.sa/Files/0060757/Subjects/%20ChE%20311.pdf)
- [27] Mohamed S, Mohamed. H. M, El-Miloudi K, Fares. C, Benghali. M.A, ‘Corrosion effects and green scale inhibitors in the fracture mechanics properties of gas pipelines, structural integrity and life, (2017), vol. 17, No 1 pp. 25–31
- [28] Benghali. M.A, Fares. C, Mohamed. H. M, Abdelkader k, Mustapha, " Optimization of the inhibition effect using acid extract of ruta chalepensis on API 5L X52 steel", 16th International Conference on New Trends in Fatigue and Fracture (2016), Dubrovnik, Croatia

References

- [29] Zhang X., Wang F., He Y., Du Y., Study of the inhibition mechanism of imidazoline amide on CO₂ corrosion of Armco iron, *Journal of Corrosion sciences*, (2001), Vol. 43, pp. 1417–1431.
- [30] Durnie. W, Marco. R.D, Jefferson. A, Kinsella. B, ‘‘Development of a structure-activity relationship for oil field Corrosion inhibitors’’, *Journal of The Electrochemical Society*, (1999), Vol. 146(5), pp. 1751-1756
- [31] Ali S.A., El-Shareef A.M., Al-Ghamdi R.F, Saeed. M.T, ‘‘The isoxazolidines: the effects of steric factor and hydrophobic chain length on the corrosion inhibition of mild steel in acidic medium’’, *Journal of Corrosion sciences*, (2005), Vol. 47, pp. 2659-2678.
- [32] Branzoi V., Branzoi F., Baibarac M., ‘‘The inhibition of the corrosion of Armco iron in HCl solutions in the presence of surfactants of the type of N-alkyl quaternary ammonium salts’’, *Journal of Materials Chemistry and Physics* , (2000), Vol. 65, pp. 288-297
- [33] Noor. E.A, ‘‘Evaluation of inhibitive action of some quaternary N-heterocyclic compounds on the corrosion of Al–Cu alloy in hydrochloric acid’’, *Journal of Materials Chemistry and Physics*, (2009), Vol. 114, pp. 533-541.
- [34] Ahmed. Y. M, Abdul A. H. K, Abu Bakar M, Abdul Razak D, Mohd. S. T, Siti K. K, Norhamidi, M, ‘‘Stability of Layer Forming for Corrosion Inhibitor on Mild Steel Surface under Hydrodynamic Conditions’’, *Int. J. Electrochem. Sci.*, (2009), Vol. 4 pp. 707 - 716
- [35] Ortega. T. D.M, Gonzalez R. J.G, Casales. M, Caceres. A, Martinez. L, ‘‘Hydrodynamic Effects on the CO₂ Corrosion Inhibition of X-120 Pipeline Steel by Carboxyethyl-imidazoline’’ *Int. J. Electrochem. Sci.*, (2011) Vol. 6, pp.778 – 792
- [36]. M. R. Ezhilarasi, B.Prabha and T.Santhi, ‘‘Corrosive inhibitive effect of pyrazole compounds towards the corrosion of mild steel in acidic medium’’, *RJC, Ested.*2008, (2015), Vol. 8, (no.1), pp. 71-83,
- [37] Corrosion-inhibitors, <https://www.uv.mx/personal/rorozco/files/2011/02/>
- [38] Nurul. I. K, Jain K, ‘‘The Effect of Temperature on the Corrosion Inhibition of Mild Steel in 1 M HCl Solution by Curcuma Longa Extract’’, *Int. J. Electrochem. Sci.*, (2013), Vol. 8 pp. 7138 - 7155
- [39] Ghulamullah k, Kazi M. S. N, Wan J. B, Hapipah B. M. A, Fadhil L. F, Ghulam M. K ‘‘Application of Natural Product Extracts as Green Corrosion Inhibitors for Metals and Alloys in Acid Pickling Processes- A review’’ *Int. J. Electrochem. Sci.*, (2015), Vol. 10, pp. 6120 – 6134
- [40] Bogumił. E. B, Iwona H. K, Adrianna S, Olga. K, Marta. P, ‘‘Organic Corrosion Inhibitors’’ <http://dx.doi.org/10.5772/intechopen.72943>
- [41] Amitha R. B. E, Bharathi. B. J. B. ‘‘Green Inhibitors for Corrosion Protection of Metals and Alloys: An Overview’’, (2011), Vol 2012, pp. 1-15

References

- [42] Hachama. K, Khadraoui. A, Zouikri, M, ‘‘Synthesis, characterization and study of methyl 3-(2-oxo-2H-1,4-benzoxazin-3-yl) propanoate as new corrosion inhibitor for carbon steel in 1M H₂SO₄ solution’’, Research on Chem. Interm. (2015), Vol. 41(5) doi: 10.1007/s11164-015-2068-4.
- [43] Khadraoui. A, Khelifa. A, Hachama. K, Boutoumi. H, Hammouti. B, Synergistic effect of potassium iodide in controlling the corrosion of steel in acid medium by *Mentha pulegium* extract, Res. Chem. Interm. (2015). Vol. 41(10): pp. 7973-7980.
- [44] Meryem. A. B, Chahinez F, Mohamed. H. M, Abdelkader. K, ‘‘Adsorption and corrosion inhibitive properties of *Ruta Chalepensis* on API X52 steel in hydrochloric acid media’’ CHEMTECH '15 / 3rd International Chemical Engineering and Chemical Technologies Conference Proceedings, November 23-24, 2015, İstanbul

Chapter III

Materials and Methods

III.1. INTRODUCTION

In this chapter, we present the materials and methods used in this experimental study. First, we will present API 5L X52 and X65 steel pipes, their chemical composition and their microstructures. Several mechanical tests are also presented along with the methodology adopted. The first one test is the Charpy test, the second is the Drop weight test, the third is the three point bending test, and the last one is tensile test.

III.2. PRESENTATION OF API 5L X52 AND X65 STEEL GRADES

III.2.1. API 5L X52 STEEL GRADE

API 5L X52 steel pipes was the most common gas pipeline material for transmission of oil and gas during 1950 until our days. The material is delivered as tubes which are manufactured by hot rolling.

The specimens used in this study, come from a pipeline manufactured for SONATRACH. This pipe is of 610 mm outer diameter and 11 mm thickness (Figure III.1) and has been in service for 20 years. The specimens were machined both from the transverse and the longitudinal direction.

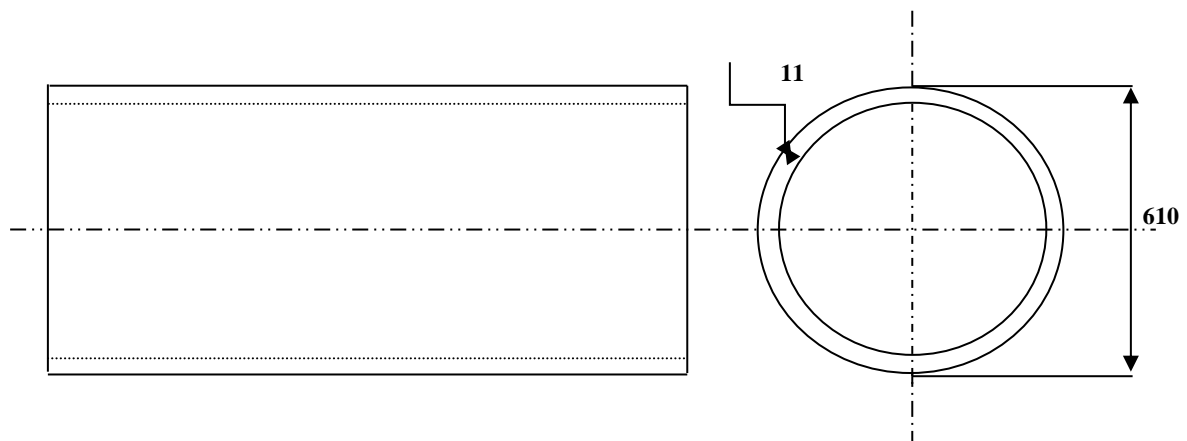


Figure. III. 1. API 5L X52 steel pipe scheme

III.2.2. CHEMICAL COMPOSITION OF X52

Chemical composition is given in Table III.1.

Table III.1 Chemical composition of API 5L X52 steel. [2]

C	Mn	Si	Cr	Ni	Mo	S	Cu	Ti	Al	Fe
0.22	1.22	0.24	0.16	0.14	0.06	0.036	0.19	0.04	0.032	97.66

III.2. Mechanical properties of API5L X52 steel [1-2]

Yield stress σ_y (MPa)	Ultimate strength σ_{tul} (MPa)	Elongation %	Reduction of area %	Fracture toughness K_{Ic} ($\text{MPa}\sqrt{\text{m}}$)
410	528	30,2	57	116.6

The mechanical properties are determined from Stress strain test of X52 pipe steel [2].

III.2.3.MICROSTRUCTURE ANALYSIS OF THE API 5L X52 STEEL

Visual inspection, optical and scanning electron microscopy are used to explore the microstructure of the material under study. These observations are necessary to have a good knowledge of the properties of the steel. Also, microstructure analysis gives information about the steel.

Figure III.2 and Figure III.3 show the microstructure of the API 5L X52 steel in different directions. Three senses are chosen: the longitudinal or rolling direction (L), the circumferential direction (T) and the direction of the thickness (E). The surfaces observed were polished up to 1 μm , cleaned with acetone and dried. The presence of non-metallic inclusions can be observed directly on the polished surface.

To visualize the different phases of the microstructure, a chemical or electrochemical attack is performed. The material was treated by Nital (4% HNO_3 solution in ethanol) for few seconds. After this attack, ferrite appears under an optical microscope as a white phase, however pearlite is darker. As shown in Figure III.2, the structure in the longitudinal direction is formed by alternating ferrite (F) and pearlite (P) rows arranged almost regularly.

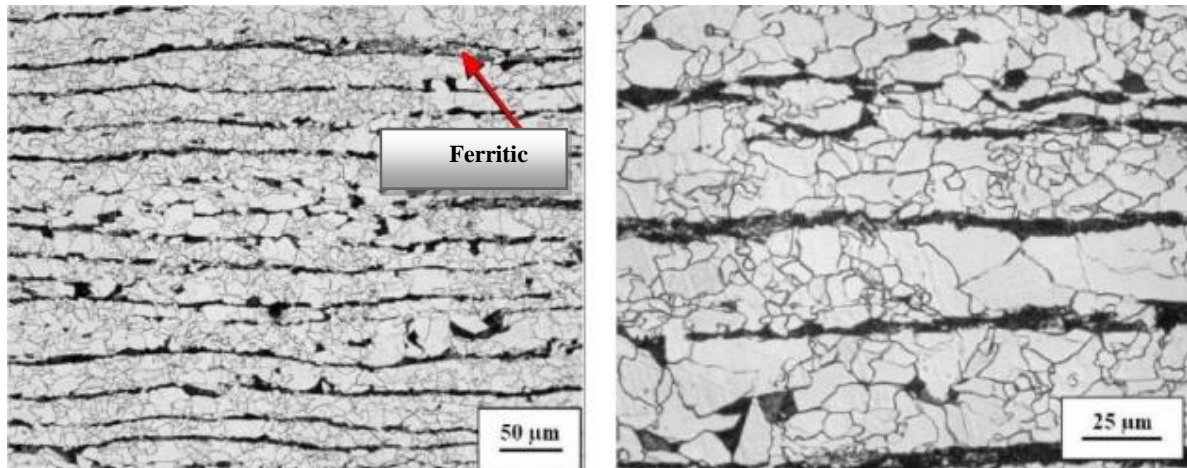


Figure. III.2: Microstructure of samples of X52 steel in the longitudinal direction. [3].

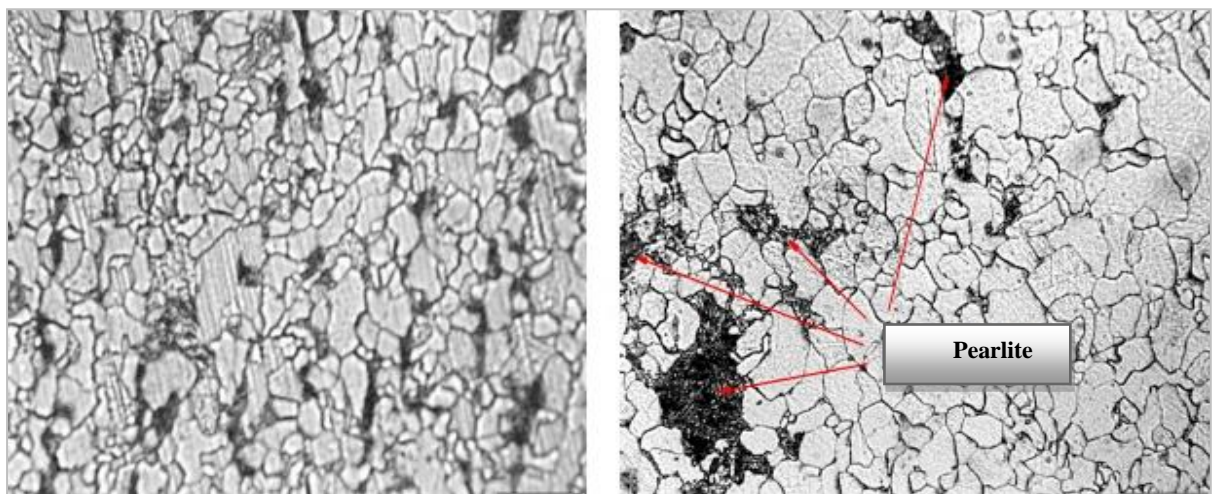


Figure. III. 3: Microstructure of samples of X52 steel. (left) the surface in the circumferential direction (right) the surface in the thickness direction. [3]

The observation of the steel has revealed significant microstructure changes between the skin and the heart. This is particularly visible in the sense of the thickness. As shown in Figure III.3, the formation of beads of martensite (metastable phase) is also noticed in the sense of thickness, and these are the preferential crack initiation sites. Figure. III.3 shows also that the steel in the circumferential direction, is generally composed of alternating rows of ferrite and pearlite formed by segregation during the solidification. The amount of pearlite is lower, and the effect of the rows is not so marked.

Purity analysis showed that API 5L X52 steel contains two types of inclusions: globular oxides and elongated manganese sulphides shown in Figure III.4. The surface of the samples were polished and observed under an optical microscope with 500x magnification. The sulphide inclusions present in the material, with a high content (0.036%), influence both the

purely mechanical aspect of crack propagation and the aspect related to the effect of the aggressive environment.

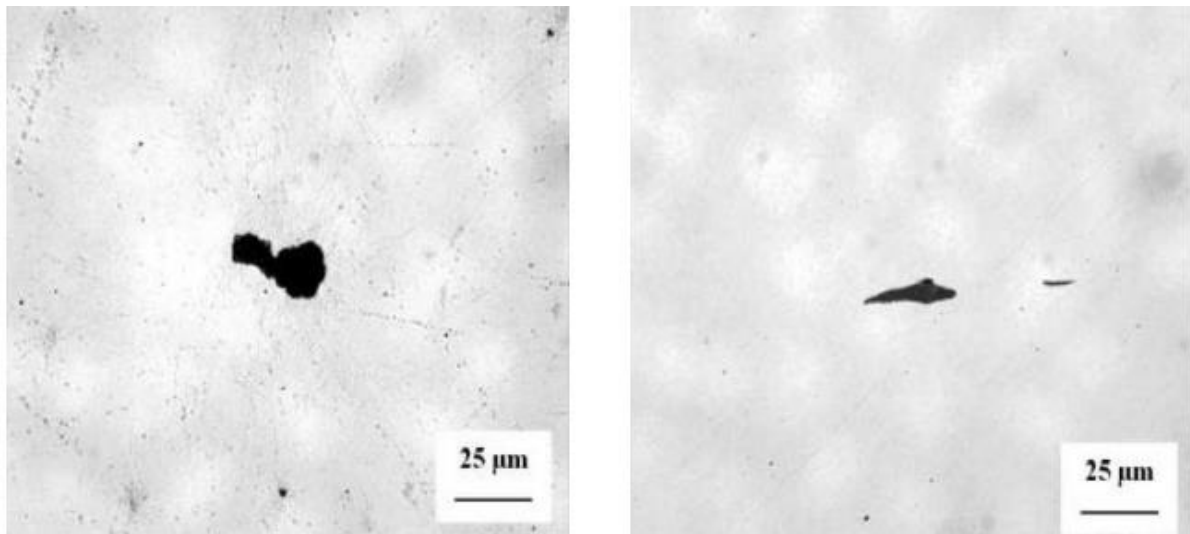


Figure. III. 4: X52 steel inclusions: globular oxides (left) and manganese sulfide (right) visible on the polished surface. [3]

To calculate the grain size, an optical microscope instrumented by a digital camera was used. Images and dimensions are processed through software calculation 'Analysis'. Table III.3 shows the different measurements in different directions of the pipe [3].

Table III.3. Summary of grain sizes in different orientations.

Orientation	Magnification	Number of grains	Size (μm)			
			Minimum	Maximum	average	Standard deviation
Longitudinal	500	157	-	-	7.88	-
Transversal		156	1.31	29.02	7.78	4.35
Thickness		147	0.98	24.36	9.29	5.22

III.2.4. API 5L X65 STEEL GRADE

API 5L X65 pipe steel is a widely used steel in the European pipe network (25%) with a minimum yield strength of 448 MPa (65 psi). Its chemical reference composition is given in Table III.4. The mechanical properties of API 5L X65 steel issued from reference [4] are reported in Table III.5.

Table III.4. Chemical composition of API5L X65 steel

C	Mn	Si	Cr	Ni	Mo	S	Cu	Ti	Al	Fe
0.14	1.5	0.231	0.016	0.25	0.25	0.005	0.001	0.003	0.04	97.564

Table III.5. Mechanical properties of API5L X65 steel [4]

Yield stress σ_y (MPa)	Ultimate strength σ_{sul} (MPa)	Elongation %	Reduction of area %	Fracture toughness K_{Ic} ($\text{MPa}\sqrt{\text{m}}$)	Hardness HV
465	558	11	57	280	205

The mechanical properties are determined from Stress strain test of API 5L X65 pipe steel



Figure III.5. Microstructure of the pipe section of API 5L X65 steel.

Figure III.5 shows that the microstructure is composed of fine grains of ferrite base and pearlite colored in white and black, respectively.

The difference between the API 5L X52 and X65 grades is the mechanical properties such as the yield strength, ultimate strength, and elongation.

III.3. CHARPY MECHANICAL TEST

Charpy impact test is a convenient and low cost mechanical test. It has been widely used to evaluate the fracture toughness of metallic materials under large deformation and high strain rate loading [5].

Two indexes could be determined from the testing. The total energy and the fracture toughness.

The instrumented impact tests on Charpy V-notch specimens are standardized in international test standards such as ISO 14556 [6] and ASTM E2298 [7]. According to these standards, the analysis of an instrumented Charpy test consists of the determination of characteristic time, force, displacement, and absorbed energy values corresponding to the following events described in Figure III. 6.

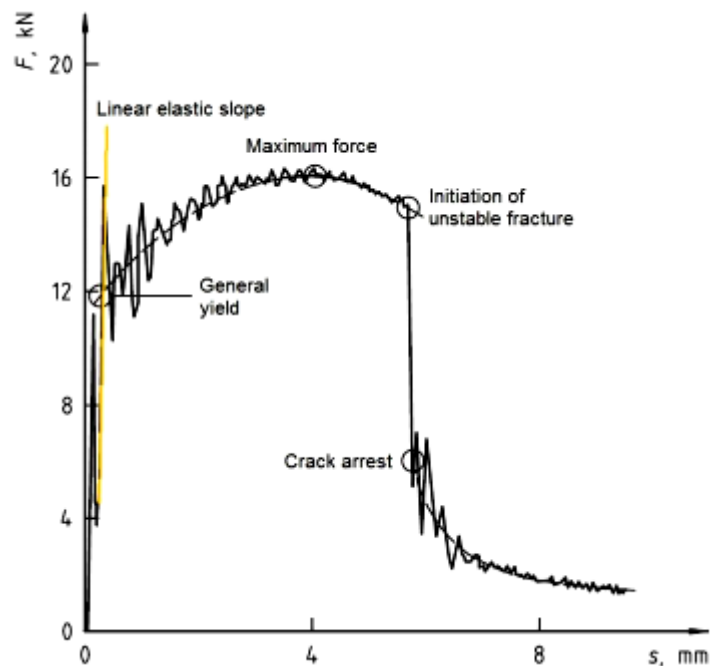


Figure. III. 6. An example of instrumented Charpy test in ductile-to-brittle transition regime.

- ✓ general yield, or yielding across the entire specimen ligament;
- ✓ maximum force;
- ✓ initiation of brittle (unstable) fracture;
- ✓ arrest of brittle (unstable) fracture, or crack arrest;
- ✓ Test termination.

The force of general yield (F_{GY}) is defined as the force at the intersection of the linear elastic part and the fitted curve through the oscillations of the force-displacement curve following the onset of general yielding of the cracked ligament.

III.3.1. OBJECTIVES OF THE CHARPY TEST

A series of Charpy V-notch impact tests were conducted to determine the fracture toughness of the provided API 5L material specimens immersed in different solution. This properties will be determined by equations in chapter IV.

III.3.2. CHARPY MECHANICAL TEST MACHINE

In this study, Charpy mechanical tests were conducted on a RKP 450 from ZwickRoell machine (Figure III.7). Instrumented Charpy hammer was used with the following characteristics:

- the measuring range of the device was from 0 J to 450 J
- digital readout on PC with resolution of 0,01 J
- The impact velocity was between 5 m/s to 5,5 m/s
- nominal impact force appears between 10 kN and 40 kN

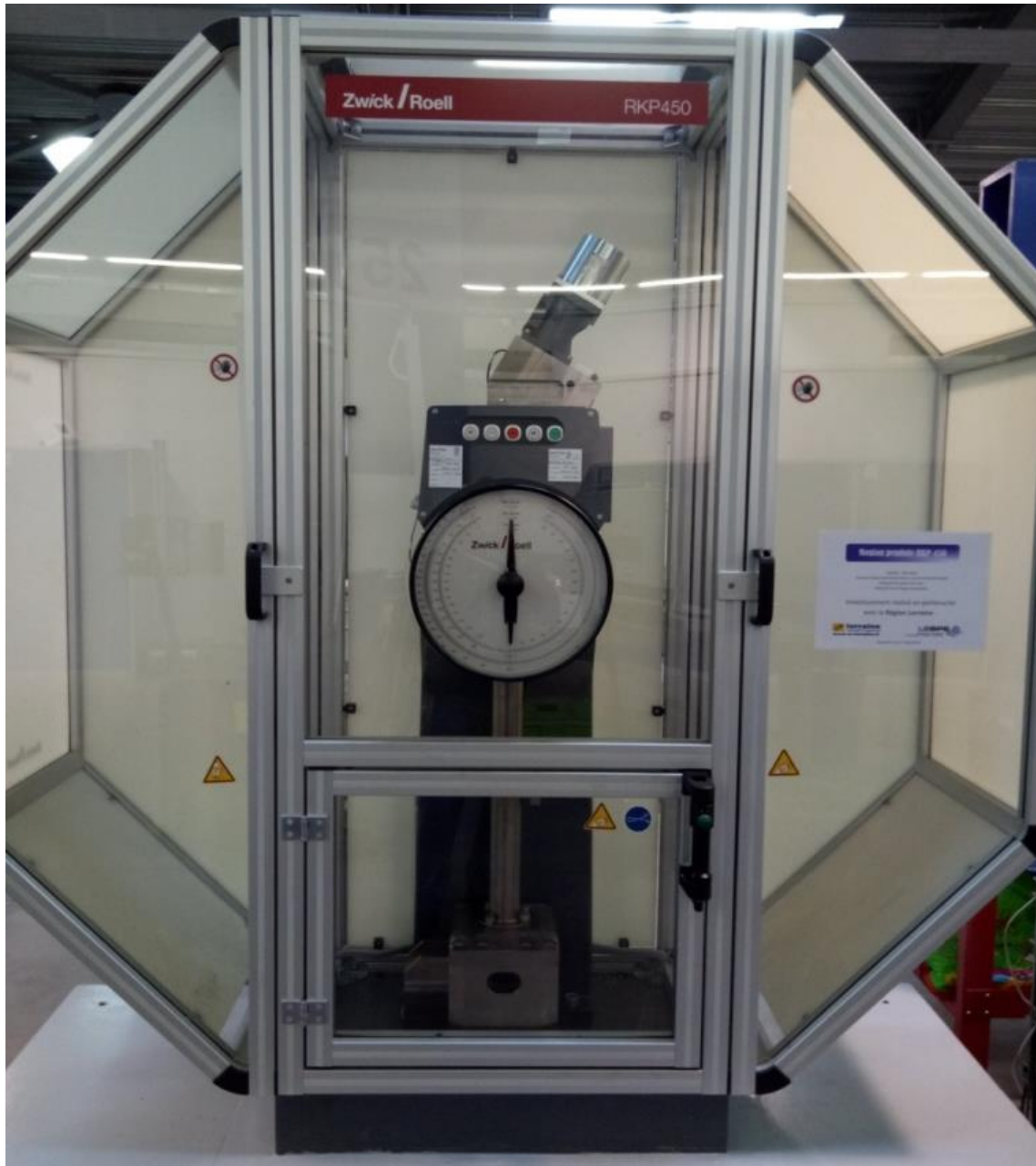


Figure. III.7. Instrumented Charpy testing machine RKP 450.

III.3.3. PRINCIPLES OF CHARPY MECHANICAL TEST

Impact Charpy test is carried out to determine the behavior of materials under impact stress. The amount of the absorbed impact energy indicates the “toughness” or the “fragility” of the material [8]. The energy needed for the fracture of the sample, which dimensions are standardized (ISO 14556), is called absorbed impact energy and it is determined by the following formula [9]:

$$K_U \text{ or } K_V = G(h_1 - h_2)$$

Equation III.1

Where the K_U or K_V is the absorbed energy (specimens with U or V notch), G is the weight of the hammer; h_1 is the initial height of the hammer and h_2 is its final height.

Figure. III. 7. Depicts a schematic view of the test.

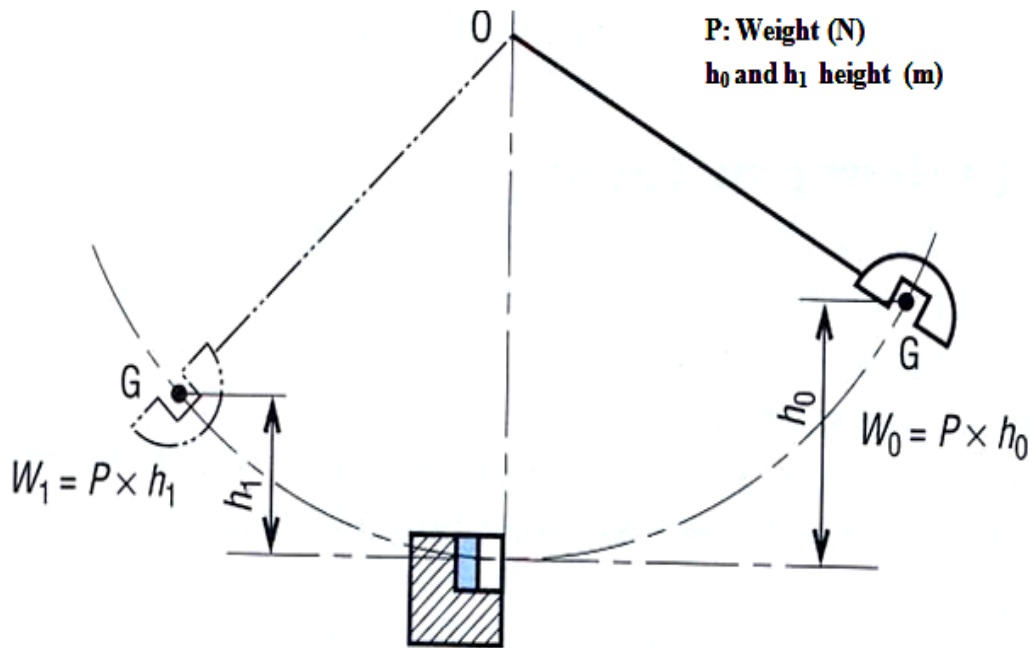


Figure. III.8 Description of the Charpy mechanical test.

III.3.4. CHARPY TEST SPECIMENS

In this study, only V-notch specimens were used. V-shaped notch machining is performed by a slot machine. Tests were carried out on standard sizes of $55/10/10 \text{ mm}^3$, V-notched depth of 2 mm, made at an angle of $45^\circ \pm 2^\circ$. All measurements were within the limit values defined in the standard ISO 14556

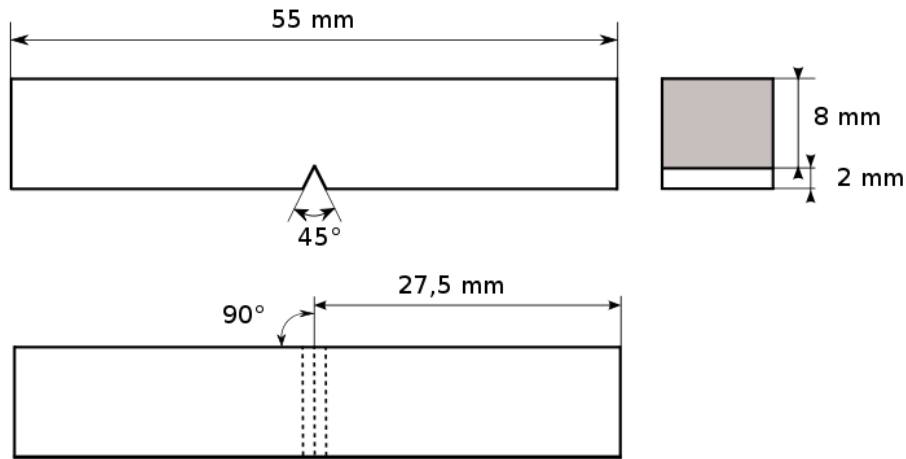


Figure. III.9 Scheme of Charpy impact test specimen

The specimen's preparation for Charpy test was performed on samples extracted from the pipe tube of 610 mm diameter and 11 mm thickness. We cut a rectangle of 400/55 mm from the pipe. Then a specimen of 10/10/55 mm was machined. Finally, a V-notch of 2 mm depth at an angle of $45^\circ \pm 2^\circ$ was performed with a broaching machine. The process is described in Figure III.10.

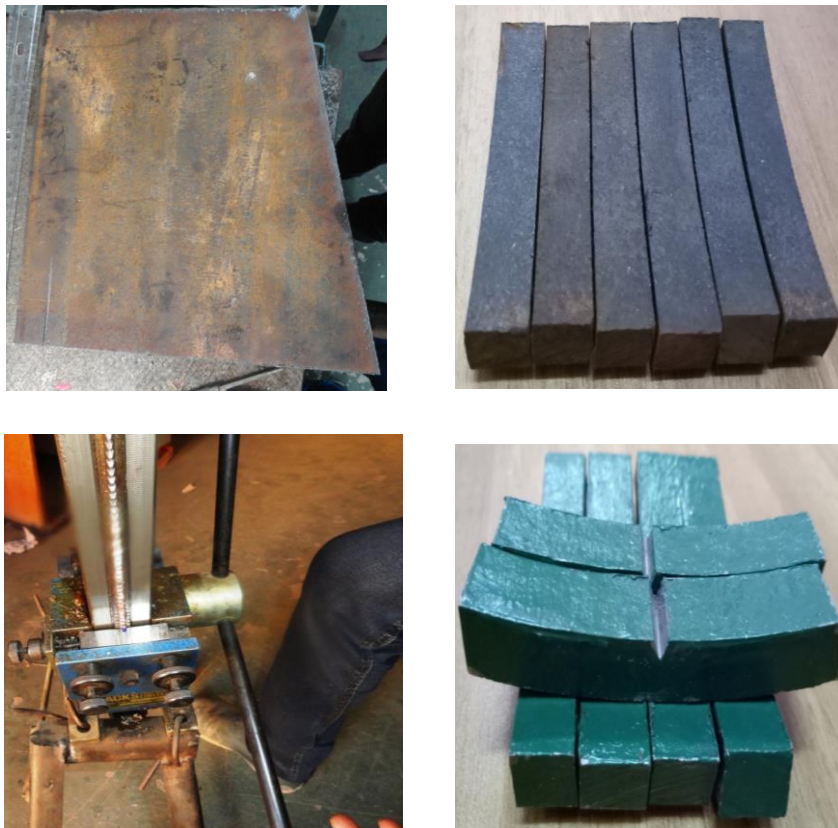


Figure.III.10 Charpy test specimen preparation

Before immersion in different solutions, the specimens were protected by a layer of varnish except the notch.

III. 4. DROP-WEIGHT TEST

The main research interest, in this study, is to assess the effect of green inhibitor of absorbed energy by specimens immersed in different concentrations from both X52 and X65 pipe steels, up to the penetration of the specimens by an impactor. This is to use the drop-weight test. The objectives of the drop-weight-test are to establish a consistent quantification of the fracture response of the material to the energy absorbed by the specimen. Drop weight machines are in use to conduct test at low velocity impact loads.

III. 4. 1. DROP-WEIGHT TEST PRINCIPLE

The drop-weight test is illustrated in Figure III.11. The input energy is determined by the weight of the steel disk (M) that is dropped on the specimen from a level (h_1). The drop height (h) is the difference between the final (h_2) and the initial (h_1) position of the steel weight. The machine principle is based on the impacts produced by dropped mass in free fall velocity under gravity which is given by:

$$E = Mg(h_1 - h_2) \quad \text{Equation III.1}$$

Where: M , g , h_1 and h_2 are the mass of the dropping disk, the acceleration due to gravity (m/s^2), the height of the dropping mass and the height of the specimen, respectively.

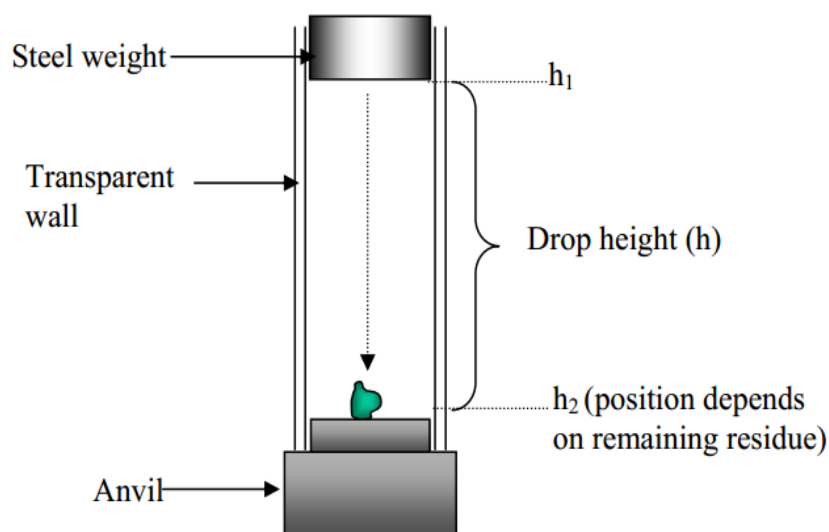


Figure III.11. Simple illustration of the drop-weight test machine

III. 4.2. DROP-WEIGHT TEST MACHINE

The drop weight machine is shown in Figure III.12. The drop weight test facility consists of various devices which are used to measure the velocity, the force and the displacement of the impactor to calculate the energy absorbed by the specimen under the test. The details of the instrumentation employed for the purpose is explained below:

- ✓ Maximum impact velocity=6m/s ;
- ✓ Maximum impact energy=340J;
- ✓ Single impact in all testing conditions;
- ✓ Possibility of varying impact energy and velocity independently;



Figure III.12. Drop weight test machine.

In this work, the testing methodology consists of a heavy anvil (21 kg) equipped with a mechanical clamping support fixture to fix the specimen, and a drop tower with two vertical rod guides on which the impactor runs by means of two roller bearings. A pneumatic braking system captures the falling mass after the first rebound in order to prevent multiple impacts on the specimen. By varying the falling mass and the drop height different impact energies and velocities can be obtained, in order to study their influence on impact effects.

III. 4. 3. IMPACTORS OF DROP-WEIGHT TEST

The impactor shapes are chosen so as to limit their deformability as much as possible and to assure their main function of transferring energy to the specimen without absorbing can be replaced, allowing us to study the influence of the size and shape of the indenter on the impact. Figure III.13 illustrates a schematic view of the impactor in the drop weight test.

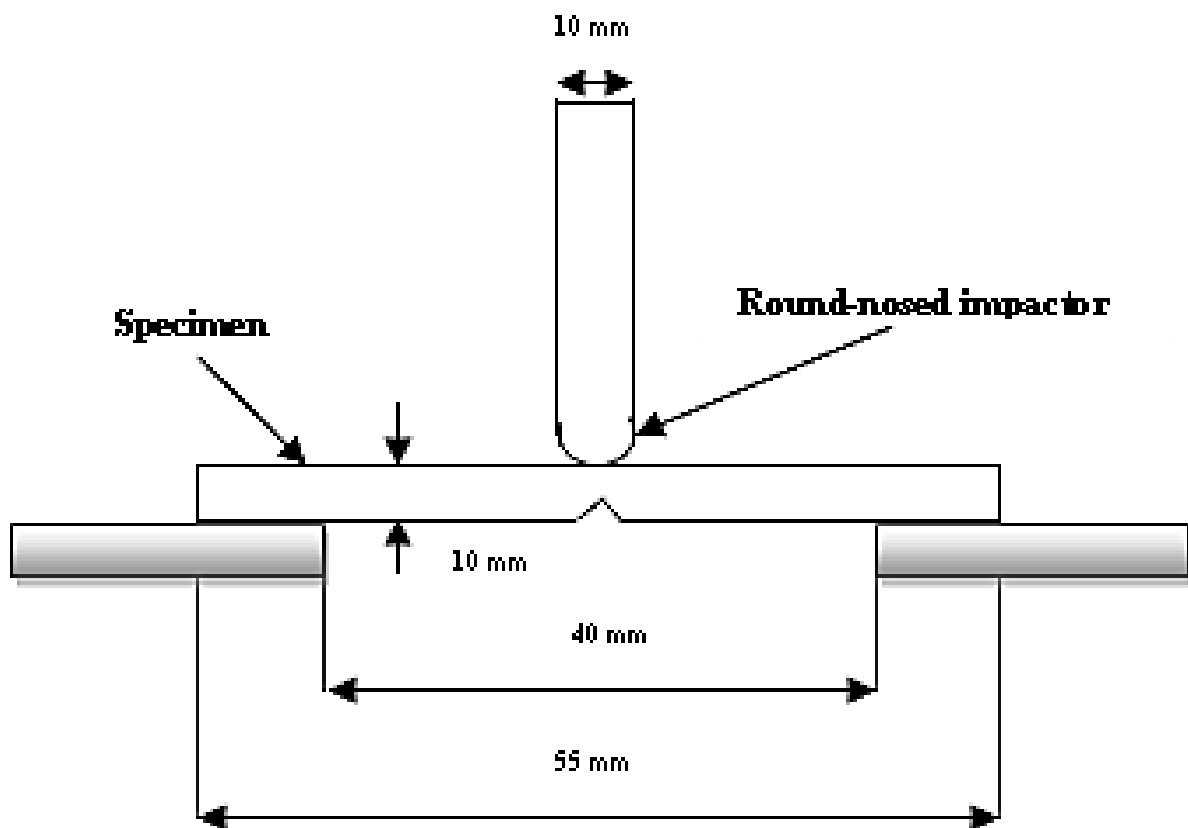


Figure III.13: Schematic of the drop weight test

III.5.THREE POINT BENDING TEST

There are several reasons why the three-point-bending test is used extensively in material characterization, of specimen preparation and testing, ease of adaptability to environmental testing, convenience for fracture toughness studies, and the availability of well documented simple formulas for analyzing materials having equal tension and compression properties [10-12].

Another important reason is that the three-point-bend test is a simple way to subject a specimen to tension, compression, and shear simultaneously. In this sense, a three-point-bend test provides a direct measure of the structural integrity of the material.

The 3-point bending test measures the breaking strength of a material. A test piece of the material to be tested is placed on two supports and a growing force is applied to the center of the bar until the rupture. Like the compression test, the bending test does not generally achieve the complete breakdown of ductile materials. [13]

This test is characterized by the simple assembly of the test pieces and its simple geometry. During the test, the upper part is in compression and the lower part is in traction.

III. 5. 1. THREE POINT TEST MACHINE

These tests were carried out on a WP 310 reaction machine, in agreement with the European standard (ISO 12135). Figure III.14 shows the three-point bending test machine, the specimen geometry is placed in a fixture attached to a materials testing machine and loaded until broken.



Figure. III. 14. Three-point bending machine, PW 310 universal machine

The force and displacement are displayed numerically and can be sent to a computer for operation. A control box allows to adjust the speed of movement, the maximum force and to control the hydraulic unit.

III. 5. 2. THREE POINT BENDING TEST SPECIMENS

The dimensions of the specimen of three point test are the same used in the Charpy test. In this study, the specimens were V-notched with the dimensions of 55/10/10mm for length, width and thickness, respectively. The specimens are schemed in Figure III.15. In this Figure, the dark lines depict the evolution transition of the test. The specimens geometry is place on two support points, and a third (loading) point applies a downward load at the mid-specimens.

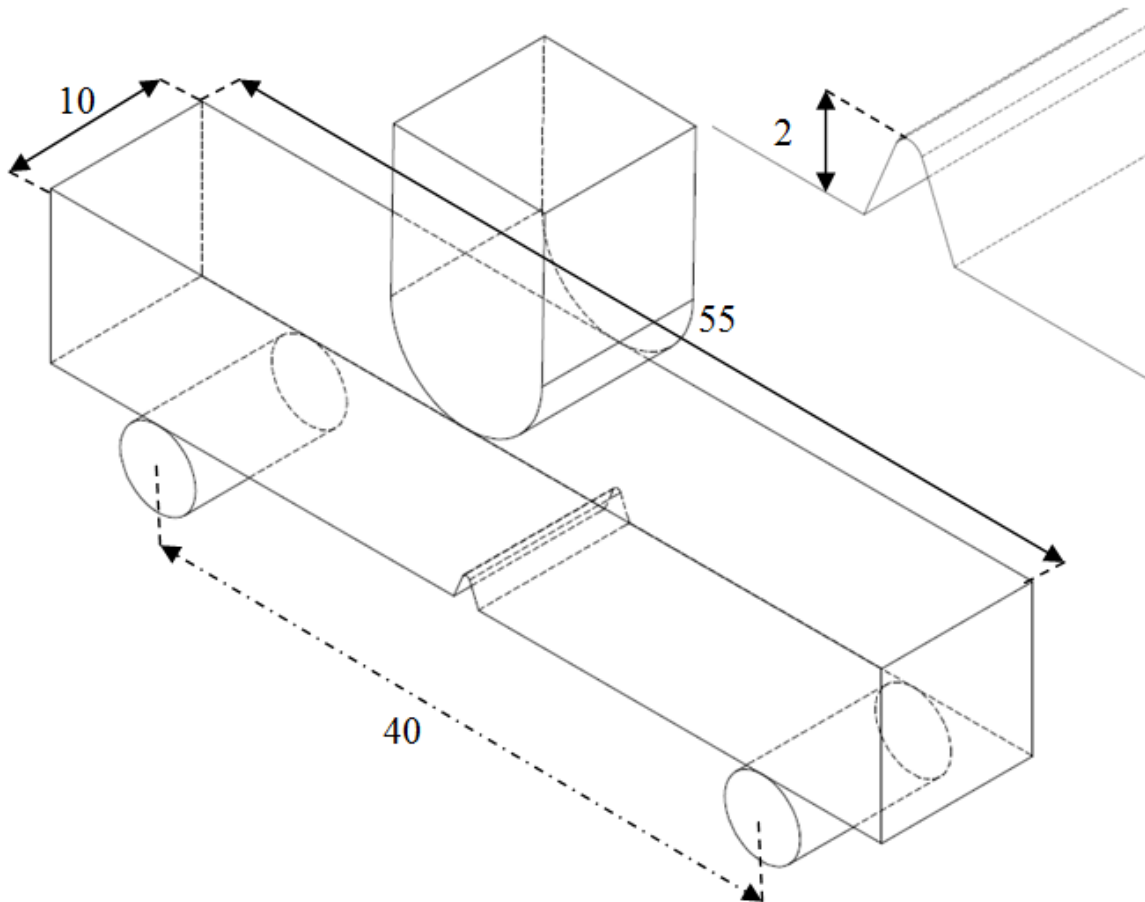


Figure III.15. Scheme of the three point test specimens

III. 5. 3. MECHANICAL PROPERTIES MEASURED BY 3-POINT BENDING TEST

A plot of the load vs. displacement data is generated for analysis as shown in Figure III.16. From the load-displacement plot, we derive a number of parameters that describe the structural properties of the API 5L X52 steel. The five parameters recommended for a basic description are: the stiffness, the yield load, the maximum load, the post-yield displacement and the work-to-fracture.

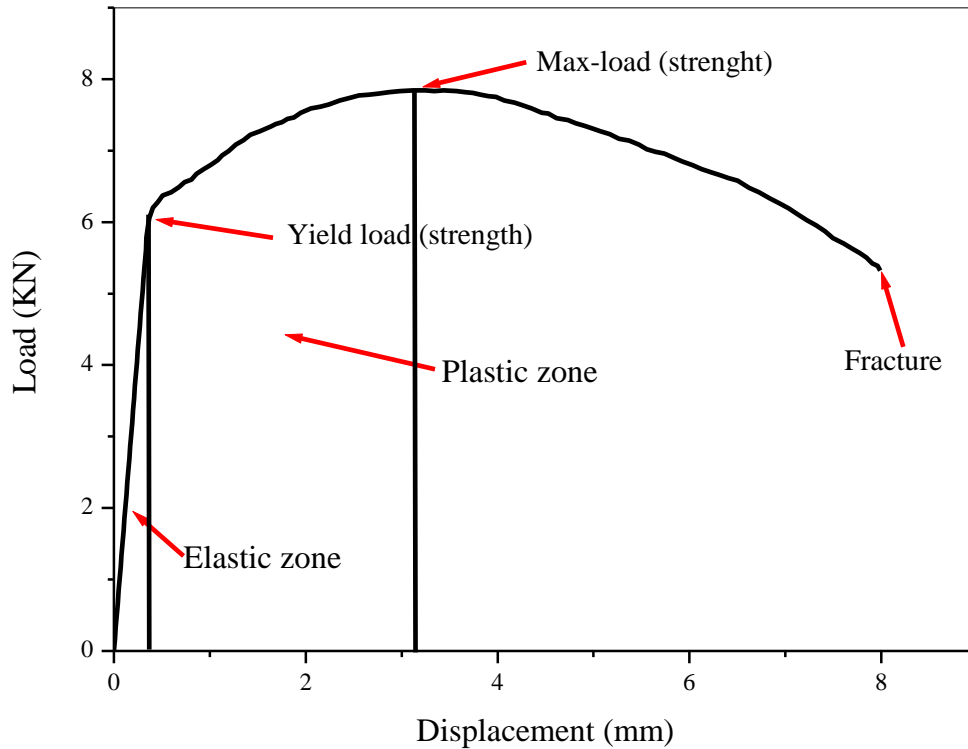


Figure. III.16: Load-displacement plot from a bending test of a specimen of API 5L X52 steel.

In this work, only the maximum load was determined from data as function the displacement.

III. 6. TENSILE TEST

The Tensile test is a mechanical test to determine the tensile properties of a material, such as, the elastic deformation properties (elasticity modulus), the strength properties (yield strength and ultimate tensile strength) and ductility properties (elongation). The tensile test is useful for the estimation of the difference in behavior of the mechanical properties between the different specimens subjected to different treatments (acidic media, green corrosion inhibitors, synthetic corrosion inhibitors...etc.).

III. 6. 1. THE TENSILE TEST MACHINE

An electric Zwick/Roell Z250 static traction machine, shown in Figure III.17, of a capacity of 250kN, has been used for carrying out the standardized characterization tests of the Young's modulus, yield strength, ultimate strength and elongation at break...etc.).



Figure III.17. Electric Static Traction Machine Zwick/Roell Z250

This machine is equipped with pneumatic jaws allowing solicitation of flat specimens of thickness ranging from a few tenths of a millimeter to 15mm. Longitudinal and transverse deformation is monitored by a video extensometer.

III. 6. 2. TENSILE TESTING SPECIMENS

The tensile test specimens were performed on samples extracted from a tube of 610mm in diameter and 11 mm thickness. A rectangle of 400/55 mm was cut from the tube. The specimens were then cut according to the NF EN 10045-1 standard.

All test specimens were machined longitudinally with respect to the rolling direction to the dimensions specified by the thickness of the pipe (11mm). The geometry of the specimens is schemed by Figure III.18 and the dimensions are indicated in Table III.7. Figure III.16 shows the rectangular sample cut from the tube and the machined test specimens.

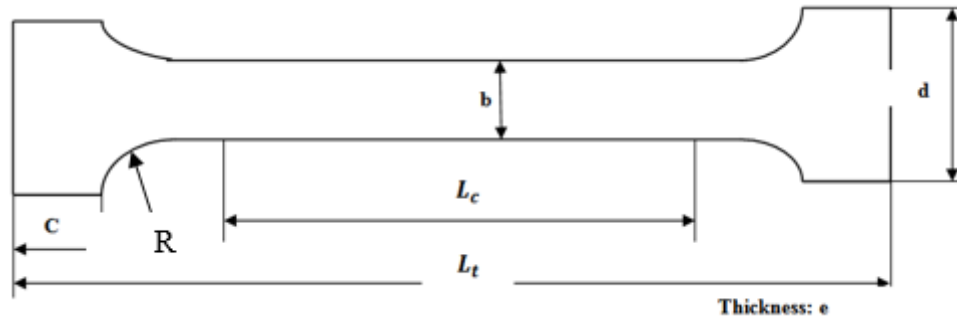


Figure.III.18. The specimen Geometry For Tensile Testing.

Table III-6: The Specimen Dimensions

Tensile Specimen machined from a $\text{Ø}610$ pipe	
Total Length L_t	150 mm
Calibrated Length L_c	60 mm
Useful Width: b	10 mm
Head Width: d	20 mm
Head Length : C	20 mm
Radius : R	12 mm
Thickness : e	11 mm



Figure III.19. The rectangular sample (left) and the tensile specimens (right)

III. 6. 3. MECHANICAL PROPERTIES MEASURED BY TENSILE TEST

A plot of the stress vs. strain data is generated for analysis as shown in Figure III. 20. From this curve, several parameters could be determined. The elastic limit, the ultimate tensile strength and the fracture point. In this work, the elongation is calculated.

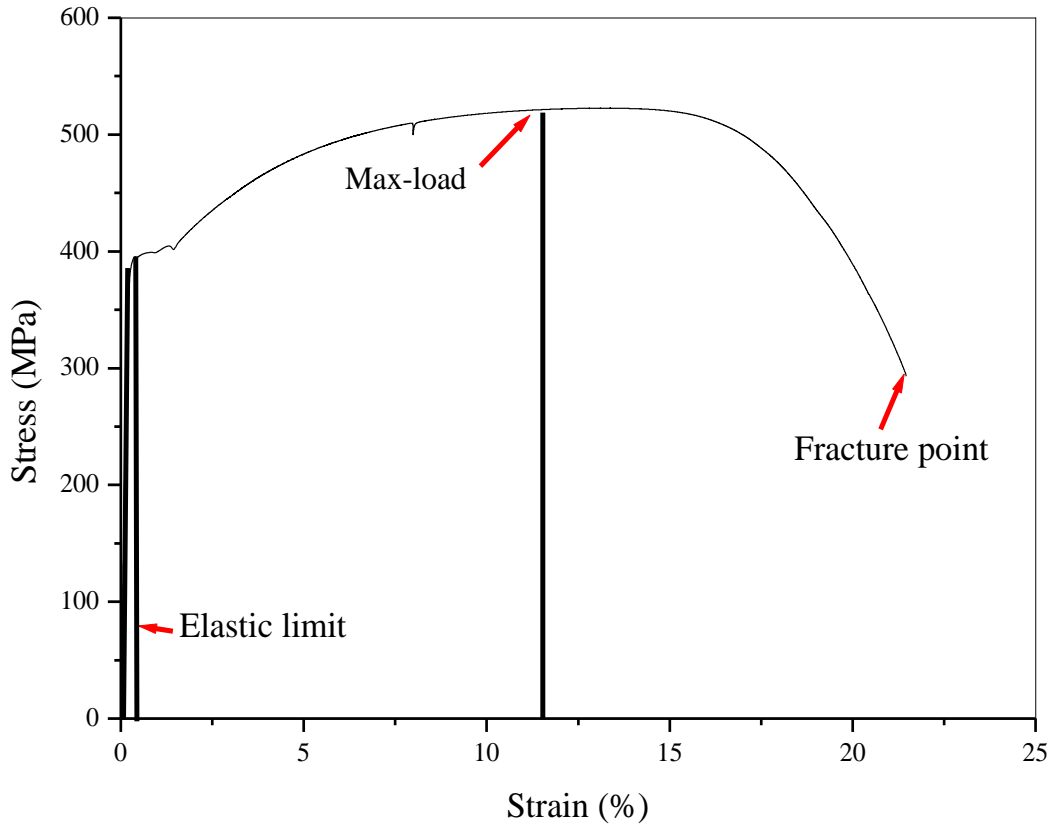


Figure III.20: Stress-strain curve of a API 5L X52 steel

The stress is related to the strain in the elastic mode by the well-known Hook equation below:

$$\sigma = E\varepsilon \quad \text{Equation III.3}$$

Where: σ , E and ε are the stress, the Young's modulus and the strain respectively. The stress is determined by:

$$\sigma = \frac{F}{A} \quad \text{Equation III .4}$$

Where: F and A are the force and the section area, respectively. The strain is determined by:

$$\varepsilon = \frac{L}{L_0} \quad \text{Equation III.5}$$

Where: L and L₀ are the length of the specimen under the test and the original length, respectively.

III.7.THE PREPARATION METHOD OF THE GREEN CORROSION INHIBITOR

III.7.1. PRESENTATION OF THE PLANT

"Green" inhibitors, as a solution for anti-corrosion to protect pipes are obtained by extraction solution from natural plants. This green name's *Ruta Chalepensis* shown in Figure III.21. A significant amelioration of mechanical properties is obtained by using this *Ruta Chalepensis* and is attributed to an inhibitor film on surface.



Figure. III.21.Green and dried plant leaves process

III.7.2. EXTRACTION METHODOLOGY

The extraction of the corrosion inhibitor was done by 10 (g) of the plant leaves *Ruta Chalepensis*, this 10 (g) was put in 1M of HCl and was then heated to boiling point. The aqueous solution is filtered. This solution is used to prepare solutions of different concentrations.

The corrosive medium that a 1M hydrochloric acid solution, is obtained by diluting the commercial concentrated 37 % HCl acid with distilled water. That by mixing 83 ml of HCl with 917 ml of distilled water



Figure. III 22. Acid grade 37% HC, Heating operation of the dried plant leaves

III.7.3. THE PREPARATION OF THE TESTING MEDIA

Different concentrations of the extract of corrosion inhibitor, were prepared by diluting the stock solution with the respective of 1 M HCl, and in the same time we are prepared 30% of the synthetic inhibitors, for example the preparation of 100 mL (green inhibitor + 1 M HCl solution) is presented by this way:

- 3% : 3mL oil extraction with 97 mL of acid solution (v/v) ;
- 5% , : 5 mL oil extraction with 95 mL of acid solution (v/v);
- 10% , : 10 mL oil extraction with 90 mL of acid solution (v/v);
- 20% : 20 mL oil extraction with 80 mL of acid solution (v/v);
- 30% , : 30 mL oil extraction with 70 mL of acid solution (v/v);

With the same amount of hydrochloric acid solution, the second and third solution are obtained, but with 30 % concentration of different synthetic inhibitor obtained from SONATRACH

References

- [1] Julien. C, Dmytrakh. I, Pluvinage, G, "Comparative assessment of electrochemical hydrogen absorption by pipeline steels with different strength", *Journal of Corrosion Science*, (2010), Vol 52 pp1554–1559
- [2] Elazzizi. A, Mohamed. H. M, Khelil, A, Pluvinage, G, Matvienko, Y.G. "The master failure curve of pipe steels and crack paths in connection with hydrogen embrittlement", *Int. J Hydrogen Energy*, (2015), Vol 40, pp, 2295-2302.
- [3] Mohammed H. M, "Approche globale a deux parametres ($K_{\rho-T}$ ρ) Estimation des contraintes de confinements dans des structures portant des entailles", University Paul Verlaine of Metz.
- [4] Momamed. S, M. Mohammed H. M, El-Miloudi. K, Azari. Z, Sorour. A. A., Merah. N, Pluvinage. G, "Reduction of hydrogen embrittlement of API 5L X65 steel pipe using a green inhibitor", *International journal of hydrogen energy xxx* (2018), pp. 1-10
- [5] Tóth, L., Rossmannith, H.P, Siewert, T.A, "Historical Background and Development of the Charpy Test", *Journal of Minerals and Materials Characterization and Engineering*, (2002), Vol.2 No.5, pp3-17
- [6] ISO 14556:2000, "Steel -- Charpy V-notch pendulum impact test -- Instrumented test method," International Standards Organization.
- [7] ASTM E2298-13a, "Standard Test Method for Instrumented Impact Testing of Metallic Materials," ASTM Book of Standards, Vol. 03.01, 2014.
- [8] Željko. A, Davor. M, Andrija. D, Matija. S, "Application of instrumented charpy Method in characterisation of materials", *Journal of Interdisciplinary Description of Complex Systems* (2015), Vol 13(3), pp 479-487,
- [9] Chris N. M. Ray A. S. *Instrumented Impact Testing: Influence of Machine Variables and Specimen Position* National Institute for Standards and Technology, Material Reliability Division, Boulder CO (USA), 2008, SCK•CEN Open Report BLG-1058 – Pp 1-45

References

- [10] Julien. C, Pluinage. G, "Modification of failure risk by the use of high strength steels IN PIPELINES, The Twelfth Meeting "New Trends in Fatigue and Fracture" (NT2F12), Romania, (27–30 May), 2012
- [11] Ogorkiewicz. R.M. , Mucci. P.E.R., "Testing of fibre-plastics composites in three-point bending", (1971), Vol 2, Issue 3, pp. 139-145
- [12] Yamamoto, C. A.: "Evaluation Techniques for Simple Mechanical Property Tests on Composite Materials. Advanced Techniques for Material Investigation and Fabrication". Western Periodicals Co., 1968, paper 1-2-3.
- [13] Bouledroua. O., Ouled Mbereick. M, Azari Z., Mohamed. H. M, "Qualification d'un Acier API 5L X70 : Etude Expérimentale et Validation Numérique", Journal of Nature & Technology, (2015), Vol 13, pp 34-39
- [14] Pluinage G " Fracture and Fatigue emanating from stress concentrators"; Editeur Kluwer, (2003).

Chapter IV

Results and Discussion

IV.1. INTRODUCTION

In this chapter, we present the results and discussion for the experiments carried out on API 5L X52 and X65 grades pipeline steel. In the first part, a macroscopic and microscopic examination of the surface of the under study materials are presented. Corrosion inspection of the surface of the steel was done with visual observation and both optical and scanning electron microscopes.

The aspect of the surface in relation with the mechanical properties is highlighted.

In the second part, we present the mechanical tests carried out in this study. Four mechanical tests were made. The fracture toughness J_c was determined from Charpy test by the equation IV.11 (dynamic test), the drop point test was carried out to estimate the energy absorbed by the specimens, the displacement was determined by three point bending (static test). Finally, the stress-strain relation was determined from tensile tests.

All the specimens were machined from an API 5L X52 and X65 steel grades taken from a gas transport pipe manufactured for Sonatrach in the transverse direction. This pipe is of outer diameter of 610mm and 11mm thickness.

IV.2. ANALYSIS OF CORROSION CAUSES

Pipeline of oil and gas transportation as faces many problems caused by internal fluids such as natural gas, oil, and water[1-2].

Internal fluids are a cause of the internal failures of component pipe network. Due to the effect of the fluid contents, metal chemical composition, microstructure, manufacturing and service defects.

The internal corrosion is one of the terrible failure of the gas and oil network transportation. Many studies and reports confirmed the internal corrosion come from the internal reaction between the internal surface of the pipe and chemical compounds such as carbon dioxide (CO_2), and hydrogen sulphide (H_2S). These compounds are responsible for various degrees of mechanical properties degradation [3-7].

From this case, we present in this section the scenario of pipe failure by some analyses below in the first part of this experimental study. At the end, some suggestions and recommendations is noted.

VI.2.1. VISUAL OBSERVATIONS

The schematic of the location of a failed pipe and the general view are presented respectively in the Figure IV.1 and Figure IV. 2.

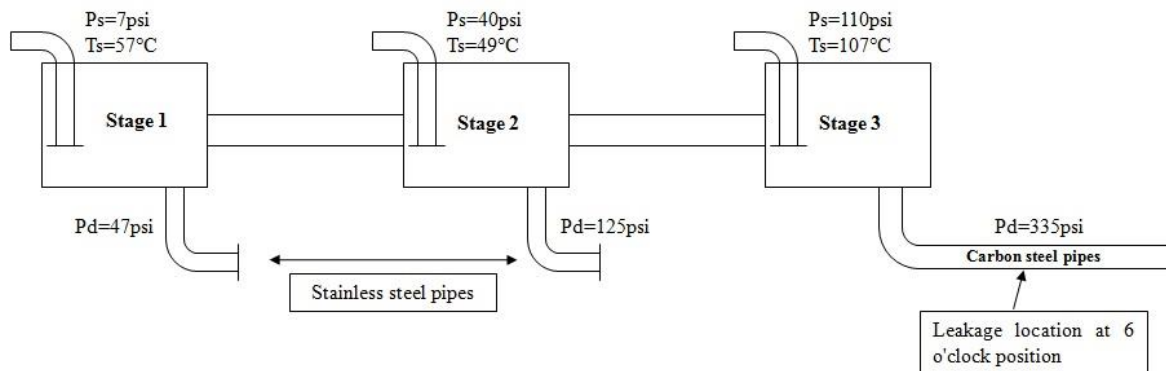


Figure IV.1. Schematic view of process diagram and the rupture location at the third stage. [8]

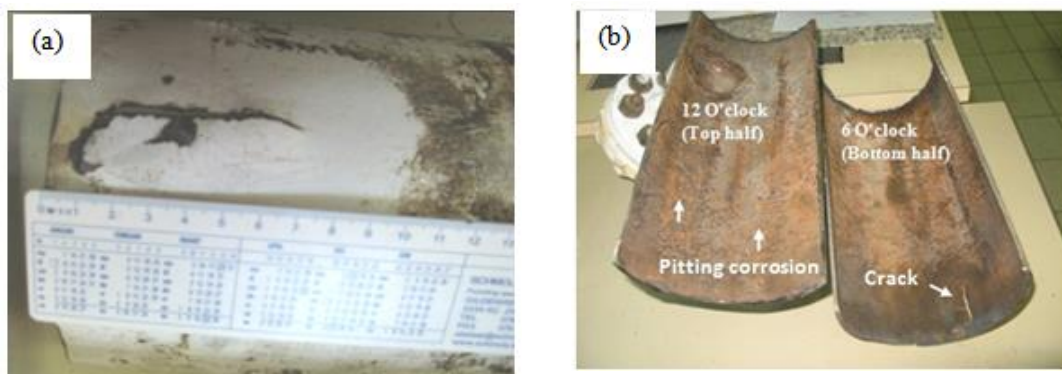


Figure IV. 2. General view of a failed gas pipe; (a) External surface and (b) internal surfaces [8]

Figure IV.2 (a) shows the crack on the ruptured external area and. Figure IV.2 (b) shows the two halves of the internal surface of the pipe.

The first half at the right (b) is the bottom part of the pipe at 6 o'clock position, where the internal surface crack is shown. The second half at the left (b) was the top part at 12 o'clock position, where the pitting corrosion is shown.

The bottom part confirmed the longitudinal crack as indicated by the white arrow in Figure IV. 2 (b).

IV.2.2. OPTICAL MICROSCOPE EXAMINATION

IV.2.2.1. EXTERNAL SURFACE

Magnified ruptured area of the external pipe surface is presented in Figure IV.3 [8].

This image shows the bulge of the pipe from the internal surface to the external surface. This bulge indicate that the model of this fracture is a ductile.

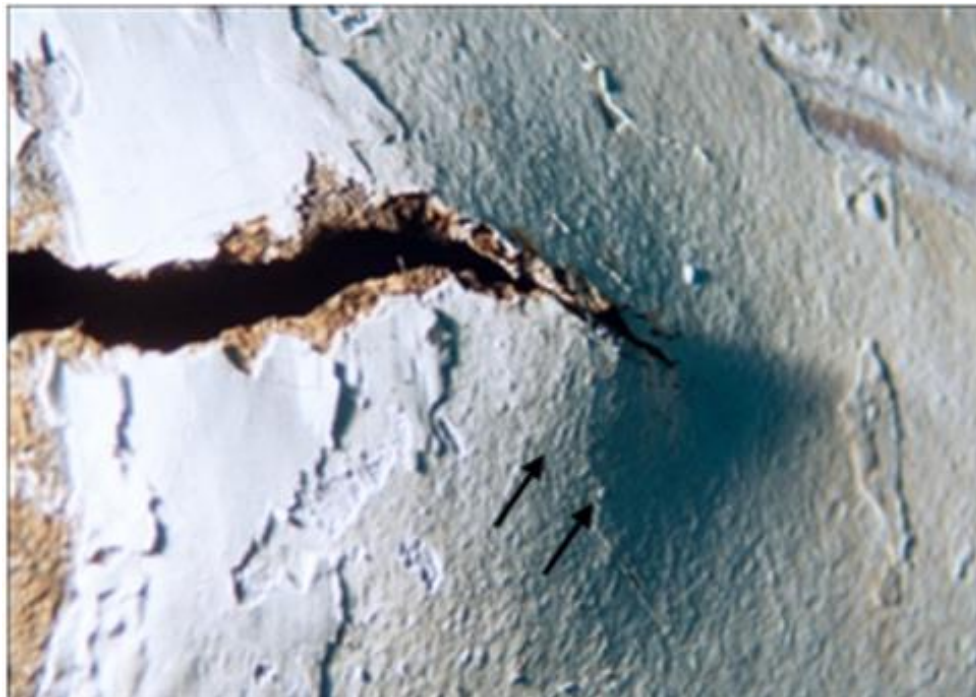


Figure. IV. 3. Macroscopic observation on the external pipe surface (50X magnification).

IV.2.2.2. INTERNAL SURFACE

Macroscopic investigation on the internal surface of the pipe was carried out to verify the wall internal condition. The verification of the wall internal condition shows the pitting corrosion was present on the pipe wall as shown in Figure IV.4 [8].



Figure IV.4. Macroscopic observation on the internal pipe surface showing pitting corrosion (50X magnification)[8]

Image in Figure IV.5 presents a crack evaluation. At the symbol I the initiated crack of the pipe is in the circumferential evolution direction and after that at the symbol II, the crack was changing to the longitudinal direction.

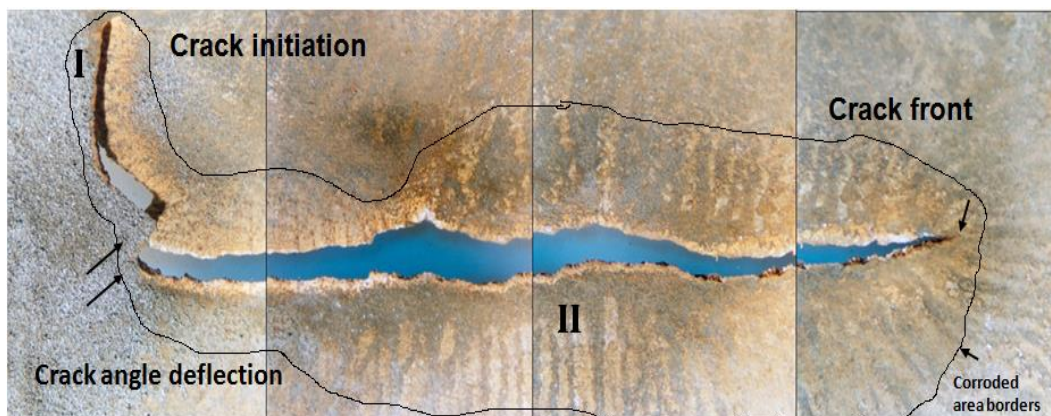


Figure IV. 5. General view of the crack on the internal surface of the pipe (100X magnification)[8]

The angle deflection crack is circumferential to longitudinal is clearly observed in this image indicated by black arrows. In general, the crack direction is propagated from the corroding area, and stopped at the front. Reduction of the thickness of the pipe is clearly noticed to a border of the area due to internal corrosion. Figure IV. 6 shows the crack propagation path, crack tip, and the wall reduced thickness

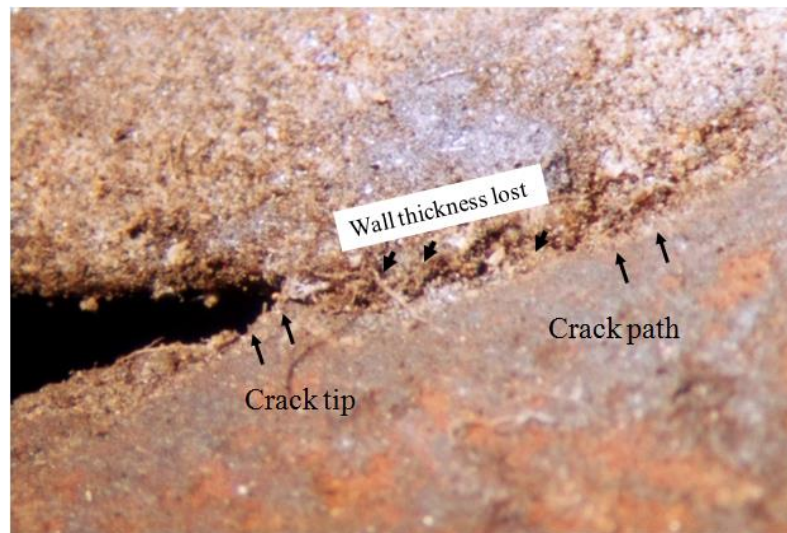


Figure IV. 6. Close view at the internal surface of the pipe shows the crack tip and the preferable path for the crack growth (150X magnification)[8]

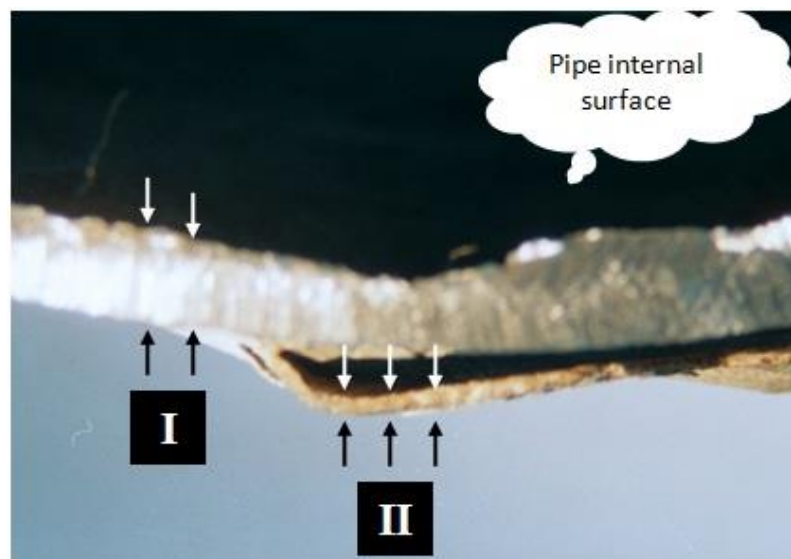


Figure IV. 7. Thickness difference between slightly corroded and ruptured area (150X magnification)[8]

Macroscopic investigation of the thickness area at the rupture and the area away from the corroded zone is shown in Figure IV.7. We noted the thickness of the corroded area by the symbol. I. and the thickness at the ruptured area by the symbol. II. This examination shows around $\approx 90\%$ of the original thickness was lost due to internal corrosion

IV.2.3. SCANNING ELECTRON MICROSCOPY EXAMINATION

Image of scanning electron microscopy was taken on the crack initiation zone as seen in (I) Figure IV.8. These observations of both optical and electron microscopy show the ductile fracture mode. The presence of bulge on the external surface supported these observations.

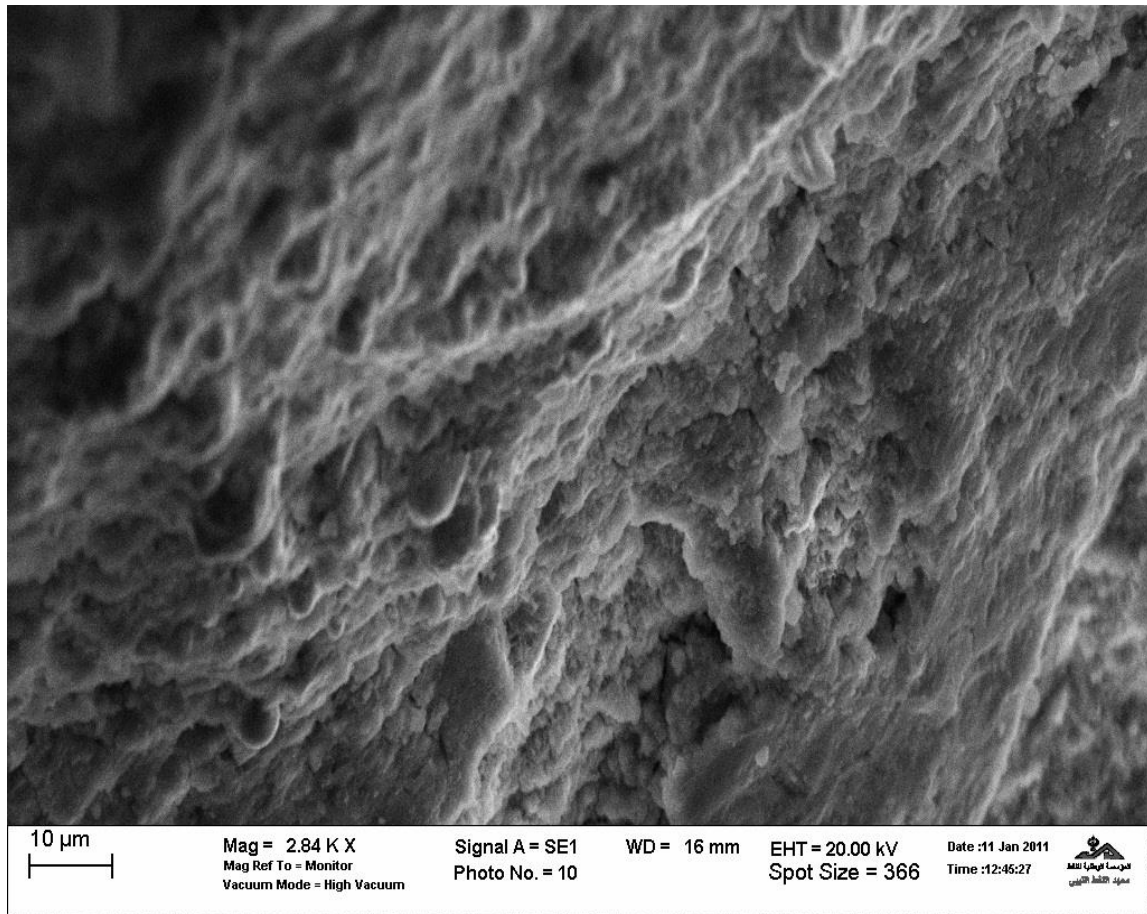


Figure IV.8. SEM image on the fracture surface. [8]

IV.2.4. CHEMICAL ANALYSIS BY XRD

Chemical analysis of the corrosion product was performed by X-ray diffraction (XRD) technique by Ital structures APD 2000 diffractometer, using Cu-K α radiation. The metal analyzer detected that the pipe chemical composition contains elements in wt % of 0.17C, 0.206Si, 1.02Mn, 0.095Cr, 0.034Ni, 0.028Mo, 0.015P, 0.036Al [8].

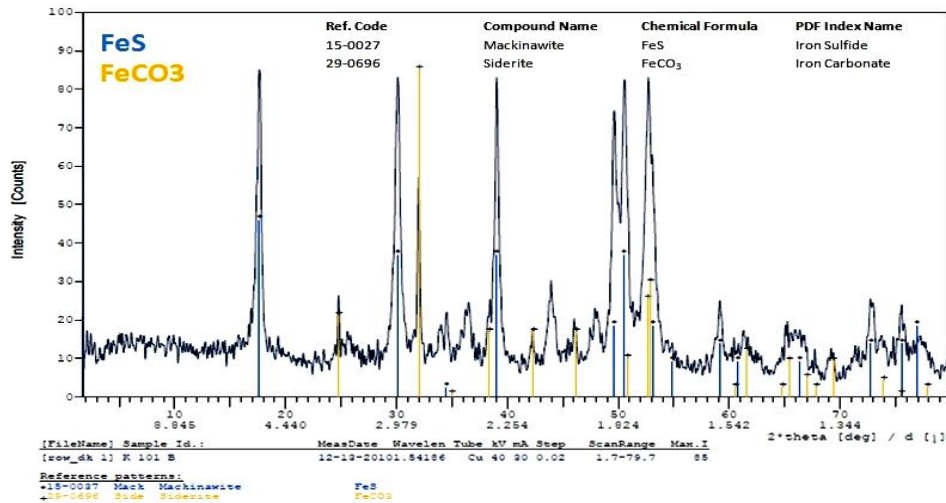
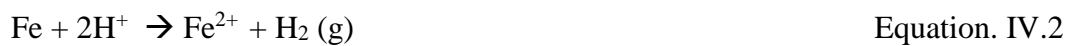


Figure IV. 9. XRD analysis of corrosion product [8]

The diffractogram shown in Figure IV.9 indicates the presence of iron sulphide at 17, 30, 39, 49, 50, 53° 2 θ [9] and iron carbonate at 25, 32, 37.2, 42.2, 46, 51, 53, 62, 65, 69, 74° 2 θ [10-11]. These two corrosion products are often the result of the chemical reaction between iron and wet H₂S and CO₂ as schemed below. These observations coincide with the experimental observations made by Schmitt et al. [12].



IV.2.5. CORROSIVE FLUID

Internal corrosion of the pipe wall is due to the presence of hydrogen sulphide, and carbon dioxide. Reduction of the pH caused by the reaction between internal surface of the pipe and the hydrogen sulphide H_2S and/or carbon dioxide CO_2 leading to the pitting corrosion and acid attack. Reduction of pH caused the increase of the corrosion evolution in gas pipelines the components of the iron sulfides FeS and iron carbonic $FeCO_3$ come from the activation of iron in solution.

This interpretation is confirmed by the experimental results in the literature [14-17]. The absence of corrosion inhibitor or internal coating, to protect the internal surface from the attack of fluids resulted in pitting and general corrosion of it.

IV.2.6.METAL WALL THICKNESS REDUCTION

Visual and microscopic analysis show the reduction of the wall thickness due to the pitting corrosion of the internal surface. This reduction leading to the degradation of the integrity of this pipe.

Carbonic acid (H_2CO_3) and hydrogen sulphide (H_2S) solution caused the corrosion reactions. Tendency to pitting corrosion of low alloy steel in carbon dioxide CO_2 increased in the temperature range of 70 to 110°C [3].

Electrochemical corrosion cells created by the corrosive acid on the pipe surface leading to metal thickness reduction at the anodic area. At the 6 o'clock position of the pipe, high rate of metal loss is located. Because this position was also in contact with wet, and fluids during the pipe service

IV.2.7.FINAL RUPTURE

The acceleration of the crack path front is initiated at the thinner area of the pipe when the failure happens. This interpretation is in agreement with the observations displayed in Figure IV. (2-6) obtained by visual and microscopic examinations.

The internal pressure lead the crack propagation to be perpendicular to the internal hoop. The crack propagated faster due to the less metal at the thinner area. As the crack propagates, the pipe bulged out and split.

The bulge explaining the failure is a ductile mode. The observed ductile fracture morphology is in agreement with visual and microscopic observations. The metal tearing at the fracture surface is in ductile mode as described in reference [17-18].

IV.2 .8. THE CORROSIVE EFFECT OF HCl

HCl is a strong acid with a corrosive effect on metals. It is used in this study to simulate the sour environment caused by H₂S and CO₂ in the hydrocarbons fluids.

A cubic sample of 10.05 g of API 5L X70 steel was immersed in 1.2M HCl solution for 10 days at 25°C. The sample was mechanically abraded with Emery paper, washed thoroughly with bi-distilled water, degreased with ethanol, dried and weighed before immersion in HCl.

After 10 days of immersion in HCl, the remaining weight was 9.25 g with 80 mg/day weight loss rate. This result suggests that, in 10 days, the steel loses 7.96% of its weight in the acidic solution. The surface of the metal was corroded by the effect of HCl and reflected by a weight loss and a dimension reduction.

This result corroborate the discussion given above for the rupture mechanism under a corrosive fluid.

IV.2.9. CORROSION RATE

To explore the kinetics of the corrosion reaction, the API 570 formula of long period corrosion rate were applied to the pipe. These methods are presented in the Annex . The parameters used in the calculation are:

1. Partial pressure: 335 psi
2. Temperature: 110°C
3. Nominal thickness: 6 mm
4. CO₂ percentage: 7.44 ppm
5. H₂S percentage: 0.01 ppm
6. The service period: one (01) year

In API 570 formula calculation, the parameters mentioned above were inserted in the software and corrosion rate was calculated [8].

The results show that, under these conditions, the rate of corrosion is 5.1 mm/y (the remaining thickness of 0.9 mm) by API 570 formula, respectively.

IV.2.10. RECOMMENDATIONS

The end user of such pipes in similar conditions can meet the following recommendations in order to mitigate this kind of degradation to reoccurrence.

1. Preventing any type of wet is necessary to avoid internal corrosion of the gas pipe.
2. Field survey of fluid chemical analysis, pH measurements and recording of the pipe thickness survey are important to keep extend the pipe life time.
3. Upgrading the pipe material to high corrosion resistant alloys is an option to mitigate the corrosion risk.
4. The existing codes and standards dedicated to the transport of fluids in pipelines have revealed that suitable guidelines for oil and gas transportation are not available and need to be revised [19].

IV.3. MECHANICAL TESTS

From the second part of this experimental study, we presented mechanical tests of the API X52 and X65 steel, such as Charpy test, Drop weight test, Three points bending test, and Tensile test, to study the effect of the green corrosion inhibitor (Ruta chalepensis), on these steel immersed in HCl acid media.

IV. 3. 1. CHARPY TEST (DYNAMIC STUDY)

A standard Charpy impact machine is used as detailed in Chapter III. This machine consists essentially of a rigid specimen holder and a swinging pendulum hammer for striking the specimen. Impact energy is simply the difference in potential energies of the pendulum before and after striking the specimen. The machine is calibrated to read the fracture energy in N-m or J directly from a pointer which indicates the angular rotation of the pendulum after the specimen has been fractured. Dynamic fracture toughness is determined from load-displacement curve obtained from instrumented Charpy impact test. A typical recorded load displacement curve is shown in Figure IV.10.

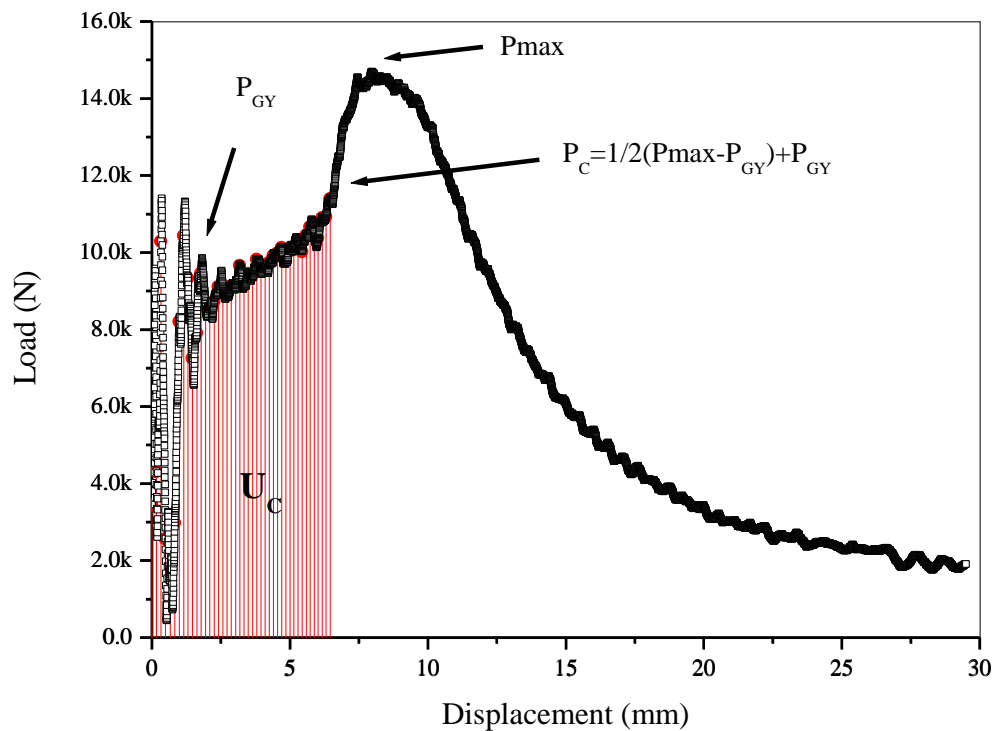


Figure IV.10. Typical load-displacement curve and the determination of the energy absorbed by the specimen

The fracture energy measured in the Charpy test is obtained directly from the apparatus or, more precisely, by integration of the load-displacement curve until the critical load. An approximate method is to define the critical load P_c as the mean value of the sum of the load at general yielding P_{gy} and the maximum load:

$$P_c = \frac{P_{Max} - P_{gy}}{2} + P_{gy} \quad \text{Equation. IV.8}$$

$$U_c = \int_0^{P_c} f(P) dP \quad \text{Equation. IV.9}$$

The work for fracture U_c which is registered during the test is used to evaluate the fracture resistance in different ways. The first one is the energy per unit area or resilience as K_{CV} (V-notched specimen) or K_{CU} (U-notched specimen) defined as:

$$K_{CV} \text{ or } K_{CU} = \frac{U_c}{Bb} \quad \text{Equation. IV.10}$$

Where B and b are the specimen thickness and the ligament width, respectively. We can also calculate the toughness J_C of the material by the following relationship:

$$J_C = \frac{\eta U_c}{Bb} \quad \text{Equation. IV.11}$$

Where (η) is a parameter for the proportionality between the fracture energy per ligament area and the notch fracture toughness. It depends on the notch radius ρ and relative notch depth a/W . Akkouri et al. [20] tabulated the values of η for different notch radii and relative notch depths. The value of 1.92 is used for a Charpy V-notched specimen.

IV.3.2. CHARPY TEST OF API 5L X52 STEEL IN ACIDIC MEDIA

In this section, we studied the influence of corrosion initiated hydrochloric acid on the mechanical properties of API 5L X52 steel. HCl concentrations of 0.25, 0.5, 0.75 and 1M were used with an immersion time of seven (07) days at 25°C.

The fractured API 5L X52 steel Charpy V-specimen is shown in Figure IV. 11.



Figure IV. 11. Fractured V-notched Charpy test specimen.

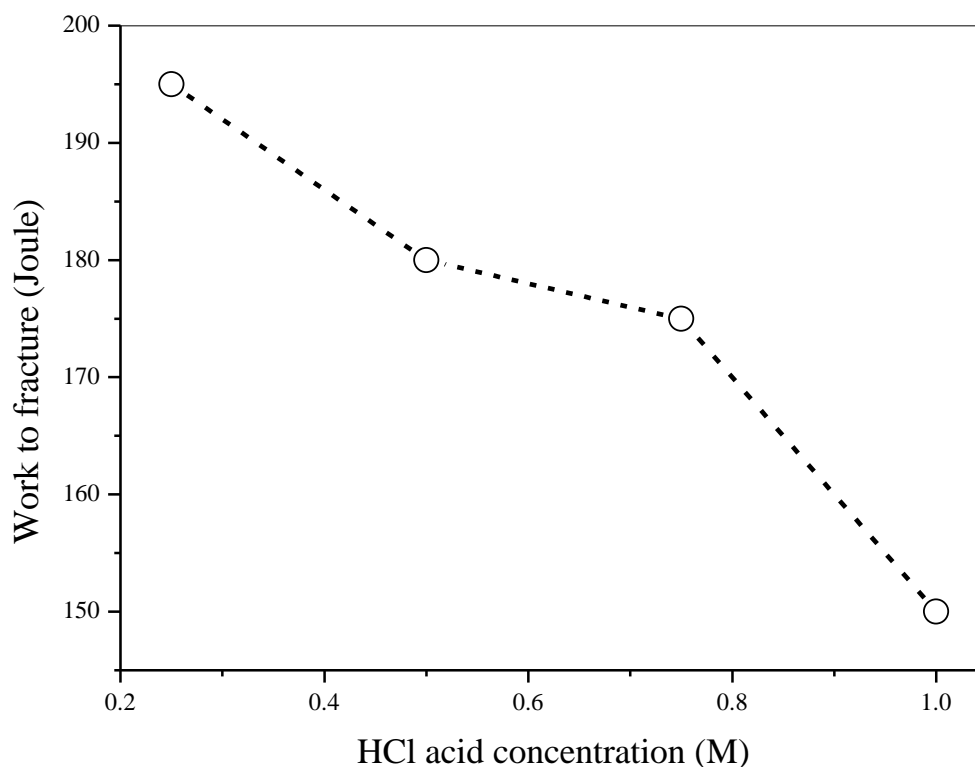


Figure. IV. 12. Variation of the work to fracture vs. HCl acid concentration

As shown in Figure IV.12, the work to fracture decreases strongly with the increase of HCl acid concentration. This is the result of continuous dissolution of the API 5L X52 steel with time in acidic media. The decrease of the toughness of this material, hence the decrease of the absorbed energy, is due to the thickness reduction.

IV.3.3. CHARPY TEST OF API 5L X52 STEEL IN THE PRESENCE OF GREEN INHIBITOR

In this section, Ruta Chalepensis plant extract was used as green corrosion inhibitor. API 5L X52 steel specimens were immersed in acidic medium of 1M for 0.25, 5, 10 and 15 days in the presence of Ruta Chalepensis of different concentrations. 5, 20 and 30 % v/v plant extract to acidic solution were used. The solutions were kept at 25°C until the Charpy tests.

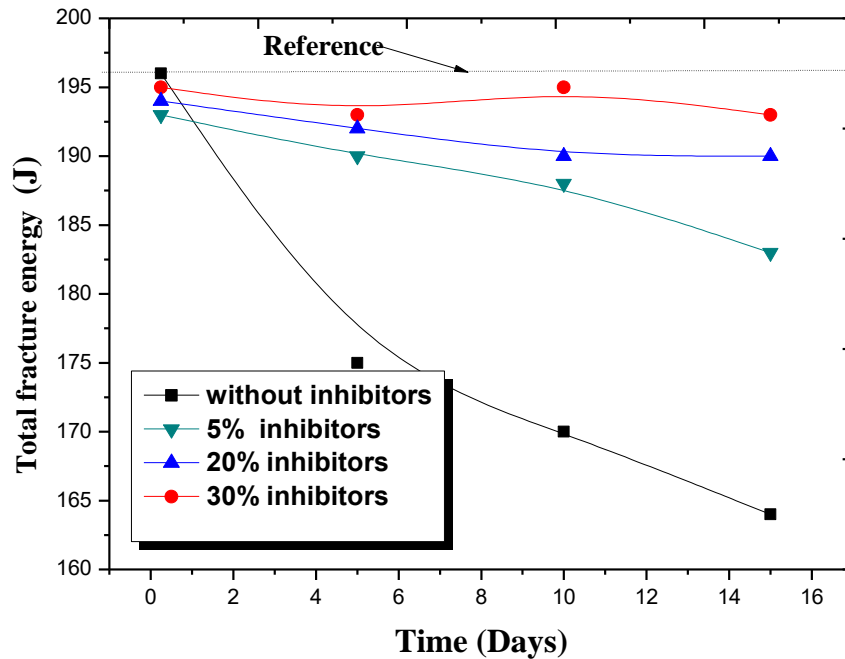


Figure. IV.13. Fracture Energy as a function of immersion time for different concentrations of the corrosion inhibitor.

Figure IV. 13. Illustrates the total energy absorbed by the specimens as function of immersion time. In the absence of corrosion inhibitors, the total fracture energy decreases from 197 to 165 J within 15 days of immersion in 1M HCl. However, in the presence of 30% (v/v) corrosion inhibitor, the decrease is only of 2 J in 15 days.

IV.3. 4. INFLUENCE OF GREEN INHIBITORS ON THE FRACTURE TOUGHNESS OF API 5L X52 STEEL

In this section, we studied the effect of corrosion green inhibitors on API 5L X52 steel in acidic media with different concentration of the inhibitors.

The experimental conditions are 25°C as the temperature, 1M as the concentration of HCl acid and 3 days as the immersion time. Figure. IV. 14 shows the evolution of the load as function of the displacement.

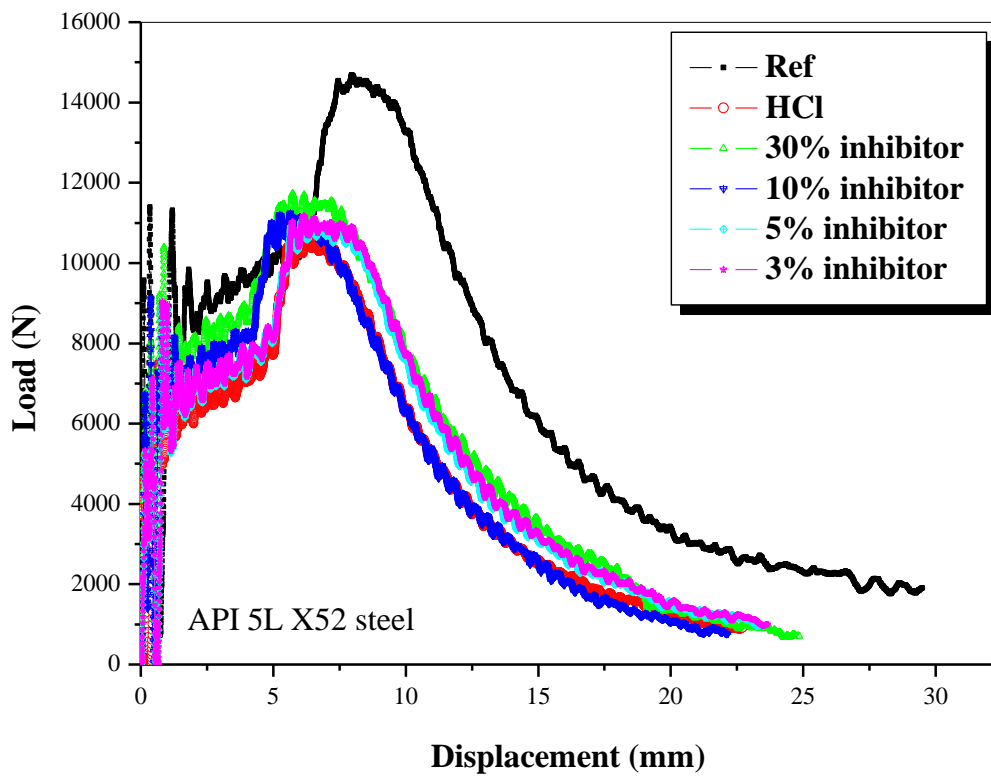


Figure IV. 14. Load vs. displacement curves obtained by instrumented Charpy impact test after immersion in hydrochloric acid solution with and without green inhibitor.

The critical load P_c is determined according to Equation IV. 1 which allows the determination of fracture energy U_C by Equation IV.2. The fracture toughness J_c , assumed to be proportional to the fracture energy U_C is determined according to Equation IV. 4 [20-21]. Accordingly, Table IV.1 gives the values of the critical loads required to break the test pieces measured at the Charpy test for 30%, 10%, 5% and 3% (v/v) concentrations of the green inhibitor. These results show the effect of the green inhibitor. In the presence of 1M HCl, the fracture toughness of the steel falls from 1.736 MJ/m² to 0.702 MJ/m². However, the presence of the green inhibitor at 30% (v/v) allows the steel to recover its toughness to 1.116 MJ/m². This is the evidence of the efficiency of our green corrosion inhibitor.

Table. IV.1. Impact testing Results

Mechanical properties	Ref	In 1 M HCl	30% (v/v) inhibitor	10% (v/v) inhibitor	5% (v/v) inhibitor	3% (v/v) inhibitor
P_c (KN)	11.87	8.37	9.47	8.57	8.88	8.77
U_c (j)	59.12	23.36	31.81	31.03	34.15	32.74
$B*b$ mm ²	68.1	66.5	57	66	62.6	61.4
J_c (MJ/m ²)	1.73	0.70	1.11	0.94	1.09	1.06

Figure. IV. 15 illustrates the results of Table 1 as the concentration of green inhibitor 3%, 5%, 10% and 30% on dynamic fracture toughness of API 5L X52 steel.

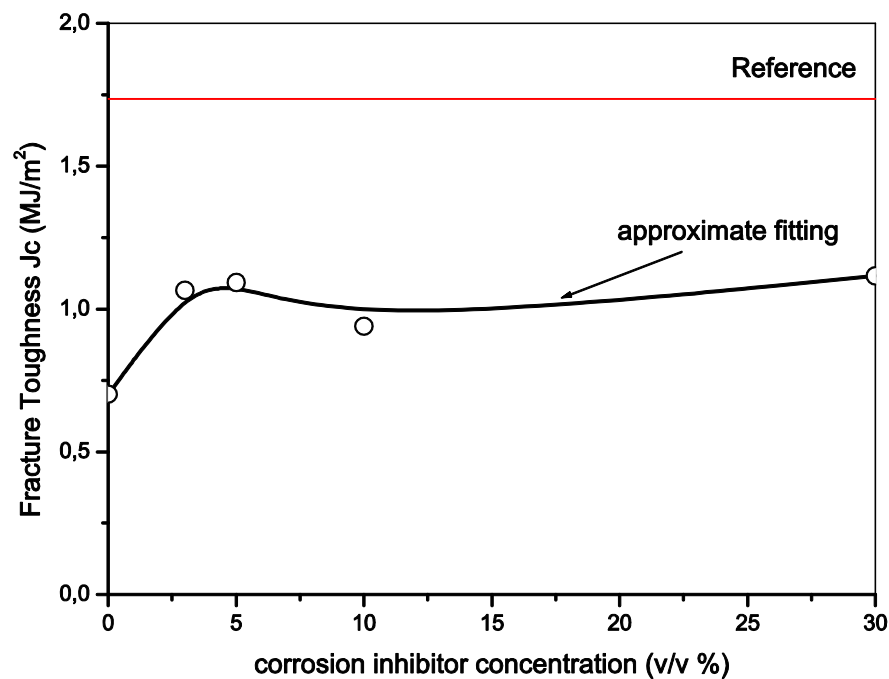


Figure. IV.15 Influence of green inhibitor concentration on dynamic fracture toughness of API 5L X52 steel after immersion in hydrochloric acid solution

IV.3.5. EFFICIENCY OF THE CONCENTRATION OF GREEN INHIBITOR ON THE X65 BY CHARPY TEST

In this section, we present our study of the effect of green corrosion inhibitors on API 5L X65 steel in acidic media, with different concentrations of the inhibitor with an

immersion time of 3 days. Figure. IV.16. shows the load-displacement curves of the steel in the presence of the green inhibitor with the concentrations of 0, 3, 5, 10 and 30 % (v/v).

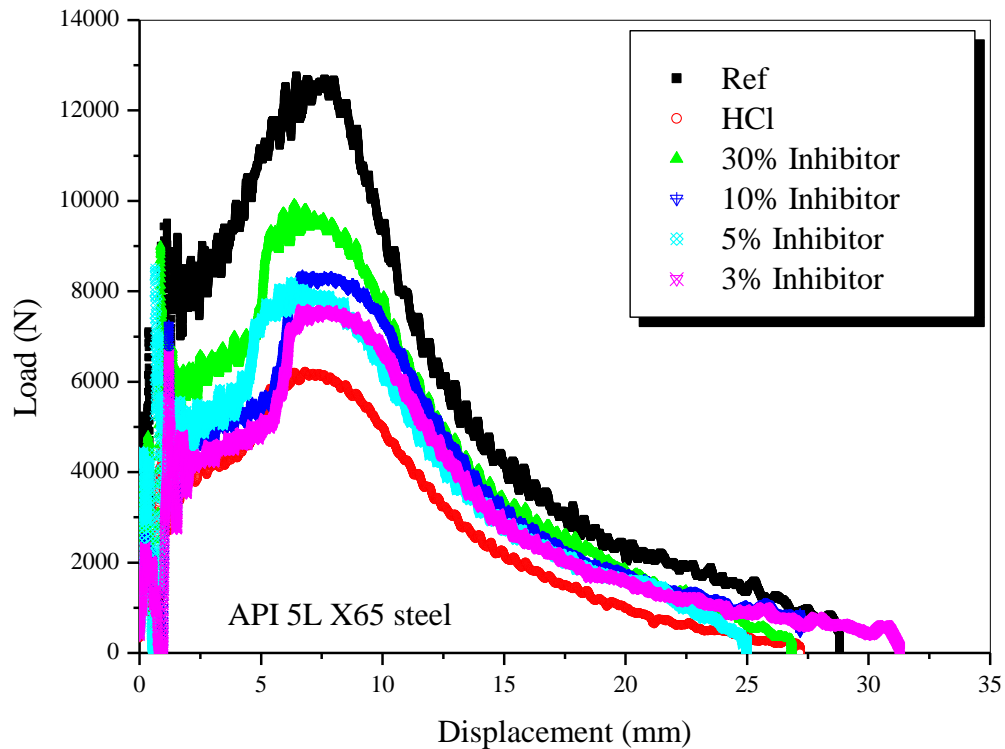


Fig IV.16 .Effect of inhibitor concentration on load-displacement curves of API 5L X65 steel.

Calculation of the mechanical properties are presented in Table IV.2. The results show the beneficial effect of green inhibitor on dynamic fracture toughness of the API 5L X65 steel after immersion in hydrochloric acid solution.

Table IV.2. Mechanical properties of the API X65 immersed in HCl compared to the different concentration (Bb is taken as 80mm²)

Mechanical properties	Ref	In 1 M HCl	30% (v/v) inhibitor	10% (v/v) inhibitor	5% (v/v) inhibitor	3% (v/v) inhibitor
P _{max} (KN)	12.67	6.21	9.77	8.08	8.05	7.57
P _{GY} (KN)	7.22	2.80	4.10	3.66	3.67	3.19
P _C (KN)	9.95	4.51	6.93	5.87	5.86	5.41
U _C (J)	31.73	15.23	26.60	23.40	21.28	22.22
J _C (MJ/m ²)	0.79	0.38	0.66	0.58	0.53	0.55

The steel is affected by HCl acid and lose its fracture toughness by 52% (from 0.79 to 0.38 MJ/m²). However, the fracture toughness drop is only 16.4% (from 0.79 to 0.66 MJ/m²) in the presence of 30 % (v/v) green corrosion inhibitor. The data are well illustrated in Figure IV.17.

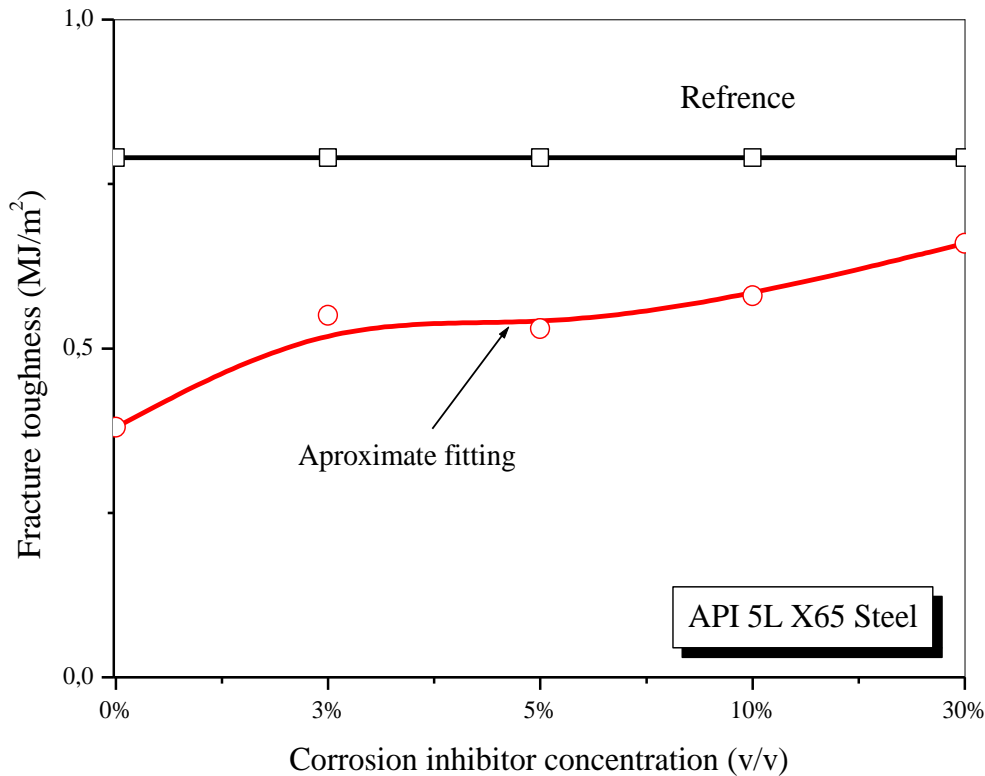


Figure. IV.17 Influence of green inhibitor concentration on dynamic fracture toughness of API 5L X65 steel after immersion in hydrochloric acid solution

IV.3. 6. THE TEMPERATURE EFFECT ON MECHANICAL PROPERTIES OF API 5L STEEL.

The failure energy K_{CV} (J) is related to temperature according to the equation below:

$$K_{CV} = A_{CV} + B_{CV} \tanh\left[\frac{T - D_{CV}}{C_{CV}}\right] \quad \text{Equation. IV.12}$$

Where A_{CV} , B_{CV} , C_{CV} and D_{CV} are constants. A_{CV} represents Charpy energy at the transition temperature D_{CV} , B_{CV} is the energy jump between the fragile and ductile plateaus. $2 C_{CV}$ is the temperature range of the Charpy energy transition.

As an example [Capelle 2013], Figure IV.18 represents a typical evolution of the failure energy with temperature expressed by Equation IV.5.

From Figure IV.18, the transition temperature is determined at the conventional level of 27 joules and called $T_{K,27}$ and also at half the jump between the brittle and ductile trays ($T_{K50} = D_{CV}$). The values of the A_{CV} , B_{CV} , C_{CV} and D_{CV} constants are shown on Figure IV.18 for API 5L X65 [22].

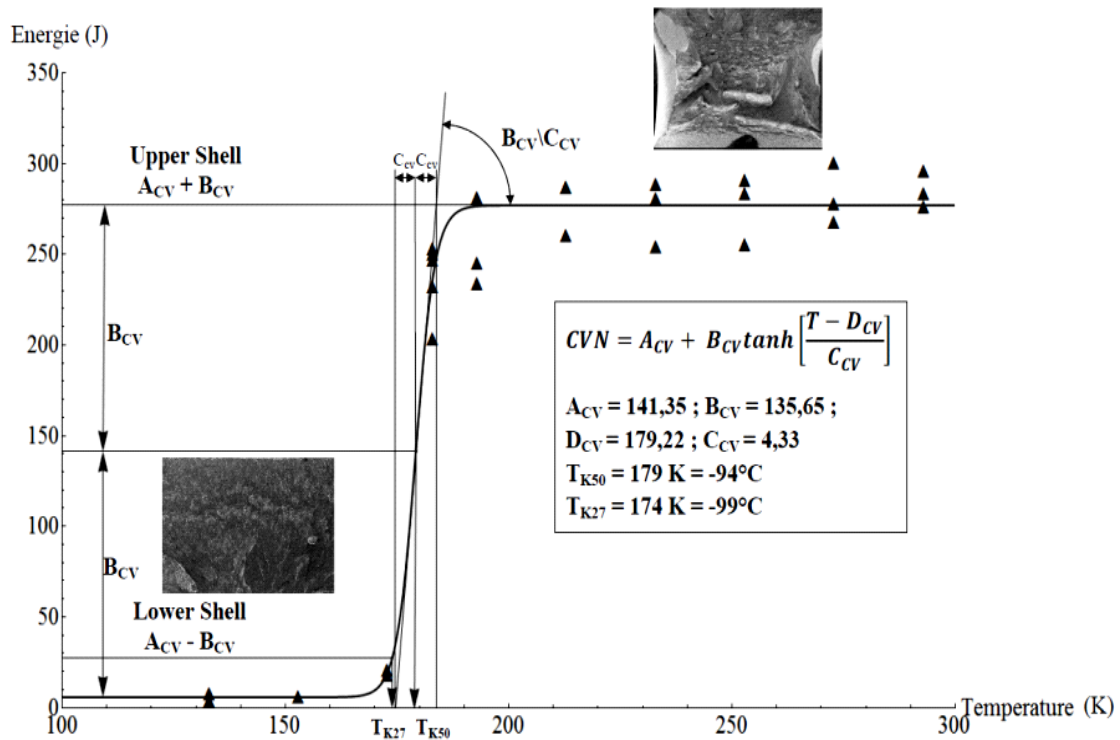


Figure.IV.18 Charpy V energy curve as a function of temperature for API 5L X65 steel.

IV.3.6.1. INFLUENCE OF IMMERSION TIME IN HCl/5 % GREEN INHIBITOR ON DYNAMIC FRACTURE TOUGHNESS OF API 5L X52 STEEL AT 80°C.

In this section of our study, Charpy specimens were immersed in 1M HCl solution with 5% (v/v) green inhibitor concentration during 3, 7 and 10 days immersion time at 80°C. Load-displacement curves were recorded and are shown in Figure. IV.19. The critical load P_c , the fracture energy U_c and dynamic fracture toughness J_c are extracted

from these recorded diagrams according to the above mentioned procedure. The results are presented in Table. IV. 3.

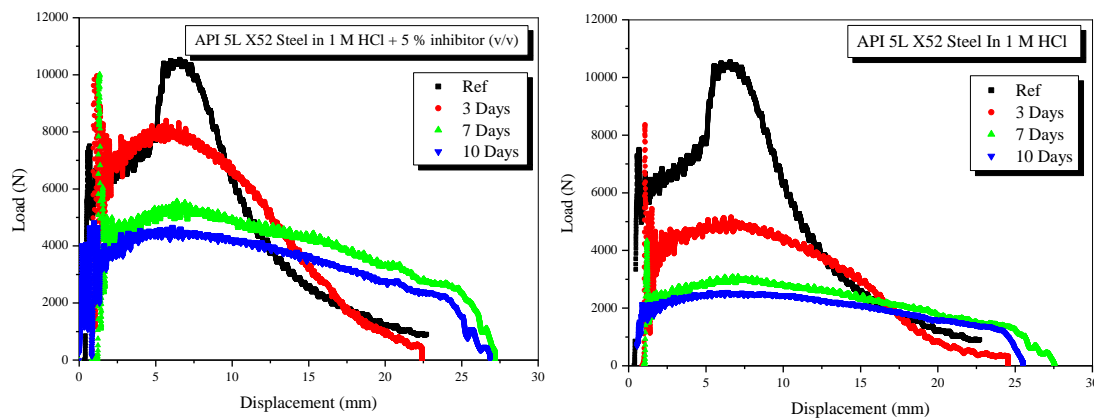


Figure IV. 19 Load-displacement curves (right) in 1M HCl acid and (left) in 1 M HCl+ 5% green inhibitor concentration at 80°C of API 5L X52 steel

Table. IV. 3 Mechanical Properties calculated for API 5L X52 steel immersed in acidic media and in the presence of 5% v/v green inhibitor (Bb is taken as 80mm²).

Mechanical properties	Ref	3days		7 days		10 days	
		Without inhibitor	5% inhibitor	Without inhibitor	5% inhibitor	Without inhibitor	5% inhibitor
$P_{max}(KN)$	10.56	5.06	8.16	3.10	5.50	2.55	4.60
$P_{GY}(KN)$	4.69	2.80	5.34	1.78	3.19	1.70	2.44
$P_C(KN)$	7.62	3.93	6.75	2.44	4.35	2.11	3.52
$U_C(J)$	27.57	4.90	9.31	3.62	7.84	3.40	5.25
$J_C(MJ/m^2)$	0.68	0.12	0.23	0.09	0.19	0.08	0.13

In Table IV.3, important loads degradation of the steel is noticed in acidic media in the absence of the inhibitor compared to the solutions where 5% (v/v) of the green inhibitor is present.

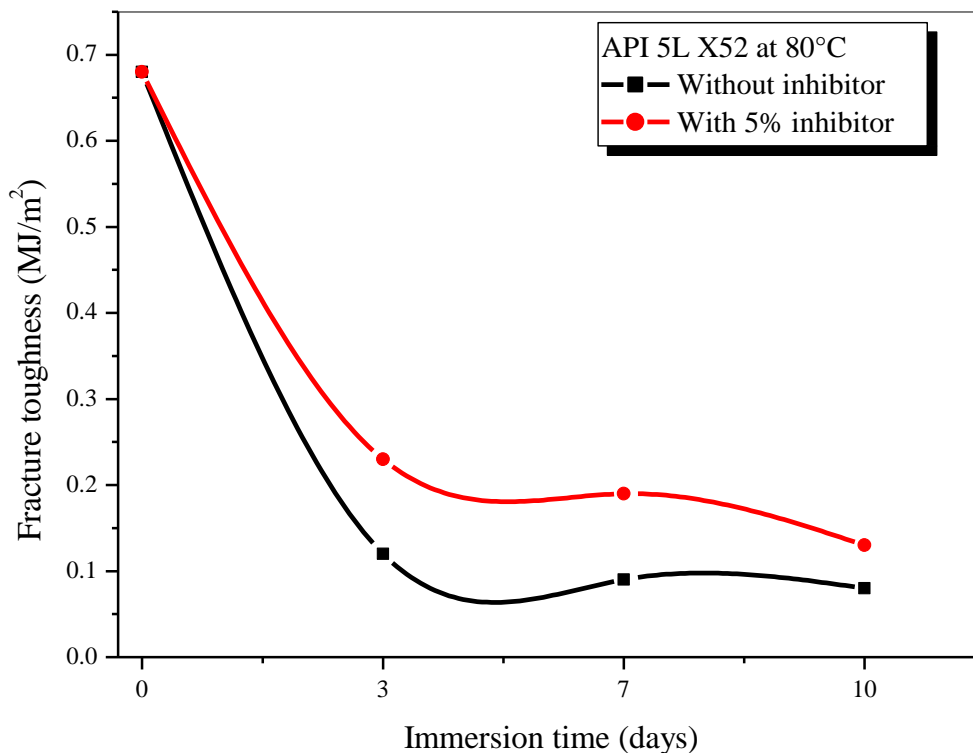


Figure IV.20: Fracture toughness vs. immersion time in 1M HCl with 5% (v/v) green inhibitor at 80°C of API 5L X52 steel

Also, it is evident from Figure IV.20 that, the decrease rate of the fracture toughness of API 5L X52 steel is higher in HCl solution than in HCl/green inhibitor solution.

IV.6.3.2. INFLUENCE OF IMMERSION TIME IN HCl/5 % GREEN INHIBITOR ON DYNAMIC FRACTURE TOUGHNESS OF API 5L X65 STEEL AT 80°C.

The green corrosion inhibitor effect is studied in the same conditions and experiments were conducted in the aim to approve the efficiency of green inhibitor to protect internal surface of the pipelines network.

Specimens of API 5L X65 steel were immersed in 1M HCl/ 5% green inhibitor solutions for 3, 7 and 10 days at 80°C. Charpy dynamic test curves are shown in Figure IV.21.

The mechanical properties calculations are gathered in Table IV.4. It is shown that the decrease of the fracture toughness is more pronounced in acidic media than the solutions were the 5% (v/v) green inhibitor is used.

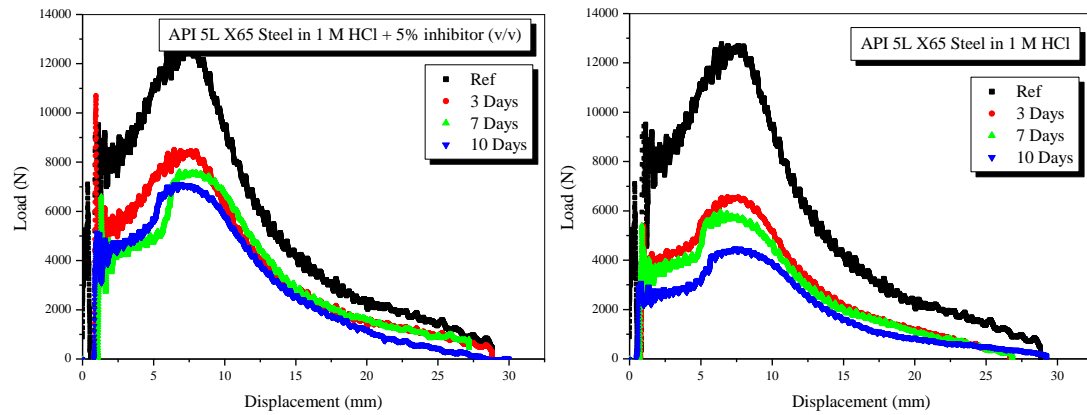


Figure IV.21: Load-displacement curves (right) in 1M HCl acid and (left) in 1 M HCl+ 5% green inhibitor concentration at 80°C of API 5L X65 steel

Table. IV. 4 Mechanical Properties calculated for API 5L X65 steel immersed in acidic media and in the presence of 5% v/v green inhibitor (Bb is taken as 80mm²).

Mechanical properties	Ref	3days		7 days		10 days	
		Without inhibitor	5% inhibitor	Without inhibitor	5% inhibitor	Without inhibitor	5% inhibitor
P_{max} (KN)	12.67	6.58	8.47	5.85	7.60	4.42	7.12
P_{GY} (KN)	7.22	2.88	4.54	2.89	3.49	2.22	3.42
P_C (KN)	9.95	4.73	6.51	4.39	5.54	3.32	4.37
U_C (J)	31.73	17.16	19.50	15.50	19.11	12.4	15.5
J_C (MJ/m ²)	0.79	0.43	0.48	0.37	0.47	0.31	0.38

Figure. IV.22 illustrates the decrease of fracture toughness after different immersion times in HCl and in HCl +5% green inhibitor at 80°C of API 5L X65 steel. After 10 days of immersion in hydrochloric acid, fracture toughness has decreased by of 61% (from 0.79 to 0.3 MJ/m²). For the same immersion time, in the presence of the green corrosion inhibitor, the decrease of J_C is only 52% (from 0.79 to 0.38 MJ/m²).

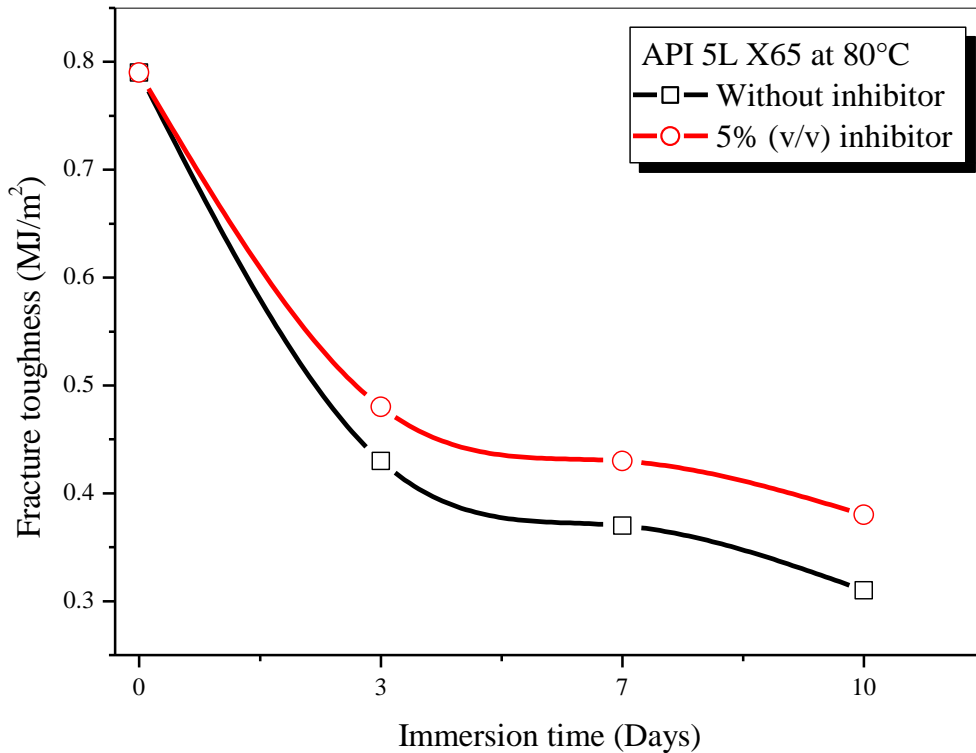


Figure IV.22: Fracture toughness vs. immersion time in 1M HCl with 5% (v/v) green inhibitor at 80°C of API 5L X65 steel

IV.3.6.3. EVOLUTION OF THE FRACTURE TOUGHNESS J_c WITH IMMERSION TIME OF THE API 5L X65 AND X52 STEEL

From both Figures IV.20 and IV.22, the decrease rate of the fracture toughness J_c with respect to immersion time less than 7 days is higher than the decrease after 10 days. A stabilization effect is noticed between 7 and 10 days. The metal is saturated by the green inhibitor and no more reaction with HCl is possible. The metal is protected by a film of the green inhibitor preventing a direct contact with the sour solution of HCl.

The API 5L X52 and X65 steels behave similarly against the HCl/green inhibitor solutions.

The fracture toughness is falling from 0.68 to 0.08 (in HCl) and 0.13 MJ/m² (in HCl/Green inhibitor) for X52 steel and from 0.79 to MJ/m² to 0.31 (in HCl) and 0.38 MJ/m² (in HCl/Green inhibitor) by the end of the 10 days experiments.

IV.3.7. THE ACTION MECHANISM OF THE GREEN CORROSION INHIBITOR

Immersion effect on steel in acid media with the corrosion inhibitor is attributed to the hydrogen embrittlement. The film absorbed of hydrogen on the metal surface due to anodic dissolution of iron



The hydronium ion is very small so it ease to diffusion into the metal surface when there is a contact. Hydrogen embrittlement in steel results generally from the enhanced plasticity [11, 23] and weakening metal links [14, 24]. The protective barrier film created by corrosion inhibitor to aim the protection of the internal surface which prevents both recombination and diffusion. The factor of the inhibitor concentration is very important in the process of the protective barrier creation. When we have the enough inhibitors concentration to create this barrier, any increase of it can give more effects on the inhibition efficiency of the system.

IV.4. DROP WEIGHT TEST APPARATUS AND SPECIMEN GEOMETRY

In this second part of mechanical testing, we used the drop-weight machine to obtain damage inflicted along of the degrees of penetration of the specimen until the fracture point. A Charpy V-notched specimens associated to a round-nosed impactor on the different steels were used as illustrated in Figure IV.23.

We studied the effect of green inhibitor on the absorbed energy of fracture of the specimens as function of the green inhibitor concentration and immersion time. Both X52 and X65 pipe steels were studied and the impactor was 21 kg mass and 3, 62 m/s maximum velocity.

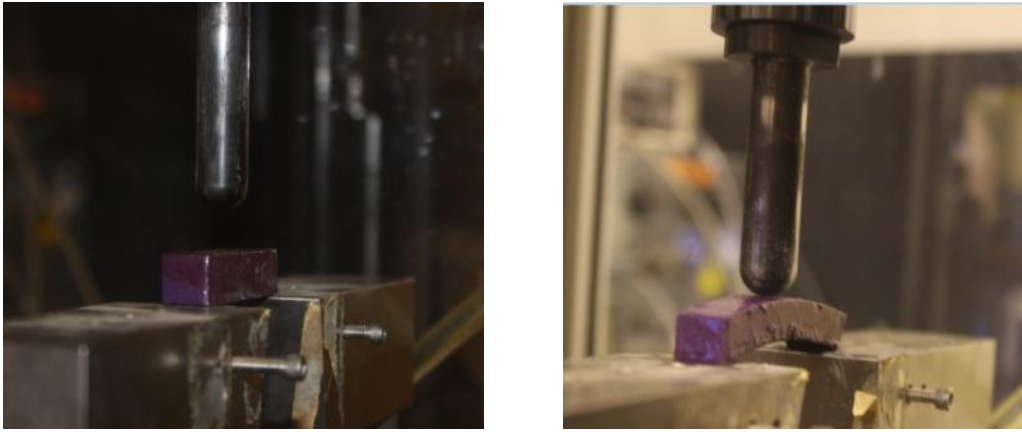


Figure IV. 23. Specimen X52 and X65 steel during drop weight test

IV.4.1. INFLUENCE OF GREEN INHIBITORS ON FRACTURE ENERGY OF THE X52 AND X65 STEEL BY THE DROP WEIGHT TEST

Three impact test specimens were prepared from X52 (55/10/9.2 dimension) and X65 (55/10/10 dimension) steels. Each specimen was immersed in 1M HCl acid with 0, 3, 5, and 10% (v/v) green inhibitor concentration. Images of the specimens after the drop weight test are shown in Figure IV.24.

The absorbed energy vs. the solution concentration along with 3, 7 and 10 days' time of immersion are drawn in the curves of Figure IV 25 and IV 26 for X52 and X65 steels , respectively.

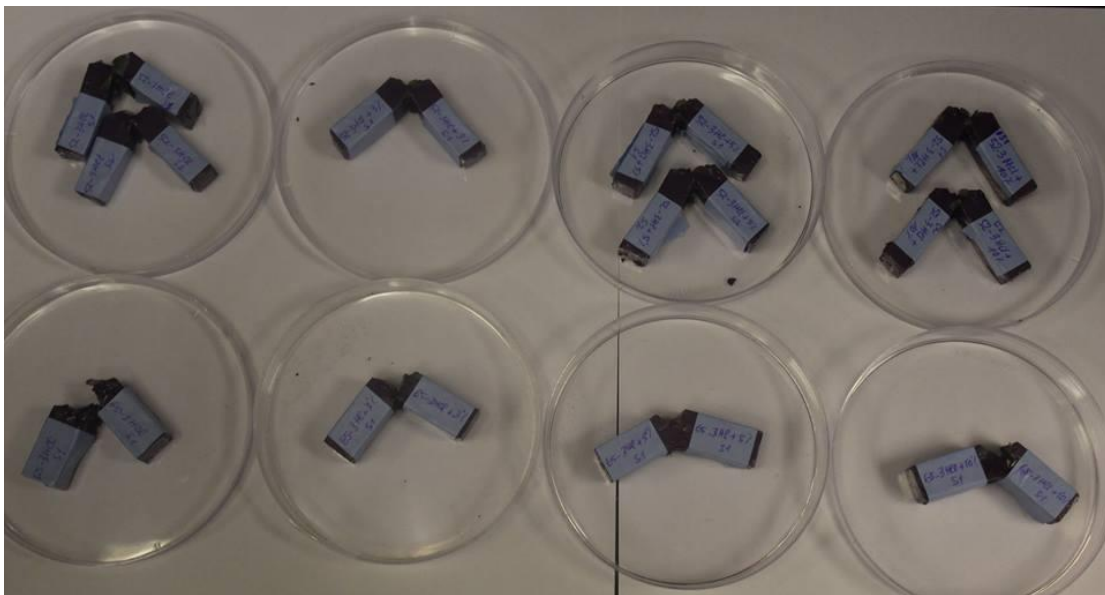


Figure. IV.24. Specimens after the drop weight test

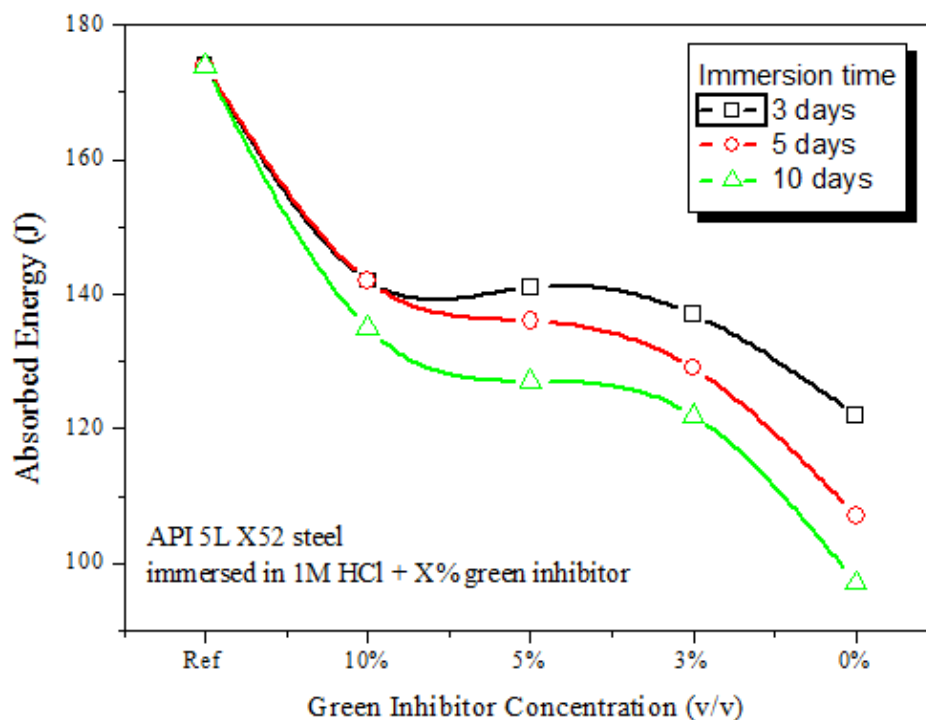


Figure. IV.25. Absorbed energy as function of the concentration of green inhibitor in 1 M HCl API 5L X52 steel with different immersion time

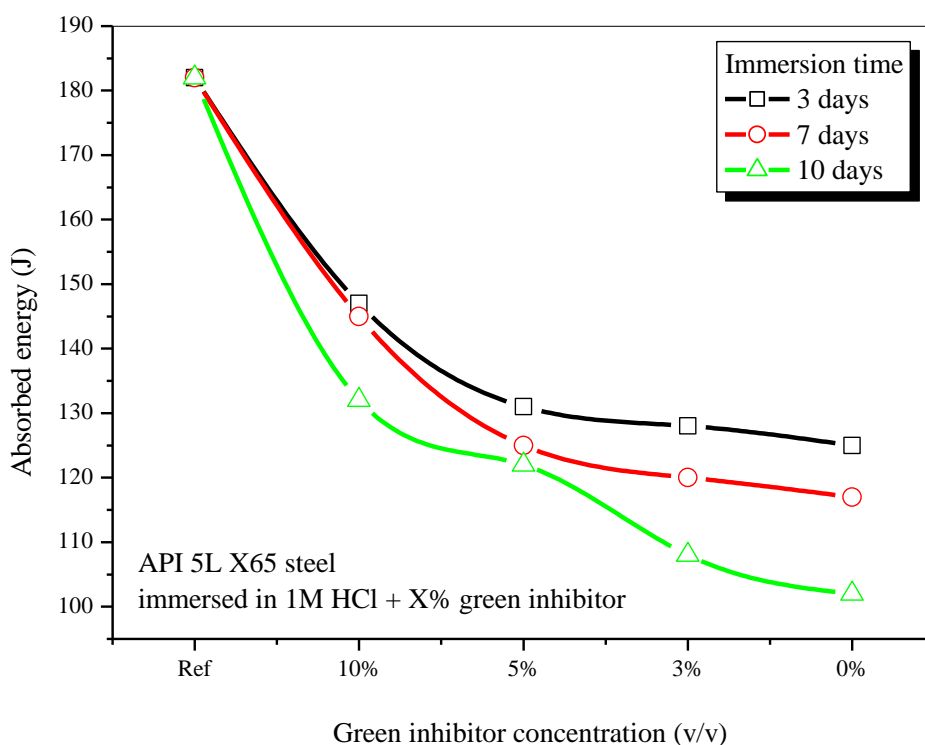


Figure. IV.26. Absorbed energy as function of the concentration of green inhibitor in 1 M HCl API 5L X65 steel with different immersion time

From Figures IV. 25 and 26, both the X52 and X65 steels behave similarly to the sour solution with or without the presence of the green inhibitor. The steel immersed in the 1M HCl loses its ability to absorb the energy of the falling weight due to the corrosive nature of the acid.

For example, the absorbed energy of the X52 steel decreases from 174 J to 122 J in 3 days and to 97 J in 10 days immersion time in HCl. However the presence of the green inhibitor, protects the steel from corrosion and increases the absorbed energy. In the presence of 10 % green inhibitor, both the X52 and X65 steels preserve up to 73% of their ability to absorb impact energy even after 10 days of immersion in 1M HCl.

IV.4.2. IMMERSION TIME EFFECT OF THE GREEN INHIBITORS ON FRACTURE ENERGY OF THE X52 AND X65 STEEL BY THE DROP WEIGHT TEST

The effect of the immersion time was also examined. Figure IV. 27 and IV.28 depicts the effect of immersion time on the absorbed energy by the X52 and X65 steel specimens, respectively. It can be seen that the addition of the green inhibitor to the acidic solution, reduces the degradation rate of the absorbed energy of the steel. From the slope of the curve absorbed energy vs immersion time, the degradation rate of the absorbed energy was determined as 3.58% per day of immersion in 1M HCl solution for X52 steel. However, the degradation rate was determined as only 0.94% per day of immersion in the presence of 10% (v/v) green inhibitor.

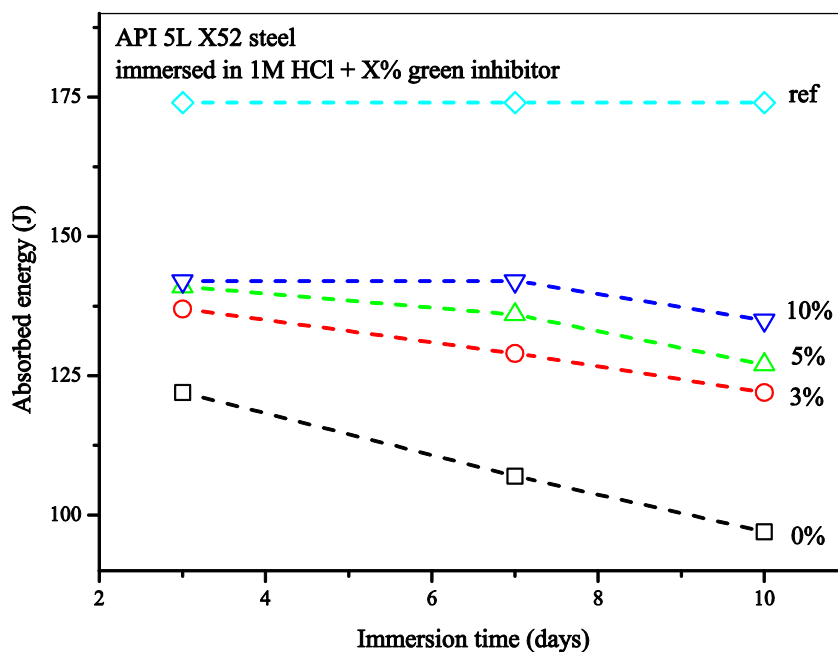


Figure. IV.27. Absorbed energy by X52 steel as function of immersion time in 1 M HCl with different green inhibitor concentration

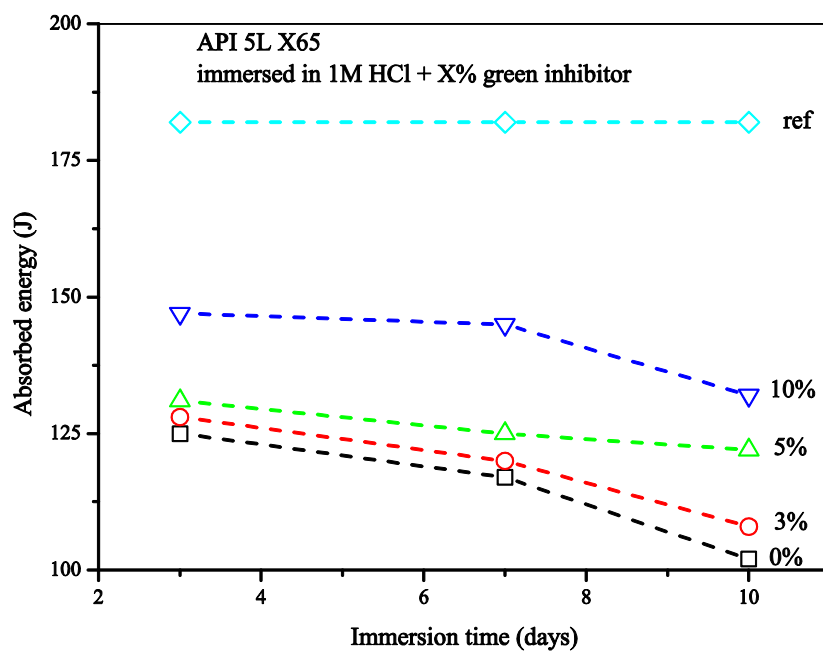


Figure. IV.28. Absorbed energy by X65 steel as function of immersion time in 1 M HCl with different green inhibitor concentration

These results show the efficiency of the green inhibitor to reduce the rate of corrosion of the X52 and X65 steels.

IV.5. THREE-POINT BENDING TEST

The bending test specimens are used to quantify the evolution of the fracture energy as a function of the presence of the green corrosion inhibitor with 0%, 5%, 20% and 30% (v/v) concentrations. Figure IV. 29 shows the specimen during the test.

IV.5.1. SPECIMENS OF STATIC THREE POINT BENDING TEST

In this part, a static three point bending test was carried out, taking into account the effect of the inhibitor concentration and comparing to the reference specimen. We used 15 V-notched specimens of API 5L X52 with 55/10/9.2 mm dimension. The specimens were immersed in 1M HCl + 0, 5, 20 and 30% (v/v) green inhibitor at 25°C for 7 days.



Figure IV. 29. Three point bending test, specimen under test (left), specimen after break (right).

IV.5.2. INFLUENCE OF GREEN INHIBITORS ON MECHANICAL PROPERTIES OF API 5L X52 STEEL BY THREE-POINT BENDING TEST

The three point bending test load-displacement curves of the specimens are shown Figure IV. 30. From the shape of the curves, three stages can be distinguished. In phase I, the load increases linearly. In the phase II, the specimen undergo non-linear variation of the load to reach a maximum value while in phase III, the load decreases until the

specimen breaks. These curves show the effect of the immersion solution on the maximum load of the specimens.

Qualitatively, it can be seen that the acidic media of HCl causes the loss of the maximum load of the specimen due to corrosion. The green inhibitor have the important effect on the degradation of these mechanical properties of steel. When it is added to the acid solution, the maximum load is increased with the inhibitor concentration. Evolution of the load as function the displacement are shown in Figure. IV. 30, and the values are shown in table. IV. 5

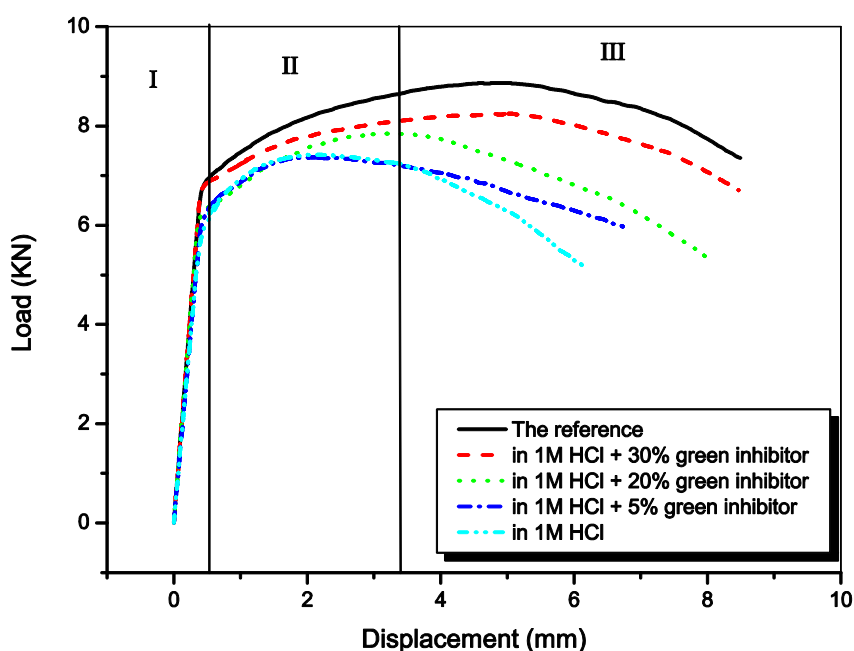


Figure IV. 30. Three point bending test load- displacement curves of the specimens immersed in as indicated solutions.

Table. IV. 5. Evolution of the maximum load and the displacement as a function the green inhibitor concentration.

Specimens	Maximum load (KN)	Displacement at max load (mm)
Reference	8.87	4.88
In 1M HCl	7.42	2.05
In 1M HCl + 5% inhibitor	7.37	2.16
In 1M HCl + 20% inhibitor	7.85	3.33
In 1M HCl + 30% inhibitor	8.25	4.87

IV.6. INFLUENCE OF SYNTETIC AND GREEN INHIBITORS ON API 5L X52 BY TENSILE TESTS IN HCl ACID SOLUTIONS

The aim of this test was to compare the efficiency of green and synthetic corrosion inhibitors X on tensile properties of API 5L X52 steel. The specimens were immersed for 7 days at room temperature in 1.2M HCl, 1.2M HCl/30% (v/v) green and 1.2M HCl/30% synthetic inhibitors X. The synthetic inhibitor X was gratefully provided by SONATRACH. Figure. IV.31 shows the reference specimens before (a) and the ruptured specimens (b) after the tensile test.



Figure IV. 31. The tensile specimens, before and, after tensile tests.

Figure IV.32 shows the stress-strain curves of the tensile testing. The data collected are averaged over two tests under the same conditions for each solution. It can be seen that the elongation at break, of the specimen immersed in 1.2HCl solution, drops from 31.5% of the reference to 17.5%. However, the use of 30% of the synthetic inhibitor have a minimal effect on the elongation at break. In the other hand, the use of the green inhibitor enhance the mechanical property against break to the original value of the reference. This is an illustration of the efficiency of the green vs. the synthetic inhibitor.

The other properties from the tensile testing as Young's modulus, yield stress and ultimate stress variation are in the limit of experimental errors.

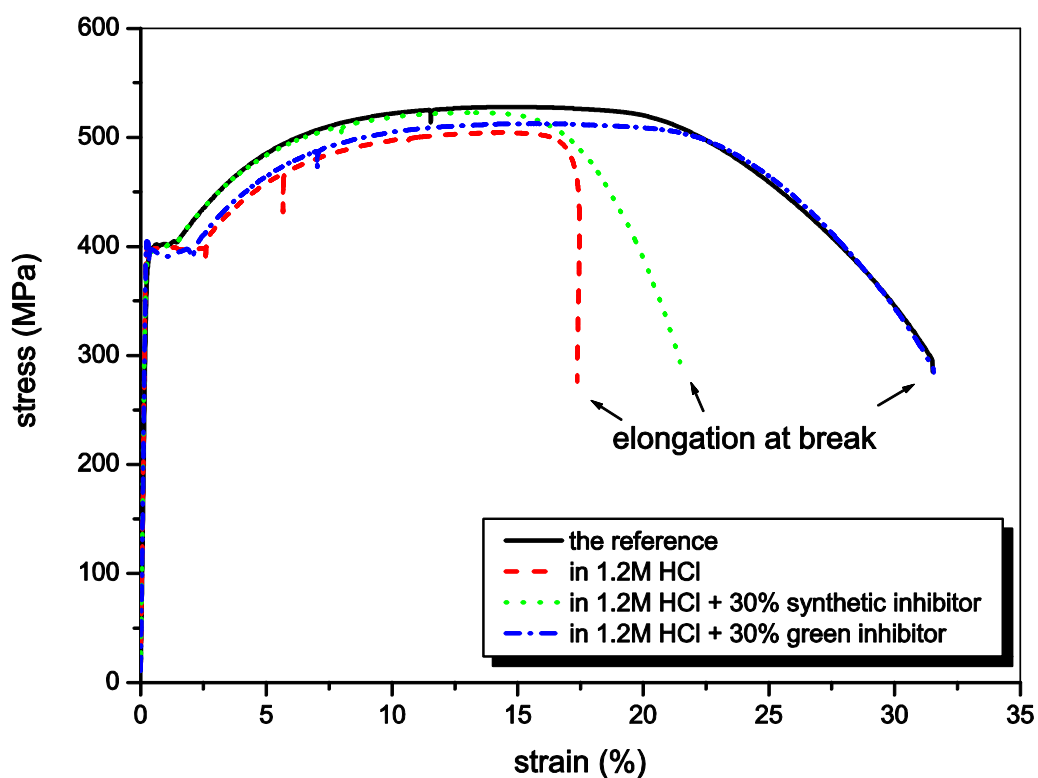


Figure IV. 32. Stress-strain curves of API 5L X52 steel after immersion in different solutions, 1.2 M HCl, 1.2 M HCl+ 30% Green and 1.2M HCl+ 30% synthetic inhibitors.

All this results from this experimental test was cumulated in table IV.6

Table. IV. 6. Tensile properties of steel API 5L X52 after immersion in different solutions from 7 days

Solution	Ref	HCl 1.2 M/l	1M HCl +30% synthetic	1M HCl + 30% Green
σ_{ul} (MPa)	527	511	502	522
A%	32.5	17.5	21.2	32.2

All the test results of the mechanical properties was cumulated in the bellow table. IV. 7, such as the Charpy test, Drop weight test, three point test, and the tensile test.

Chapter II

Inhibitors of corrosion

Table IV.7. Cumulated the results of the experimental test

Energy absorbed by the specimens from the Charpy test of the API 5L X52									
Experimental technique	API 5L steel	Mechanical properties	Ref	In 1M HCl	30% (v/v) inhibitor	10% (v/v) inhibitor	5% (v/v) inhibitor	3% (v/v) inhibitor	
		J _c (MJ/m ²)	1.73	0.70	1.11	0.94	1.09	1.06	
Energy absorbed by the specimens from the Charpy test of the API 5L X65									
Experimental technique	API 5L steel	Mechanical properties	Ref	In 1M HCl	30% (v/v) inhibitor	10% (v/v) inhibitor	5% (v/v) inhibitor	3% (v/v) inhibitor	
		J _c (MJ/m ²)	0.79	0.38	0.66	0.58	0.53	0.55	
Energy absorbed by the specimens from the Charpy test of the API 5L X52 Steel at the 80°C									
Charpy test	X52	Mechanical properties	Ref	3days		7 days		10 days	
				Without inhibitor	5% inhibitor	Without inhibitor	5% inhibitor	Without inhibitor	5% inhibitor
		J _c (MJ/m ²)	0.68	0.12	0.23	0.09	0.19	0.08	0.13
Energy absorbed by the specimens from the Charpy test of the API 5L X65 Steel at the 80°C									
Charpy test	X65	Mechanical properties	Ref	3days		7 days		10 days	
				Without inhibitor	5% inhibitor	Without inhibitor	5% inhibitor	Without inhibitor	5% inhibitor
		J _c (MJ/m ²)	0.79	0.43	0.48	0.37	0.47	0.31	0.38

Energy absorbed by the specimens from the Drop weight test of the API 5L X52 Steel							
Drop weight test	X52		Ref	10% inhibitor	5% inhibitor	3% inhibitor	0% inhibitor
		3 Days	174	142	141	137	122
		7 Days	174	142	136	129	107
		10 Days	174	135	127	122	97
Energy absorbed by the specimens from the Drop weight test of the API 5L X65 Steel							
Drop weight test	X65		Ref	10% inhibitor	5% inhibitor	3% inhibitor	0% inhibitor
		3 Days	182	147	131	128	125
		7 Days	182	145	125	120	117
		10 Days	182	132	122	108	102
Energy absorbed by the specimens from the three point bending test API 5L X52 Steel							
Three point bending	X52	Specimens		Maximum load (KN)		Displacement at max load (mm)	
		Reference		8.87		4.88	
		In 1M HCl		7.42		2.05	
		In 1M HCl + 5% inhibitor		7.37		2.16	
		In 1M HCl + 20% inhibitor		7.85		3.33	
		In 1M HCl + 30% inhibitor		8.25		4.87	

IV.7. CONCLUSION

From this chapter, we can conclude at the first part of the corrosion inspection pipe transportation gas, some analyses important in the aim detection the corrosion causes. We presented in this part microscopy optical observation, from the different view of the corrosion position (internal and external), and also the chemical analyses.

In another hand we presented the discussion of the cases of the corrosion activation in pipe, at the end we presented some recommendations in aim to control corrosion.

At the second part we have some mechanicals tests of API 5L X52 and X65 steel, in aim to study the efficiency of the green inhibitors extracted from the Ruta Chalepensis on the both types. We are studied the degradation of the both total energy fracture, and the fracture toughness of these steels, by Charpy test in the absence and presence of the green inhibitors corrosion.

At the second test we study the effect of the concentration and time immersion of the green inhibitor by the Drop weight test, when we calculate the energy absorbed by specimens. The third test we study the degradation of the load- displacement by the three points bending test in the presence and absence the green inhibitors corrosion.

In the last test we study the effect of the green inhibitors corrosion and synthetic inhibitors of the degradation of the mechanical properties, spicily on the elongation steel

All these mechanical test was give important results, the extracts of this plant have showed a great ability to enhance the efficiency against degradation of mechanical properties such as the total energy, fracture toughness, absorbed energy and the elongation at fracture.

References

- [1]. George. A, "Piping and Pipeline Engineering, Design, Construction, Maintenance", Integrity, and Repair, Aiken, South Carolina, U.S.A, (2003)
- [2]. Elazzizi. A, Hadj M. M, Khelil. A, Pluvinage. G., Matvienko, Y.G, "The master failure curve of pipe steels and crack paths in connection with hydrogen embrittlement", International Journal of Hydrogen Energy, (2015), Vol. 40, pp. 2295–2302.
- [3]. Nordsveen. M, Nes̃ic. S, Nyborg. R, Stangeland. A., "A Mechanistic Model for Carbon Dioxide Corrosion of Mild Steel in the Presence of Protective Iron Carbonate Films—Part 1: Theory and Verification", Journal of Corrosion science section, (2003), Vol. 59, No. 5, pp 443-456
- [4]. Hadj Meliani, M., Azari Z., Pluvinage G., Matvienko Yu.G, "Two parameter engineering fracture mechanics: Integrity of Pipelines Transporting Hydrocarbons", (2010), Biskra-Algeria.
- [5]. Soudani. M, Hadj Meliani. M, K. El-Miloudi, Fares. C, "Corrosion effects and green scale inhibitors in the fracture mechanics properties of gas pipelines", Journal – structural integrity and life. (2017), pp. 25–31.
- [6]. Hadj-Meliani. M, Azari. Z, Matvienko. Y, G, Pluvinage. G, "The effect of hydrogen on the master failure curve of APL 5L gas pipe steels". Procedia Engineering, (2011). Vol. 10, pp. 942-947.
- [7] Trabaneli. G, Frignani. A, Monticelli. C, Zucchi.F, "Alkyl-benzotriazole derivatives as inhibitors of iron and copper corrosion", Int. J. Corros. Scale Inhib., 2015, 4, no. 1, pp. 96-107
- [8] Soudani. M, Bouledroua. O, Hadj Meliani M, El-miloudi K, Muthanna. B. G. N. Khelil. A, Elhoud. A, Matvienko, Y. G, Pluvinage. G, "Corrosion Inspection and Recommendation on the Internal Wall Degradation Caused Rupture of 6" Gas Line Pipe", Journal of Bio- and Tribo-Corrosion (2018),
- [9] Qiliang L, W, Zhang. Z, Amy. K, Momson. T, " Kinetics and inhibito of ferrous sulfide Nulleation and precipitation", Socierty of petroleum Engineers, 2014.
- [10] Shouhu. X, Mingwei. C, Lingyun. H, Wanquan. J, Xinglong. G, Yuan H, Zuyao C, "Preparation and characterization of microsized FeCO_3 , Fe_3O_4 and Fe_2O_3 with ellipsoidal morphology", Journal of Magnetism and Magnetic Materials, (2008), Vol. 320, pp. 164-170
- [11] Hirnyi. S. I., "Corrosion of iron in a carbonate-bicarbonate solution, Part1. Crystallographic analysis of passive films", Materials Science, (2001), Vol. 37, pp. 76 -80
- [12]. Richard L. M, "Corrosion Consequences of Oxygen Entry Into Sweet Oilfield Fluids", Society of Petroleum Engineers Inc, (2001).

References

- [13]. Forero, A. B., Milagros, Núñez, M.G., Bott, I. S "Analysis of the Corrosion Scales Formed on API 5L X70 and X80 Steel Pipe in the Presence of CO₂". *Materials Research*.(2014), Vol 17(2): 461-471.
- [14] Chaoyang F, Jiashen Z (1998). "Corrosion fatigue behavior of carbon steel in drilling fluids". *Journal of Corrosion Engineering Section*, (2016), Vol 8, pp 651–656.
- [15] Hu, Z. Y, Duan, D. L, Jiang, S. L, Ding, X. J., Li, S "Pure Mechanical Wear Measurement of Carbon Steel in Oil–Water Fluids". *J Bio Tribo Corros* (2015). Vol 1(17), pp1-10
- [16] Nwanonenyi. S. C, Arukalam. I. O, Obasi, I. O., Ezeamaku. U. L, Eze. I. O, Chukwujike. I. C, Chidiebere. M. A "Corrosion Inhibitive Behavior and Adsorption of Millet (*Panicum miliaceum*) Starch on Mild Steel in Hydrochloric Acid Environment". *J Bio Tribo Corros*. (2017), Vol 3(54)
- [17] API 5L, "Specification for Line Pipe" (Washington, DC: API, 2016).
- [18] ASTM , *Metals- Mechanical Testing; Elevated and low – Temperature Tests; Metallography*. (2016), E (03.01) 1382.
- [19] Hadj Meliani, M, "The Inspections, Standards and Repairing Methods for Pipeline with Composite: A Review and Case Study". 17th International Conference on New Trends in Fatigue and Fracture, (2017), pp 147-156.
- [20] Akourri O , Louah M, Kifani A, Gilgert J, Pluvinage G. "The effect of notch radius on fracture toughness", *Journa of Engineering Fracture Mechanics* 65 (2000) pp 491-505
- [21] Pluvinage G "Fracture and Fatigue emanating from stress concentrators"; Editeur Kluwer, (2003).
- [22] Meryem. A. B, Chahinez. F, Abdelkader K, Mohamed H. M, adsorption and corrosion inhibitive properties of *Ruta Chalepensis* on API X52 Steel In Hydrochloric Acid Media. *Chemtech'15 3rd international chemical engineering and chemical technologies conference proceedings*, (2015), İstanbul.
- [23] Coseru A., Julien. C, Pluvinage. G. "On the use of Charpy transition temperature as reference temperature for the choice of a pipe steel". *Journal of Engineering Failure Analysis*, ,(2014).Vol 37, Pp 110-119
- [24] Cervantes. T. A, Godínez. S. J. G., J. González. V. L, Díaz. C. M. "Corrosion Rates of API 5L X-52 and X-65 Steels in Synthetic Brines and Brines with H₂S as a Function of Rate in a Rotating Cylinder Electrode" *Int. J. Electrochem. Sci.*, (2014) Vol 9, pp 2454 - 2469
- [25]. Hanneken J. W. *Hydrogen in metals and other materials: a comprehensive reference to books, bibliographies, workshops and conferences*, *International Journal of Hydrogen Energy*, (1999) , Vol 24, pp 1005-1026.

References

- [26] Lufrano J. and Sofronis P. Enhanced hydrogen concentrations ahead of rounded notches and cracks – competition between plastic strain and hydrostatic stress. *Acta Metalurgia*. (1998), Vol 46, No 5, pp 1519-1526.
- [27] Lunarska E., Ososkov Y., Jagodzinsky Y. Correlation between critical hydrogen concentration and hydrogen damage of pipeline steel. *International J. Hydrogen Energy*, (1997), Vol 22 No. 2/3 pp 279-284.
- [28] Gulbrandsen. E, Nyborg. R, Trine L, Nisancioglu. K, *CORROSION/2000* No. 23, (Houston, TX: NACE, 2000).
- [29] Green, A. P., and Hundy, B. B. "Initial plastic yielding in notch bend tests", *Journal of Mechanics and Physics of Solids*, (1956). Vol 4, pp 128-144
- [30] Julien. C, Dmytrakh. I, Azari. Z, Pluvinage. G. "Evaluation of Electrochemical Hydrogen Absorption in Welded Pipe", *Science Direct, Procedia Materials Science*, (2014), Vol 3, 550–555
- [31] Kamel. H, Abdelkader. K, Mohamed. Z, Mohamed. K, Abdellah. K, Khadidja. E, Belkheir. H, "Synthesis, characterization and study of methyl 3-(2-oxo-2H-1,4-benzoxazin-3-yl) propanoate as new corrosion inhibitor for carbon steel in 1M H₂SO₄ solution", *Journal of Res Chem Intermed*, (2015),

General Conclusion

General Conclusion

This work presented from this thesis interested to study the effect of the synthetic and green inhibitors on the degradation of the mechanical properties pipe steel of API 5L X52 and X65.

- ❖ From the inspection part we can quite the following conclusions be drawn:
 - From the inspections part, achieved by visual, optical observation and also the metallurgical analysis of the corroded surface of the pipe.
 - From this Investigation the corroded surfaces analysis by X-Ray Diffraction showed the presence of the carbon dioxide CO₂ and hydrogen sulfide H₂S content.
 - Absence of the internal chemical treatment or internal coating leads the contact between fluid and pipe wall.

- ❖ From the experimental part we studied the degradation of the mechanical properties of API 5L X25 and X65 steels, we can quite the following conclusions be drawn:
 - The Ruta Chalepensis plant extract was successfully than the synthetic inhibitors when we compared the mechanical properties from each one of them.
 - From the Charpy test the values fracture toughness increase with the increase of the concentration of green inhibitors. In the presence of 1M HCl, the fracture toughness of the X52 steel is 1.736 MJ/m² to 0.702 MJ/m². However, the presence of the green inhibitor at 30% (v/v) the steel to recover its toughness to 1.116 MJ/m²
 - Drop weight test, in the presence of 10 % green inhibitor, both the X52 and X65 steels preserve up to 73% of their ability to absorb impact energy even after 10 days of immersion in 1M HCl.
 - Three points bending test, the degradation of the load-displacement curve as function the concentration of the green inhibitors solution.
 - From the tinsel test, it can be seen that the elongation at break, of the specimen immersed in 1.2HCl solution is 17.5% . , and 31.5% from, 30% of the synthetic inhibitor, and the 31.2 % of the 30 green inhibitors at break.

This study could be improved in the future by the chemical isolation of the active ingredient from the Ruta Chalepensis extract to a full physico-chemical characterization. Also, it is recommendable to carry out in situ experimental study to explore the possibility to use this green corrosion inhibitor in the field in real operating conditions.

Annexe

API 570 CALCULATIONS SUMMARY SHEET- 2016

API 570	
<p>MAWP (Half-life Concept)</p> <p>In corrosive service- Recalculate MAWP</p>	$P = \frac{2SEt}{D}$ (This is "MAWP" Per 570) <p>Here, $t = t_{act}-2(CR \times \text{Inspection Interval})$ $S = \text{Allowable Stress, } E = \text{Joint Efficiency, } D = \text{OD} = \text{Out Dia}$</p>
Corrosion Rates	$\text{Corrosion Rate (CRLT)} = \frac{t_{\text{initial}} - t_{\text{actual}}}{\text{time (years) between } t_{\text{initial}} \text{ and } t_{\text{actual}}}$ $\text{Corrosion Rate (CRST)} = \frac{t_{\text{previous}} - t_{\text{actual}}}{\text{time (years) between } t_{\text{previous}} \text{ and } t_{\text{actual}}}$
Remaining Life	$\text{Remaining Life, RL (years)} = \frac{t_{\text{actual}} - t_{\text{required}}}{\text{corrosion rate (Highest)}}$
Inspection Interval	Inspection Interval = Lesser of 1/2 of RL or Table 2
Fillet Welded Patch	\sqrt{Dt} Minimum distance between the toes of the fillet. Here, $D = \text{ID, } t = \text{Min required thickness of fillet weld patch}$
API 574	
Min. Required Thick Pipe	$t_{\text{min required}} = \frac{PD}{2SE} + CA$ (Alternative Barlow formula from API RP 574)
Min. Required Thick Flanged Fittings	Old/corroded: $t_{\text{min required}} = \frac{1.5PD}{2SE} + CA$ If Unknown materials, use 7000 for S.
Min. Required Thick Valves Body	Old/corroded: $t_{\text{min required}} = \frac{1.5PD}{2SE} + CA$ If Unknown materials, use 7000 for S.
ASME B31.3	
Min. Thick / Retirement /Required Thick/Pressure Design Thick Pipe	$t_{\text{min}} = \frac{PD}{2(SE + PY)}$ or $t_{\text{min}} = \frac{PD}{2SE}$ Here, $P = \text{Design Pressure, } D = \text{OD}$ $S = \text{Allowable Stress, } E = \text{Joint Efficiency, } Y = \text{Coefficient Factor} = .4$
Min. Required Thick Pipe	$t_{\text{min required}} = \frac{PD}{2(SE + PY)} + CA$ or $t_{\text{min required}} = \frac{PD}{2SE} + CA$ Here, $P = \text{Design Pressure, } D = \text{OD, } CA = \text{Corrosion Allowance}$ $S = \text{Allowable Stress, } E = \text{Joint Efficiency, } Y = \text{Coefficient Factor} = .4$

API 570 CALCULATIONS SUMMARY SHEET-2016

Cost effective Schedule/Order Thick Pipe	$\frac{t_{min} + CA}{.875}$ (For Seamless Pipe) $t_{min} + CA$ (For ERW Pipe)
Retirement Thick Blanks/ Blind Flg.	$t_{min} = dg \sqrt{\frac{3P}{16SE}}$ Here, dg = Gasket ID, P = Design Pressure, S = Allowable Stress, E = Joint Efficiency.
New/Cost Effective/ Order Thickness Blanks/ Blind Flg.	$t_{min} = dg \sqrt{\frac{3P}{16SE} + CA}$ Here, dg = Gasket ID, P = Design Pressure, S = Allowable Stress, E = Joint Efficiency. CA = Corrosion Allowance
Thermal Expansion/ Thermal Growth	$G = \frac{FxL}{100}$ Here, G = Growth in inch, F = Factor, L = Length in Feet
Fillet Welds	LEG = 1.414×THROAT, THROAT = .707×LEG Xmin(REQUIRED LEG) for Socket/ Slip on flanges $t_c = .5 t_r$ or .7t min. (required throat) for Branch Connections/repads
Hydro Pressure Pipe	Hydro test Pressure (H.T) = $1.5 \times P \times \frac{S_t}{S_d}$ Here, P = Design Pressure S_t = Stress @ Test Temp, S_d = Stress @ Design Temp
Pneumatic Pressure Pipe	$1.1 \times P$ Here, P = Design pressure
Joint Efficiency/ Quality Factor	Piping Table A-1B (See Table 302.3.4)
Preheat Temp.	See Table 330.1.1
PWHT	See Table 331.1.1
Defect and Acceptance Criteria	See Table 341.3.2 and Table 341.3.2
MDMT	See Table A-1 and Table 323.2.2A and Fig. 323.2.2B
B16.5	
Flanges	Max Hydro Press – 1.5 X system design pressure-rounded to 25 psi (whole) Types 150, 300, 400, 600, 900, 1500, 2500 NPS ½ thru NPS 24
Hydro Pressure (Fittings)	Max Press = 1.5 X 100 th Flange rating (Round to next 25 PSI) 1 min for NPS 2 and ↓ and 2 min for NPS 2 1/2-8 3min 10 ↑
Flanged Fittings Areas below Min. T	Diameter = $.35 \sqrt{dtm}$ d = ID Meas Thk = .75tm Area = πR^2 Dist Appart = $1.75 \sqrt{dtm}$ t = Min Wall From Charts Tables 13-28
Tension Test/ Rupture Stress/ UTS	Load/Area (ASME Sec. IX)